Journal of Rheology

PERSPECTIVE | DECEMBER 31 2025

Ring polymer physics and rheology: Challenges and opportunities

Charles M. Schroeder ; Ralf Everaers ; Kurt Kremer ; Margarita Kruteva ; Christos N. Likos ; Gregory B. McKenna ; Thomas O'Connor ; J. Ravi Prakash ; Dieter Richter ; Rae Robertson-Anderson ; Michael Rubinstein ; Kenneth S. Schweizer ; Dimitris Vlassopoulos

J. Rheol. 70, 183–216 (2026)
https://doi.org/10.1122/8.0001099

Ring polymer physics and rheology: Challenges and opportunities

Charles M. Schroeder,[1,a)] Ralf Everaers,[2] Kurt Kremer,[3] Margarita Kruteva,[4] Christos N. Likos,[5] Gregory B. McKenna,[6] Thomas O'Connor,[7] J. Ravi Prakash,[8] Dieter Richter,[4] Rae Robertson-Anderson,[9] Michael Rubinstein,[10,11] Kenneth S. Schweizer,[12,13,14] and Dimitris Vlassopoulos[15,16]

[1]*Department of Chemical and Biological Engineering, Princeton University, Princeton, New Jersey 08544*
[2]*ENS de Lyon, CNRS, Laboratoire de Physique and Centre Blaise Pascal, F-69342 Lyon, France*
[3]*Max-Planck-Institut für Polymerforschung, Ackermannweg 10, Mainz 55128, Germany*
[4]*Forschungszentrum Jülich GmbH, Jülich Centre for Neutron Science (JCNS), 52425 Jülich, Germany*
[5]*Faculty of Physics, University of Vienna, Boltzmanngasse 5, 1090 Vienna, Austria*
[6]*Department of Chemical and Biomolecular Engineering, North Carolina State University, Raleigh, North Carolina 27695*
[7]*Department of Materials Science and Engineering, Carnegie Mellon University, 5000 Forbes Avenue, Pittsburgh, Pennsylvania 15213*
[8]*Department of Chemical Engineering, Monash University, 20 Research Way, Melbourne, VIC 3800, Australia*
[9]*Department of Physics and Biophysics, University of San Diego, San Diego, California 92110*
[10]*Thomas Lord Department of Mechanical Engineering and Materials Science, Biomedical Engineering, Physics and Chemistry, Duke University, Durham, North Carolina 27708*
[11]*Institute for Chemical Reaction Design and Discovery (WPI-ICReDD), Hokkaido University, Sapporo 001-0021, Japan*
[12]*Department of Materials Science and Engineering, University of Illinois at Urbana-Champaign, Urbana, Illinois 61801*
[13]*Department of Chemical and Biomolecular Engineering, University of Illinois at Urbana-Champaign, Urbana, Illinois 61801*
[14]*Materials Research Laboratory, University of Illinois at Urbana-Champaign, Urbana, Illinois 61801*
[15]*Institute of Electronic Structure and Laser, FORTH, Heraklion 71110, Crete, Greece*
[16]*Department of Materials Science and Engineering, University of Crete, Heraklion 71003, Crete, Greece*

(Received 4 August 2025; final revision received 17 November 2025; published 31 December 2025)

Abstract

Understanding the structure and dynamics of ring or cyclic polymers is a long-standing challenge in polymer science, with important implications for emerging biological phenomena such as chromosome territories. This Perspective article provides a comprehensive overview of the current state of ring polymer physics and rheology, highlighting emerging challenges and opportunities for future research. Key scientific questions are considered regarding the properties of synthetic and biological ring polymer systems using theory, simulations, and experiments. This article was inspired by stimulating discussions at a CECAM Flagship workshop on Ring Polymer Dynamics in Prato, Italy, in June 2023. Several of the concepts and results discussed here are also presented in the *Journal of Rheology* virtual issue on ring polymers (https://pubs.aip.org/jor/collection/1392/Ring-Polymers). Broadly, this article aims to spark conceptual advances in polymer physics and rheology by exploring new phenomena and open scientific questions that are unique to ring polymer systems.
https://doi.org/10.1122/8.0001099

I. INTRODUCTION

A key challenge in developing new functional materials lies in understanding how molecular architecture affects bulk viscoelastic properties [1,2]. Ring polymers (or cyclic or circular polymers) have a unique molecular architecture lacking chain ends, which results in qualitatively different structure and dynamics compared to linear chains [3,4]. Ring polymers call into question our fundamental understanding of polymer dynamics because the absence of free ends alters flow behavior [5,6], diffusion [7], phase behavior [8], and ordering transitions [9] compared to linear macromolecules. Their cyclic topology [10] gives rise to unusual viscoelastic properties that cannot be explained by classic theories based on the tube model [1,2]. The unique properties of ring polymers makes them promising candidates for several materials science applications [11,12]. Moreover, ring polymers are essential to fundamental life processes and play a key role in

[a)]Author to whom correspondence should be addressed; electronic mail: cschroeder@princeton.edu

biology and biotechnology, including DNA replication and maintenance of circular genomes [13], DNA looping [14], and biologically active macrocycles such as drugs [15].

Structure-property relationships for polymeric materials critically depend on macromolecular architecture and composition, which ultimately governs their bulk-scale viscoelastic properties. A relevant fundamental material function describing the mechanical response of a polymer is the stress relaxation modulus $G(t)$. For entangled linear polymer melts (with molecular weight exceeding the critical entanglement molecular weight M_e), the dynamics are described by the tube model [1,2], which is a single-chain approximation to uncrossability topological constraints imposed by neighboring chains. In linear polymer melts, individual chains reptate, i.e., relax stress by diffusing curvilinearly along a confining tube, a process facilitated by the presence of free ends. Complementing reptation with additional nonreptative processes such as contour length fluctuations and constraint release yields quantitative predictions of rheological data for linear chains [2,16]. In general, the stress relaxation modulus $G(t)$ for linear polymer melts shows a plateau at intermediate times and exponential decay at longer times. However, the stress relaxation response for branched polymers is qualitatively different. Star polymers are the simplest branched architecture and relax stress by arm retraction because one end of each arm is fixed to the core [2,16]. Macromolecules with more complex branched architectures (e.g., combs) relax hierarchically in the melt state: branching generations relax sequentially starting from the outermost dangling ends and moving inward, often combining retraction and reptation [17]. Up to this point in the discussion, stress relaxation critically relies on a free chain end. A natural question then arises: how is stress relaxed in ring polymer melts given the absence of polymer chain ends? The answer lies in considering the topology of polymeric materials.

The microscopic topology of polymeric materials is governed by molecular architecture. In turn, the dynamic motion of polymer chains is subject to topological constraints [18,19], an effect which is familiar to the common human experience of untangling knotted strings. The topological constraints of linear polymers are *transient* and tend to dominate the viscoelastic behavior of high molecular weight polymeric liquids by slowing down chain equilibration after a deformation or during diffusion. In contrast, the microscopic topological state of ring polymer systems is *fixed* during synthesis [18,19], at least in terms of the presence or absence of interlocked rings or concatenated structures. In ring polymer systems, all subsequent conformational changes preserve such topology together with invariants characterizing the internal degree of knotting or the degree of linking of pairs, triplets, and higher order linkages of rings. The ring polymer analog of the transient network structure in linear chain melts is an arrangement of several adjacent rings with interacting or interpenetrating loopy segments. Understanding how the microscopic topological structures in ring polymers lead to stress accumulation and relaxation in high molecular weight systems is an open challenge in the field.

For identical chemical composition, molecular weight, and density, the large-scale structure and dynamics of ring polymers can be radically different than their linear chain counterparts. Figure 1 illustrates the differences between linear and ring polymers by comparing simulation results for the prototypical equilibrium structure in the melt state. In the well-known case of linear polymer chains [1,24], polymer molecules mutually and strongly interpenetrate and exhibit nearly ideal Gaussian chain statistics [Fig. 1(a)]. In contrast,

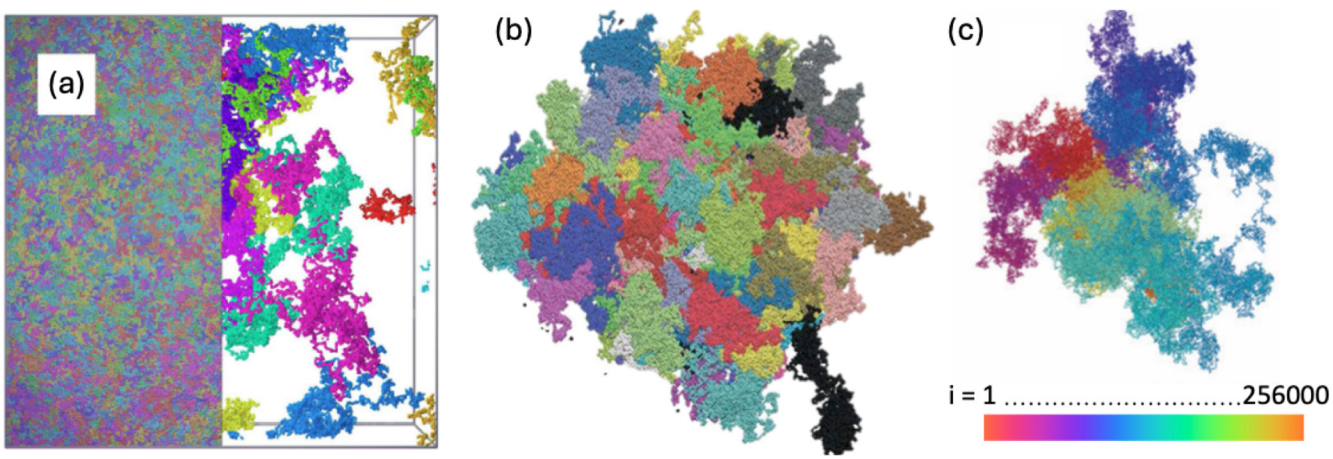

FIG. 1. Simulations of linear chains and nonconcatenated ring polymers in the melt state: (a) Visualization of a melt of $N = 1000$ linear polymer chains of $N_b = 15\,000$ beads with periodic boundary conditions with individual chains shown with randomly chosen colors. To illustrate the mutual interpenetration of chains, all polymers are shown in the left-hand side of the box. In the right-hand side of the box, ten randomly selected polymers are shown to illustrate the random walk-like single chain structure. Reproduced with permission from Svaneborg *et al.*, Phys. Rev. E **94**, 032502 (2016). Copyright 2016, American Physical Society [20]. (b) A melt of $N = 142$ nonconcatenated ring polymers of $N_b = 10\,082$ beads with periodic boundary conditions shown without projecting the beads back into the central simulation box [21]. Individual ring polymers are represented with individual colors to show their territorial packing. Reproduced with the permission from Vettorel, *et al.,* Phys. Today **62**, 72 (2009) [22]. Copyright 2009, AIP Publishing LLC. (c) An individual hierarchically crumpled ring polymer of length $N_b = 256\,000$ beads from a similar melt of $N = 629$ rings. The cyclic color code following the monomer index reveals the fractal nature of the territorial packing. Although most of the ring contour length appears to be tucked into densely crumpled sections, the randomly chosen ring also displays a large penetrable open loop. Reproduced with permission from Schram *et al.*, Soft Matter **15**, 2418–2429 (2019) [23]. Copyright 2019, Royal Society of Chemistry.

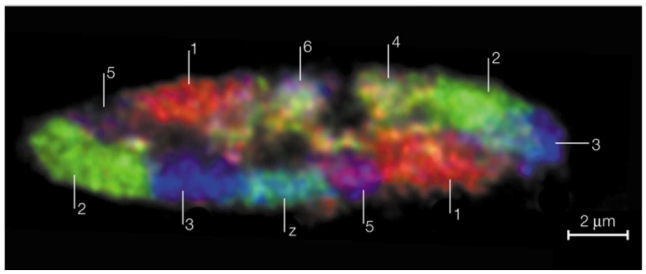

FIG. 2. Midplane light optical section through a chicken fibroblast nucleus showing segregated chromosome territories rendered visible via chromosome painting using fluorescence *in situ* hybridization (FISH). Reproduced with permission from Cremer and Cremer, Nat. Rev. Genet. **2**, 292–301 (2001) [30]. Copyright 2001, Nature Portfolio.

in a melt of unknotted nonconcatenated rings, individual ring polymer molecules interpenetrate to a lesser degree and exhibit territorial behavior [Fig. 1(b)] [6,22,23,25–28], with high molecular weight rings further displaying self-similar territorial packing in their crumpled internal structure [Fig. 1(c)]. The stark differences in molecular structure between linear and ring polymers hold important implications for understanding their dynamics and thermodynamics in the melt state.

Implications for understanding ring polymer physics extend beyond synthetic ring systems. A common real world example of long linear unentangled macromolecules [29] is found in the cell nuclei of eukaryotic organisms, where the chromosomes occupy territories [30] resembling those found in ring polymer melts (Fig. 2) [31]. Although the crumpled internal structure of chromosomes [32] was theoretically predicted [33] on topological grounds, the applicability of the analogy to linear chromatin fibers depends on a separation of time scales [34,35]. Notably, computer simulations of decondensing model chromosomes [35] revealed territories that are stable over biologically relevant time scales and chain structures, in good agreement with both experimental data for chromosomes and the local crumpled equilibrium statistics for corresponding melts of nonconcatenated rings [35,36]. More recent work has shown how biological processes like loop-extrusion can drive chains to adopt nonequilibrium conformations with higher fractal dimensions, altering their function and rheology [37]. Overall, these studies have motivated new research on understanding chromosome territorial arrangement and related biophysical problems that define the current state of the art in ring polymer physics.

A. Brief history: From early studies to recent developments

The study of ring polymers has a rich history spanning experiments, computational modeling, and theory. In the early to mid-20th century, scientists identified naturally occurring cyclic DNA molecules, including the genomes of bacteriophages [38] and extrachromosomal circular DNA molecules in eukaryotic organisms [39]. In terms of synthetic ring polymers, experimental studies in the 1970s and 1980s focused on preparing and characterizing synthetic nonconcatenated rings in dilute solutions and melts [40]. Early work focused on ring polymer chemistries including poly(dimethylsiloxane) (PDMS), polystyrene (PS), and polybutadiene (63% 1,2-addition and 37% 1,4-addition) [40–48], and rings were typically purified and characterized using a variety of methods including size-exclusion chromatography, light scattering, and shear rheology. In the regime corresponding to the moderately entangled equivalent linear chain system [$Z = M_w/M_e < 15$, where M_w is the mass average molar mass (referred to as molecular weight) and M_e is the entanglement molecular weight of the equivalent linear chain], linear viscoelastic (LVE) measurements on ring polymers revealed a weak rubbery plateau region with a modulus that was approximately 20%–50% compared to linear chain counterparts [47,48], though it was shown much later that no plateau was observed in molecular dynamics simulations of ring melts in this Z regime [27,49]. At high molecular weights, the viscosity of linear polymer melts was reported to significantly exceed that of ring polymers [47,50]. Addition of linear chains to ring polymer melts was reported to increase the viscosity of these materials [47,51,52].

Early work on ring polymers began to reveal the influence of linear chain impurities on the rheological properties of ring polymer melts, which motivated methods to improve ring purity. Initial ring synthesis work used fractional precipitation of PS rings from benzene-methanol solutions, and purity was monitored by gel permeation chromatography and ultracentrifugation sedimentation [44]. Fractionate precipitation was also used to study the effects of linear chain addition on refractionated ring samples, which were (at the time) thought to be of the highest purity available [51]. Additional attempts to further purify rings focused on subjecting ring polymer samples to extensive refractionation by size-exclusion chromatography [48]. Overall, these early studies highlighted the need for improved methods for ring polymer purification while further revealing the complexities in preparing high purity ring polymer samples.

In the early 2000s, the development of liquid chromatography at the critical condition (LCCC) was shown to provide enhanced purification of ring polymers [53,54], which set the stage for subsequent rheological characterization of ring polymer melts. In the LCCC method, the critical condition for a linear polymer of a given chemistry is determined: the entropic repulsion that a polymer feels with respect to the packing material used in a column for conventional size exclusion chromatography is balanced by the enthalpic attraction of interaction chromatography when a temperature gradient is introduced. At the critical condition, all linear polymers chains are eluted at the same time regardless of molecular weight and, therefore, separated from rings whose elution depends on their molecular weight [53]. Using LCCC-purified rings [55,56], it was reported that low to moderate molecular weight ring polymer melts ($Z \leq 11$) do not exhibit an entanglement plateau, but rather show power-law stress relaxation behavior [5], consistent with predictions from the lattice animal model [4,5,57,58]. This work further showed that the viscoelastic properties of rings are extremely sensitive to the presence of linear chains [5], in qualitative agreement with simulations [6], as discussed in more detail in Secs. II–IV. Taken together, these early studies motivated

the need for additional synthesis, preparation, and characterization methods for rings discussed in this article.

B. Motivation, goals, and overview of article

In this Perspective article, we discuss the current state of ring polymer physics and rheology, focusing on recent progress in experiments, theory, and computational modeling. We further discuss emerging challenges and opportunities in the field, highlighting several fundamental questions that need to be addressed at the interface of polymer chemistry and polymer physics. Broadly, this article highlights the need for new synthetic strategies to enable the design and preparation of scalable quantities of high molecular weight rings. New methods are needed for the enhanced purification of ring polymers to understand and control the influence of linear polymer chains in ring polymer samples. In addition, an improved understanding of structure-property relationships, specifically focusing on the nonlinear rheological response of rings and ring-based mixtures, is necessary to advance the current state of the art and to elucidate methods and strategies for polymer processing. Major opportunities lie in exploiting nonconcatenated rings for developing new material structures and applications [59]. Additional research is needed to further advance basic scientific knowledge in the field, which will enable the development of ring polymers as versatile building blocks for materials engineering with unique topological interactions and corresponding flow properties.

A primary goal of this Perspective article is to identify open scientific questions that can only be solved by a united community approach and meaningful collaborations to address such important interdisciplinary challenges. This article was prepared based on extensive discussions from a recent Ring Polymer Workshop held in Prato, Italy between June 14 and 16, 2023, which provided a venue for in-depth discussions on a relevant set of publications included in the recent virtual issue on ring polymers in the Journal of Rheology. We also refer the reader to a recent review article focusing on the internal structure and dynamics of ring polymer systems at relatively small length and time scales [60]. This article is organized by discussing the state of the art of the field and emerging challenges facing the preparation and study of ring polymers in dilute solutions (Sec. II), melts and concentrated solutions (Sec. III), and the study of biological and active ring polymers (Sec. IV).

II. SYNTHESIS AND DILUTE SOLUTION PROPERTIES OF RINGS

A. Synthesis and characterization of rings

The synthesis, preparation, and characterization of ring polymers have been extensively discussed in prior literature. We refer the reader to textbooks edited by Semlyen [61] and Tezuka [62], and a book chapter coauthored by Ederle *et al.* [42] for detailed discussions of early efforts in the synthesis and preparation of ring polymers. In addition, a more recent review article by Grayson and co-workers [63] provides extensive discussions of synthetic strategies for cyclic macromolecules. In general, ring polymers are typically prepared by ring-closure reactions, which involve end-to-end cyclization reactions of linear polymers synthesized by ionic polymerization methods [42]. As discussed below, the ring-closure reaction plays a key role in the structural properties and the purity of ring polymer samples.

Experimental measurements of dilute solution properties are commonly used as a principal means of characterizing linear polymers [16,64] and model polymers of different molecular architectures [65–78]. In addition, such measurements are frequently used to test predictions of molecular theories and simulations [65,70,75,79,80]. Ring and linear polymers are commonly characterized in dilute solutions in either theta or good solvents to determine radius-of-gyration R_g by static light scattering, hydrodynamic radius R_H by dynamic light scattering, or the effective size obtained from intrinsic viscosity measurements $[\eta]$. The dilute solution properties of model polymers such as rings can also be characterized using small angle x-ray scattering and small angle neutron scattering (SANS), for example, in determining the particle scattering function (or form factor) $P(q)$ [81,82]. Additional characterization methods commonly rely on bulk rheology (linear or nonlinear viscoelastic measurements), single molecule polymer dynamics [83], atomic force microscopy (AFM), electron microscopy, nuclear magnetic resonance (NMR), mass spectrometry, and infrared spectroscopy.

In the following discussion, we consider a few key properties of rings and linear chains, including the ensemble-averaged root-mean-square radius-of-gyration R_g and the θ-temperature for dilute solutions of rings and linear chains. Interestingly, Zimm and Stockmayer predicted the ratio of the R_g of a ring to that of a linear polymer of the same molecular weight (R_{gR}/R_{gL}) for ideal Gaussian chains several years before its experimental measurement [84]. Subsequent to the first systematic investigation of dilute ring solutions by Semlyen [85], several studies focused on the characterization of ring polymers by measuring dilute solution properties [7,81,82,86–92]. Experimental measurements have been accompanied by extensive analytical [65,70,84,93–97] and simulation-based [98–102] property predictions.

A significant aspect of dilute ring polymer solutions is that the unique topology of having no chain ends leads to the θ-temperature for solutions of rings, Θ_R, being lower than that for linear polymer solutions, Θ_L, in identical solvents [81,82,88,90,92]. For example, experiments on solutions of ring or linear PS chains of identical and high molecular weight M_w in d_{12}-cyclohexane revealed a ring θ-temperature of $31.5 \pm 1\,^{\circ}\mathrm{C}$, whereas the linear chain counterpart has a value of $38.3\,^{\circ}\mathrm{C}$ [82]. Consequently, a ring polymer at a given temperature essentially experiences better solvent conditions than a linear chain with the same molecular weight. The improved solvent quality for ring polymer solutions is considered to arise from both 3-body interactions and topological constraints [101]. Ensuring that solutions of rings and linear chains with identical chemistry and molecular weight have the same solvent quality requires that their temperatures, T_R and T_L, are equally distant from their respective θ-temperatures. Using the definition of the solvent quality parameter [94,103–107] $z = k_0\,(1 - \Theta/T)\sqrt{M_w}$, where T is

TABLE I. Reported values of ratios of various observables for ring polymers and their linear counterparts including radius-of-gyration R_g, hydrodynamic radius R_H, and intrinsic viscosity $[\eta]$. Subscripts R and L indicate rings and linear chains, respectively. Symbols with θ as a superscript indicate θ-conditions for the particular architecture, while the remaining symbols represent measurements carried out under good solvent conditions.

Variable	Definition	Experiment	Theory	Simulation
g^θ	$(R^\theta_{gR}/R^\theta_{gL})^2$	0.50 [81,82,88], 0.56–0.73 [113]	0.500 [84,94,97]	0.50 [97,114]
g	$(R_{gR}/R_{gL})^2$	0.55 [82], 0.53 [86,90] 0.47–0.51 [61]	0.568 [95], 0.516 [65]	0.536 [98], 0.56 [99,102], 0.55 [114], 0.53 [115]
g^θ_H	$R^\theta_{HR}/R^\theta_{HL}$	0.84 [87], 0.86–0.89 [88]	0.848 [65]	0.833 [114]
g_H	R_{HR}/R_{HL}	0.89 [81], 0.83–0.9 [116], 0.74–0.79 [7]	0.85 [65]	0.89 [115]
g'^θ	$[\eta]^\theta_R/[\eta]^\theta_L$	0.60–0.66 [116], 0.66 [90]	0.658 [117], 0.645 [118], 0.662 [65]	0.57 [119]
g'	$[\eta]_R/[\eta]_L$	0.57–0.63 [120], 0.56–0.67 [116], 0.71–0.74 [90]	0.673 [65], 0.561 [121]	0.59 [115], 0.58 [119], 0.58–0.64 [120]

the temperature, Θ is the theta temperature, and k_0 is a chemistry-dependent constant, the two temperatures are related by the expression, $T_R = (\Theta_R/\Theta_L)T_L$. Finally, the effect of knots on the θ-temperature of ring polymers has been studied using simulations [100], revealing a decrease in the ring θ-temperature upon introducing trefoil or fivefold knots in an unknotted ring but no difference in the θ-temperature between these two knotted molecules.

B. Ring-closure reactions and solvent quality effects

It is well known that the overall size of a polymer chain in dilute solutions depends on the molecular architecture, molecular weight, and solvent quality [16]. In contrast to linear and branched polymers, the size of ring polymers also depends on the preparation conditions. For example, rings formed by end-to-end cyclization reactions of linear polymers in a theta solvent and subsequently characterized in good or theta solvents are smaller than the same molecular weight rings formed by end-linking the same linear polymers in a good solvent. The reason for this difference is that the size of ring polymers depends on the number and distribution of knots locked-in during the ring-closure process. This phenomenon created significant controversy in the 1980s, when it was argued that there is a higher probability of knot formation for rings synthesized in theta solvents (rather than good solvents) [90], which leads to more compact conformation and reduced size [108]. Knots formed during ring-closure reactions in synthetic polymers are permanent due to cyclization.

A ring polymer with a particular knot (e.g., trefoil knot) has a well-defined size. More and higher order knots are thought to be locked-in during ring-closure reactions in theta solvents than in good solvents, resulting in smaller sizes of rings prepared in theta-solvent conditions. The complexity of knots locked-in at preparation increases with the molecular weight of the ring; that is, the order of Alexander polynomial increases as the 1/4 power of molecular weight in theta-solvent prepared rings. The ratio of the sizes of ring and linear chains in a particular solvent (theta or good) depends on the preparation condition of rings through the distribution of locked-in knots and also on the measurement technique and corresponding quantity: radius-of-gyration $R_g = \langle R_g^2\rangle^{1/2}$, hydrodynamic radius $R_H = k_BT/6\pi\eta_sD$, where k_B is the Boltzmann constant, η_s is the solvent viscosity, and D is the long-time diffusivity, or effective size obtained from intrinsic viscosity measurements $[\eta]$. Comparison of different molecular architectures is often performed using the following parameters: [94] $g = (\langle R_g^2\rangle_R)/(\langle R_g^2\rangle_L)$, $g_H = (\langle R_H^2\rangle_R^{1/2})/(\langle R_H^2\rangle_L^{1/2})$, and $g' = [\eta]_R/[\eta]_L$, where the subscripts R and L refer to rings or linear chains (Table I). These quantities are typically determined using ring and linear polymer samples of the same chemistry and molecular weight under identical conditions. However, the ratio of sizes quantified by g, g_H, and g', measured by different techniques under different solvent conditions, are of similar order of magnitude. In addition, the relatively small size differences of ring and linear polymers make their separation during purification challenging, requiring more advanced techniques, such as LCCC to enable purification (Sec. I A). Interestingly, supercoiled rings [109,110] can be significantly larger than nonsupercoiled polymers with the same molecular weight. Moreover, the distribution of knots in ring DNA can be modified by enzymes (Sec. IV).

The phenomenon of knot formation in rings was addressed by performing ring closure reactions for linear PSs in a good solvent (tetrahydrofuran, THF) [43,81,90,111] or a theta solvent (cyclohexane at the theta temperature) [44,88]. The two sets of rings exhibited nearly identical values of R_g and $[\eta]$ at the theta condition in cyclohexane for a range of molecular weight up to nearly 200 000 g/mol, where a deviation was attributed to the effect of solvent during synthesis. A compilation of the PS ring data [43,44,81,88,90,111] reveals the following: in theta conditions, a universal value is observed for $g^\theta \approx 0.5$, whereas in good solvent conditions, g varies between 0.47 and 0.51 [61], with some additional publications reporting slightly larger values of g [86,89,90]. Recent work by Takano and co-workers focused on the synthesis of knotted PS rings, which indeed exhibit a size that decreases as the estimated fraction of knots increases [112]. The same research group synthesized and critically purified a series of PS rings with molecular weights ranging between 17 000 and 570 000 g/mol and reported g^θ values between 0.557 and 0.73 in theta solvent conditions (cyclohexane) [113]. In terms of the hydrodynamic radius, g_H was 0.89 for

PS rings synthesized in good solvent [81], and g_H^θ varies in the range 0.86–0.89 (depending on the molecular weight) for rings synthesized in theta solvent [88].

In terms of intrinsic viscosity, a nearly universal value of $g'^\theta \approx 0.64$ was determined from PS data in theta solvents, with small deviations appearing with increasing molecular weight and being more pronounced around 100 000 g/mol and above. Positive deviations are thought to reflect the presence of linear chains. Closer inspection by analyzing individual pairs of linear and ring polymers indicates that g'^θ values range between 0.64 and 0.68, with the larger values suggesting linear chain contamination. Experimental evidence suggests that g'^θ values for rings synthesized in theta conditions slowly decrease with increasing molecular weight [88], which was attributed to the presence of knots [43]. Whereas the knots indeed yield a decrease in g, g_H, and g' [122], it was reported that the ring polymer samples were contaminated by linear chains of lower (approximately half) molecular weight, which could explain the results [44,61]. It was further argued that the available experimental results suggest that, even if knots exist in ring polymers, the related difference of expansion will be small. In good solvents, the average value of g' was found to be 0.64, but with much larger variations in the data at different molecular weights compared to theta solvents [61]. A recent study of a series of PS rings from 16 000 to 370 000 g/mol, synthesized in THF and critically fractionated, revealed that the values of g' in THF ranged from 0.57 to 0.63 with increasing molecular weight, in agreement with simulations [120]. Finally, it is possible that there are subtle changes in the solvent draining through the linear and cyclic polymer coils, which could influence the g' values in different solvents.

A summary of experimental measurements, theoretical predictions, and simulation results for several properties of rings and linear chains is shown in Table I. The citations are not exhaustive but rather serve to illustrate characteristic values for these quantities. The main takeaway message is that any ratio of the observable quantities of the ring to the linear polymer is less than unity. In many cases, prior literature generally does not report all experimental values with a careful consideration of the difference between the solvent quality of ring and linear polymer solutions (e.g., for experiments performed at the same temperature), as discussed above. In addition, the precise values of these quantities depend on the solvent quality and relative "goodness" of the solvent in the thermal crossover regime. The simulation results shown in Table I have all been obtained using coarse-grained models for polymers using a variety of techniques. In simulations, the determination of the intrinsic viscosity is particularly challenging due to the need to account for hydrodynamic interactions (HI), the influence of boundaries, and the presence of significant noise. Its calculation for linear chains has required the adoption of variance reduction methods [80,123]. Undoubtedly, this will be required for the estimation of the intrinsic viscosity of ring polymer solutions. As pointed out in prior work [70], although there are predictions of ratios of the intrinsic viscosity [120] of rings to linear polymers listed in Table I, they may not reliable due to their inadequate treatment of HI.

It is important to make a distinction between the static and dynamic properties of polymer chains. In the case of linear polymer chains, experimental measurements have shown some apparent differences between static and dynamic properties in terms of their molecular weight M scaling in good solvents. For instance, the radius-of-gyration R_g (a static property) has been reported to scale as $R_g \sim M^{0.59}$ and the hydrodynamic radius (a dynamic property) has been reported [124–127] to scale as $R_H \sim M^{0.55\pm0.02}$. However, we note that the apparent exponents in these scaling relations sensitively depend on several factors, including the solvent quality in the thermal crossover regime between theta and athermal solvents, and hence should be considered as effective exponents.

There is a long history of theoretical attempts to explain the molecular weight scaling behavior of linear and ring polymers, which is beyond the scope of this Perspective article [128–131]. First, the long-time diffusivity D is a dynamic property [132] requiring the presence of fluctuating HI to be taken into account in order to obtain a precise estimate [133]. Second, accurately predicting the scaling behavior of a dynamic property in theta and athermal solvents not only requires accounting for the presence of fluctuating HI, but also the development of a systematic procedure to compute properties in the long chain limit that establishes the universal nature of the predictions, free from finite size effects and independent of the choice of simulation parameters. In the case of linear chains, this was demonstrated [80] for theta solvents using Brownian dynamics (BD) simulations [79,134–138] along with a variance reduction technique. Third, in the thermal crossover regime ($0 \leq z < \infty$), it is necessary to account for solvent quality. Recent work has used parameter-free BD simulations that account for fluctuating HI, a narrow Gaussian potential that accounts for solvent quality, and an extrapolation procedure to obtain results in the asymptotic limit of long chains, enabling prediction the observed swelling of R_g, R_H, and the viscosity radius for linear chains with quantitative accuracy [123,130,138,139]. Ratios of quantities involving the long-time diffusion coefficient for rings were also recently reported using BD simulations with fluctuating HI [114].

C. Single polymer dynamics

The dynamics of DNA-based ring and linear polymers have been extensively studied using single molecule techniques (Fig. 3) [83]. Single molecule experiments allow for the direct observation of linear chains or architecturally complex polymers at equilibrium [7] or under nonequilibrium conditions in shear and extensional flow [137,143,144]. In recent years, experiments on single polymer dynamics have expanded the field of molecular rheology, focusing on dynamics in shear, extensional, and mixed flows across concentration regimes spanning dilute, semidilute unentangled, and entangled [83].

Single molecule experiments on ring polymers are generally carried out using monodisperse DNA-based rings [83,145]. High molecular weight DNA rings are readily prepared using plasmids and fosmids [145,146]. In extensional

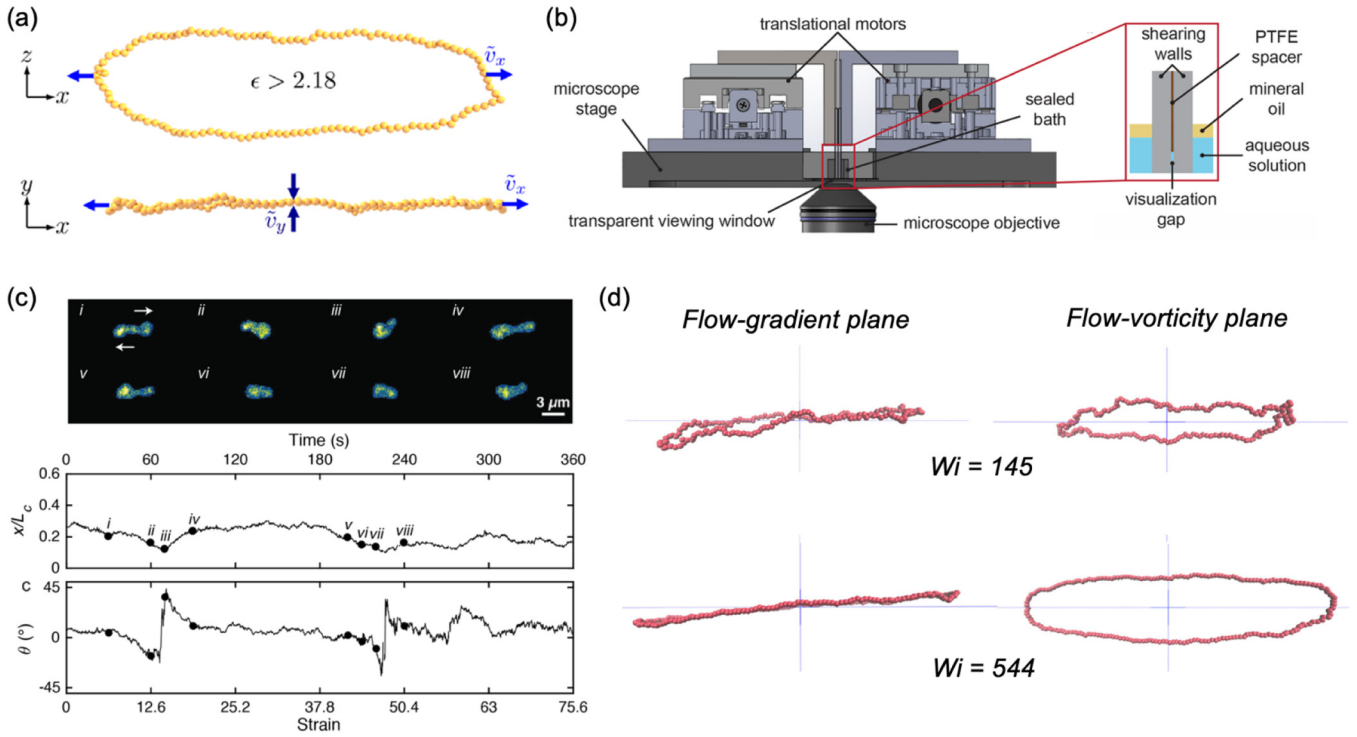

FIG. 3. Single molecule experiments and simulations reporting ring polymer dynamics in dilute solution extensional flow and shear flow. (a) Coarse-grained Brownian dynamics (BD) simulations showing "swelling" of ring polymers in the direction orthogonal to flow (z-direction) in planar extensional flow, where the x-direction is the extensional flow axis. Reproduced with permission from Hsiao *et al.*, Macromolecules **49**, 1961–1971 (2016) [140]. Copyright 2016, American Chemical Society. (b) Schematic of the custom feedback-controlled shear flow device allowing for single molecule imaging in the flow-gradient plane of shear. Reproduced with permission from Tu *et al.*, Macromolecules **53**, 9406–9419 (2020) [141]. Copyright 2020, American Chemical Society. (c) Single molecule snapshots and transient measurements of ring DNA polymer extension x/L and orientation angle θ in the flow-vorticity plane of shear flow at Weissenberg number $Wi = \dot{\gamma}\tau = 6.2$, where $\dot{\gamma}$ is the shear rate and τ is the longest relaxation time of ring conformation determined from single molecule imaging. Ring DNA molecules consisted of a 114.8 kbp bacterial artificial chromosome (K16). Reproduced with permission from Tu *et al.*, Macromolecules **53**, 9406–9419 (2020) [141]. Copyright 2020, American Chemical Society. (d) Simulations showing vorticity-direction swelling of ring polymers in steady shear flow at $Wi = 145$ and $Wi = 544$, respectively. Reproduced with permission from Liebetreu and Likos, Commun. Mater. **1**, 1–11 (2020) [142]. Copyright 2020, Nature Portfolio.

flow, single molecule experiments were used to study the nonequilibrium dynamics of DNA rings in dilute solution, revealing an unexpected shifted coil-stretch transition and a less diverse set of transient stretching pathways compared to linear chain analogs [147]. Intramolecular HI was found to induce an "open loop" chain conformation for rings in the direction perpendicular to flow in planar extensional flow [Fig. 3(a)] [140], giving rise to the shifted coil-stretch transition compared to linear chains.

In shear flow, single molecule experiments provided for the direct observation of ring DNA stretching using a custom feedback-controlled flow device allowing for imaging in the flow-gradient plane of shear [Fig. 3(b)] [141]. Ring polymers were observed to undergo repeated end-over-end tumbling events in steady shear flow, qualitatively similar to linear chains, determined from direct measurements of transient ring extension x/L and orientation angle θ [Fig. 3(c)] [141]. In addition, multiparticle collision dynamics (MPCD) simulations provided a new understanding of ring polymer dynamics in steady shear, reporting a vorticity-direction swelling of ring polymers in steady shear flow [Fig. 3(d)] [142,148]. The MPCD technique has further shed light on the emergence of new tumbling modes for ring-based, topologically complex molecules, namely, mechanically linked poly[2]catenanes (PC) and pairs of chemically bonded rings (BR) [149]. Indeed, the vorticity swelling mechanism present for single rings is ineffective for PC's due to the high twisting penalty at the mechanical junction that would be associated with the alignment of both rings on the flow-vorticity plane. Accordingly, the PC rings attain double-folded configurations in shear flow and exchange positions via *slip tumbling*. On the contrary, the BR rings swell but the random lack of synchronization in their vorticity swelling sets in rotational motions around the gradient axis, in a mode termed *gradient tumbling* [149]. Shear flow has also been shown to convert writhe to twist for supercoiled rings (see also Sec. IV), which are in general more robust under shear than their relaxed and flexible counterparts regarding their deformations and orientation in shear flow [150]. In semidilute solutions, ring polymers were observed to undergo large fluctuations in chain extension in background solutions of majority linear chains in extensional flow [151]. Fluctuations in ring extension generally arise due to ring-linear threading events (Sec. III B 2) [151]. Additional studies of biologically relevant ring polymers (e.g., relaxed or supercoiled DNA ring polymers) are discussed in Sec. IV.

D. Challenges, opportunities, and open questions

The synthesis and preparation of ultrahigh molecular weight rings with controlled levels of purity and dispersity remains an open challenge. Broadly, there is a need for new

synthetic strategies to enable the synthesis and preparation of scalable quantities of high molecular weight rings with high degrees of purity. At present, the conventional methods used for ring polymer synthesis provide samples in small amounts, typically less than 200 mg, which become even smaller by 50% or more after purification by LCCC or related methods. Moreover, continuous rheological characterization and thermal treatment of a ring polymer sample will inevitably lead to some degree of degradation via unlinking of the precursor's chain ends. From this view, the development of new ring synthesis methods that avoid the need for ring-closure reactions (e.g., ring-expansion synthesis methods) [63,152,153] could improve both the yield and purity of ring polymer samples, while further avoiding potential complications arising from knot formation during ring-closure reactions.

In addition to ring-expansion synthesis methods, additional degrees of control can be brought to bear on intramolecular cyclization strategies for high molecular weight linear polymer chains. Recent work has demonstrated the synthesis of rings with high degrees of spatiotemporal control over intramolecular cyclization that avoids undesired side reactions that can compete with target ring synthesis [154]. In particular, ultrahigh molecular weight (>2M g/mol) cyclic polythioesters were recently prepared using ring-opening polymerization of gem-dimethylated thiopropiolactone, followed by macromolecular cyclization triggered by protic quenching [154]. Such strategies enable selective access to desired cyclic polythioesters, while avoiding the need for high dilution to suppress linear polymer contaminants during ring-closure reactions. In addition to synthetic methods, new strategies are needed for the enhanced purification of ring polymer samples to control and ultimately minimize the influence of linear polymer chains.

Additional investigations of ring polymer solutions are needed that focus on both structure and dynamics, including linear and nonlinear dynamics, single polymer dynamics [83], rheology, and center-of-mass (COM) diffusion experiments [155–157]. Bulk rheology and single molecule experiments should be combined with simulations to achieve a deeper understanding of the underlying physics in dilute and semidilute solutions. Regarding nonequilibrium dynamics, additional single molecule experiments are needed to directly observe the stretching dynamics of rings in time-dependent, oscillatory flow fields [158,159] or 3D flow fields such as uniaxial extensional flow or biaxial extensional flow, which has been enabled by recent advances in automated flow control [160]. Such molecular-scale experiments will provide a window into viewing and understanding how the unique molecular architecture of rings results in a rich set of dynamics under nonequilibrium conditions. Additional work is also needed to understand the LVE properties of rings in dilute and semidilute unentangled solutions, in addition to COM diffusion behavior, over a wide range of solvent qualities in the thermal crossover regime.

Additional progress is also needed in the development of numerical methods and computational modeling of rings in solution. Significantly extended numerical simulations will require large computational resources, which will greatly benefit from new hardware-specific optimized simulation codes. From this view, computational modeling under realistic solution conditions (e.g., including solving quality effects and HI) is not just a problem of running the existing simulations longer, in part, due to the cost and energy requirements for high-performance computing.

III. MELTS AND NONDILUTE SOLUTIONS OF RINGS

A. Current state of the field: Theory/simulation

1. Double-folded randomly branched ring model

Early theories of polymer dynamics and rheology [1,2] were originally developed for individual molecules topologically confined and diffusing through an array of fixed obstacles. In the case of linear chains, the presence of the obstacles has no effect on the chain conformations, but on short time scales suppresses chain motion to a tubelike region [161] and forces the chains to diffuse (reptate [162]) along the tube contour. This reptation process results in the delay of the loss of the memory of initial chains' conformations. The experimentally observed signature of this delay is the rubbery plateau of the stress relaxation function of entangled linear polymers. Note that the concept of the confining tube was first proposed for polymer networks with entangled strands [161]. On the microscopic scale, tube confinement has been observed by several numerical simulations and experiments such as neutron spin echo (NSE) experiments in terms of the dynamic structure factor [163,164].

The interest in understanding the structure and dynamics of nonconcatenated rings traces back to early studies in the mid-1980s [4,57], which predicted several peculiar properties of topologically constrained rings based on the idea that ring polymers confined to a lattice of obstacles behave as double-folded randomly branched lattice animals (Fig. 4). Although it is far from obvious that the obstacle model applies to ring melts [165], the analogy suggests that the crumpling of rings in a melt can be understood as the successive application of three different strategies for entropy maximization: double-folding, branching, and swelling. First and most importantly, the theory predicts that rings adopt double-folded configurations to minimize the threadable surface as this reduces the importance of the topological constraints they impose on each other (or which are imposed by the obstacles in the model). Second, and in contrast to linear chains, double-folded rings

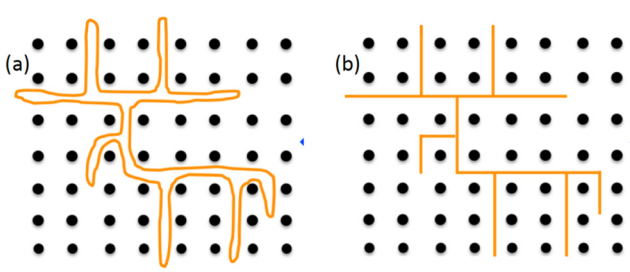

FIG. 4. Double-folded randomly branched lattice animal models for ring polymers. (a) A ring polymer constrained in a matrix of fixed obstacles can be mapped to (b) a randomly branching tree [4,57]. Reproduced with permission from Rosa and Everaers, J. Chem. Phys. **145**, 164906 (2016) [172]. Copyright 2016, AIP Publishing LLC.

can increase their entropy by branching, suggesting that much about the ring systems can be understood by studying random trees [4,58,166–168], which are tightly wrapped by ring polymers [169]. Finally, as systems exhibiting random branching become too dense, rings and trees in the melt state adopt territorial conformations exhibiting the minimal required amount of swelling due to a combination of path swelling and a modification of the branching statistics [28,170–172]. However, we note that such double-folded structures have not yet been identified by experiments [173].

The dynamics of a ring polymer in an array of fixed obstacles was described analytically [58] as the self-similar diffusive transport of the mass stored in smaller side branches of a tree along larger branches and finally along the tree trunk; this model was further confirmed using Monte-Carlo (MC) simulations. Later, the model was extended to include excluded volume interactions in good solvents or at melt densities [174,175], including predictions for rheological properties [174]. Recently, MC simulations of double-folded, randomly branched rings were used to explore the mesoscopic dynamics that emerge from local dynamical modes [176]. However, predictions for the static and dynamic structure factors that would allow for a quantitative comparison with scattering experiments [177–180] are still missing. Nevertheless, we note that the static structure factor for rings in the melt has been developed on the basis of elementary loops and experimentally verified [173].

2. Fractal loopy globule model

If most of the contour length is neatly tucked away in crumpled, double-folded ring sections, then rings can safely open *some* loops *without* violating topological constraints. The decorated loop model [181] and the fractal loopy globule (FLG) model [182] allow double-folds to open up on all length scales in a self-similar way (Fig. 5). As a consequence, smaller loops can penetrate larger ones and the "fat" branched assembly of loops of all sizes gains in entropy compared to skinny double-folded lattice animal configurations (Fig. 4). The self-similarity of loopy globules was imposed by topological constraints of fixed number of loops overlapping with each other on all length scales so that the fractal dimension of nonconcatenated ring polymers is equal to three.

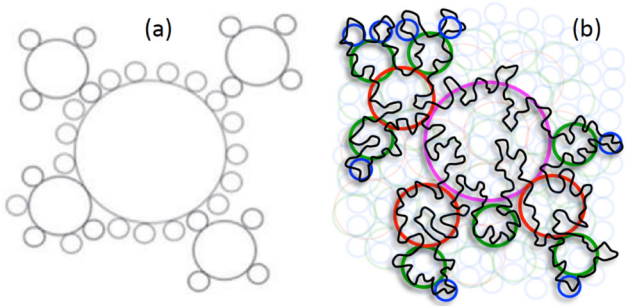

FIG. 5. Theoretical models for ring polymer melts. (a) The decorated loop model [181] and (b) the FLG model [182] allow double-folds to open up on all length scales. Reproduced with permission from Obukhov *et al.*, Europhys. Lett. **105**, 48005 (2014). Copyright 2014, IOP and Ge *et al.*, Macromolecules **49**, 708–722 (2016) [181,182]. Copyright 2016, American Chemical Society.

The dynamics of the FLG model proceeds by a combination of self-similar reptation and constraint release [182]. The stress relaxation modulus $G(t)$ predicted by the FLG model for entangled nonconcatenated rings is

$$G(t) \approx G_e \left(\frac{t}{\tau_e}\right)^{-(d_f-(1-\theta)d_p)/(2d_f+(1-\theta)d_p+\theta)}, \quad \tau_e < t < \tau_{relax}, \tag{1}$$

where G_e is the entanglement plateau modulus for the corresponding linear chain, θ is the tube dilation parameter ($\theta = 1$ corresponds to full tube dilation), d_f is the fractal dimension of a nonconcatenated entangled ring, d_p is the fractal dimension of the primitive path of a ring, τ_e is the relaxation time of an entanglement strand, and τ_{relax} is the relaxation time of a ring [182]. With complete tube dilation ($\theta = 1$) and a fractal dimension $d_f = 3$, the FLG model predicts a power-law stress relaxation function $G(t)$,

$$G(t) \approx G_e \left(\frac{t}{\tau_e}\right)^{-3/7}, \quad \tau_e < t < \tau_{relax}. \tag{2}$$

The power-law stress relaxation behavior has been observed in experiments for low to moderate molecular weight ring polymer melts [5]. In the FLG model, the dynamic behavior is presumed to occur only on length scales larger than the entanglement length or tube diameter of the equivalent linear chain. On smaller length scales, rings behave similarly, albeit not identically, to unentangled chains. The open question is whether such self-similar dynamics continues on *all length and time scales beyond the entanglement length scale*, or whether there is another qualitatively different dynamical process that cuts it off on some large enough length scale. Which of the competing models (randomly branching double-folded model or FLG model) provides a better description of the conformations and dynamics of nonconcatenated entangled ring polymers? The difference between the predictions of these models is not very large, and in order to distinguish between them, careful simulations and experiments are required. A detailed primitive path analysis provided additional insight into these issues [182,183].

Before proceeding, a few comments about the key role of molecular simulations are warranted. As discussed above, simulations play a key role in both testing and validating theoretical models, while also providing critical insight into polymer structure and dynamics at the molecular scale. The following sections discuss key results from molecular simulations, including coarse-grained molecular dynamics (MD) simulations, that continue to inform our understanding of ring polymer systems by complementing and adding to the body of knowledge provided by theoretical models and experiments. As one example, a single-chain slip-spring model was recently developed to describe the behavior of entangled melts of nonconcatenated ring polymers [184].

3. Force-based theory for ring polymer liquids

A statistical mechanical theory for the COM dynamics of dense solutions and melts of flexible and semiflexible rings was recently constructed [185]. This force-level theory focuses on unconcatenated rings and captures the effects of strong intermolecular interactions and topological compaction on ring dynamics. Intermolecular ring-ring packing correlations are determined from the polymer reference interaction site model (PRISM) integral equation theory [186]. The theory enables predictions of the COM diffusion constant D, the longest conformational relaxation time, and the intermediate-time non-Fickian transport of dense ring solutions and melts [185,187]. The central idea is that high molecular weight rings behave like fluctuating soft particles that significantly interpenetrate to a degree that depends on molecular weight, concentration, and backbone stiffness. The interpenetration of neighboring rings imposes dynamic constraints on their motion due to long-lived correlations in intermolecular excluded volume forces [185,187].

In the force-level theory, the new physics enters via correlations of intermolecular forces exerted on ring segments. The theory is described by two key regimes: a "weak-caging" regime and a "strong-caging" regime [49,188]. The onset of the weak-caging regime corresponds to the initial breakdown of the Rouse model as the ring molecular weight increases and interpenetrations begin to play a role on dynamics. In the weak-caging regime, intermolecular ring-ring excluded volume force correlations relax on the longest fractal Rouse timescale, and a molecular weight-dependent slowing down of ring COM diffusion is predicted. A key variable is N_D, which is a DOP that defines the onset of the weak-caging regime and quantifies a dynamic crossover beyond which intermolecular effects are nonperturbative. At the onset of the weak caging regime, the intermediate non-Fickian time-dependence is predicted to change at a DOP around N_e (entanglement DOP), because it is at this scale that single ring conformations crossover from ideal coils to compact globules due to topological effects. The parameter N_D is a function of the macromolecular packing fraction, Kuhn length, chain equivalent N_e or tube diameter, and liquid dimensionless compressibility, which quantifies the amplitude of nm-scale density fluctuations. In the weak-caging regime, the theory predicts the COM diffusion constant $D \sim N_D/N^2$, which differs from the FLG prediction of $D \sim N_e^{2/3}/N^{5/3}$ [182]. Quantitative comparisons with simulations for flexible and semiflexible ring melts and semidilute stiff ring solutions show good agreement [185,187,189] and provide a framework to qualitatively interpret new experimental observations for high molecular weight rings [188]. However, extension of this theory to predict stress relaxation has not yet been achieved, and hence, the existing theory cannot make direct predictions for $G(t)$.

At very high molecular weight, the weak-caging scenario of COM ring diffusion eventually breaks down. To address this regime, a self-consistent strong-caging theory has been constructed for both ring melts and semidilute solutions with variable backbone stiffness [187,188]. The theory predicts a second crossover for $N > N_{on} > N_D$, where N_{on} is a DOP beyond which ring COM diffusion becomes thermally activated (Fig. 6). The theory predicts that $N_{on} \propto N_D$, and systematic analysis of MD data for ring melts over a range of backbone stiffness values found that $N_{on} \approx 30N_D$ collapsed all results onto a universal curve [189]. The specific value of N_{on} and its dependence on molecular model parameters is thus inherited from N_D, and decreases dramatically with increasing backbone stiffness. Drawing on the analysis in recent work [189], Fig. 7 shows how both N_e and N_{on} vary with the underlying chain stiffness in the Kremer–Grest bead-spring model. For the typical range of bead-spring stiffness coefficients $k_\theta/k_BT = 0-5$, the analysis predicts N_{on} varies from 6210 to 90 monomers, or equivalently Z_{on} varies from 138 to 9 entanglements. Physically, the strong-caging

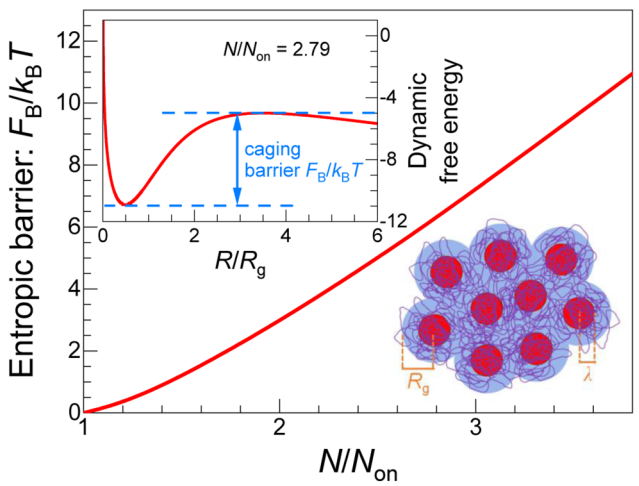

FIG. 6. Entropic activation barrier F_B relative to thermal energy (k_BT) as a function of ring degree of polymerization (DOP) N normalized by the onset value N_{on} [187], where k_B is Boltzmann's constant and T is absolute temperature. Inset: Dynamic free energy in units of thermal energy (k_BT) as a function of the ring COM displacement in units of distance relative to the radius of gyration R_g for a specific value of N/N_{on}, where N_{on} is a DOP beyond which ring COM diffusion becomes thermally activated. In the lower right schematic, λ indicates the entanglement length. Reproduced with permission from Mei *et al.*, ACS Macro Lett. **10**, 1229–1235 (2021) [187]. Copyright 2021, American Chemical Society.

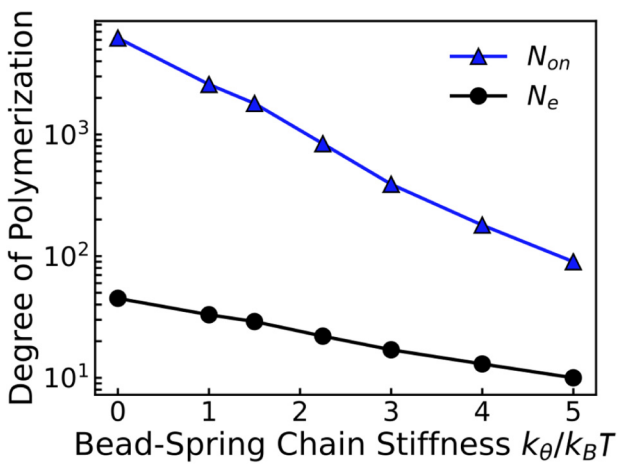

FIG. 7. The dependence of the linear entanglement DOP N_e and the onset DOP for strong caging N_{on} with varying backbone stiffness k_θ/k_BT. Model melts were simulated at a monomer number density $\rho = 0.85\sigma_{LJ}^{-3}$ and $k_BT = 1\epsilon_{LJ}$ [189].

regime corresponds to when the intermolecular force-time correlations acquire a transiently arrested component and long-time dynamics are described by an activated process with an entropic barrier that grows linearly with N (Fig. 6). Recent evidence for a crossover to an exponentially slow regime was observed in ring melt simulations [189]. Moreover, results from NSE experiments showed evidence of a crossover from two different subdiffusive regimes to a Fickian regime in the short time COM diffusion of high molecular weight poly(ethylene oxide) (PEO) rings [190]. However, the mechanistic origins of slow dynamics in high molecular weight rings are not yet fully understood (Sec. III C 4).

B. Current state of the field: Experiments

1. Stress relaxation & ring purity

Understanding the rheological properties of ring polymer melts and concentrated solutions is a frontier problem in polymer physics. As discussed in Sec. I, the development of LCCC (critical condition for linear chains) provided a method for enhanced purification of synthetic rings, setting the state of the art for preparing and characterizing ring polymer melts [53,54]. Using LCCC-purified samples of PS rings, it was found that rings with $Z = M_w/M_e$ values corresponding to moderately entangled conditions for the equivalent linear chains ($Z < 11$) do not exhibit an entanglement plateau but rather show power-law stress relaxation behavior (Fig. 8), such that $G(t) \sim t^{-\alpha}$, where $0.4 \leq \alpha \leq 0.5$,

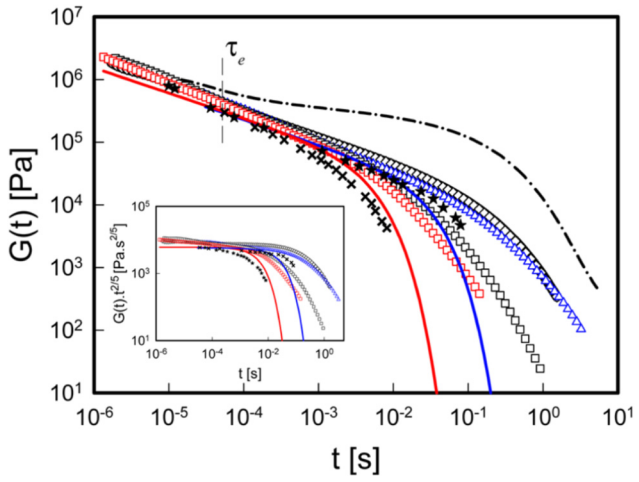

FIG. 8. Stress relaxation modulus $G(t)$ for polyisoprene (PI) rings and PS rings at $T - T_g = 65\,^{\circ}\mathrm{C}$. Data showing experiments from PI rings $M_w = 38$ kDa (red squares, $Z = 6.1$), PI 81 kDa (blue triangles, $Z = 12.9$), PS 160 kDa (black squares, $Z = 9.3$), PS 198 kDa (black diamonds, $Z = 11.5$). Stars and crosses are results from MD simulations on coarse-grained bead-spring chains with $Z \approx 3.6$ and 14.4 [49]. Red and blue lines are predictions from the lattice animal model for PI 38 kDa and PI 81 kDa rings, respectively, and predictions from the FLG model are similar [182,195]. The dashed-dotted line is the relaxation modulus for the PI 81 kDa linear polymer, showing an entanglement plateau. The Rouse time for entanglements τ_e of the linear PI 81 kDa is shown. Inset: Scaled version of the same plot, without the linear polymer data. Power-law scaling is consistent with the lattice animal model such that $G(t) \sim t^{-0.4}$. Reproduced with permission from Pasquino *et al.*, ACS Macro Lett. **2**, 874–878 (2013) [191]. Copyright 2013, American Chemical Society.

consistent with predictions from the lattice animal model $G(t) \sim t^{-0.4}$ (see Sec. III A 1) [5,191]. Note that the power-law exponent of $\alpha = -0.4$ is indistinguishable experimentally from -0.43, the FLG exponent, as discussed in Sec. III A 2.

It was reported that the viscoelastic properties of rings (including the stress relaxation power-law exponent α) are extremely sensitive to the presence of linear chains, suggesting great sensitivity of rheological properties to linear chain contaminants even below linear chain volume fractions 0.001 (corresponding to 0.1% v/v) [5,47,51,191,192]. These findings were confirmed by MD simulations, which, however, provided qualitative confirmation that the sensitivity of rings to linear chains was less significant than that reported experimentally [6]. These results prompted concerns about the stability of the synthetic rings because the amounts available after LCCC fractionation are very small (typically less than 100 mg), and the continuous deformation and thermal treatment of these samples during rheological characterization may cleave the ring backbone, opening the ring and resulting in linear chain contamination. Nevertheless, the power-law stress relaxation behavior for ring melts was further observed with different polymer chemistries (e.g., PS, 1,4-polyisoprene, and polybutadiene rich in vinyl content) in the range $3.9 \leq Z \leq 22$ [191–194]. Prior work has shown that the stress relaxation modulus $G(t)$ [or complex modulus $G^*(\omega)$] in LCCC-purified ring polymer melts is well described by the ring Rouse model for relatively low molecular weight rings [193].

2. Threading interactions

The power-law stress relaxation behavior of ring polymer melts ($Z \lessapprox 22$) at intermediate times or frequencies [195,196] is well described by the FLG model (see Sec. III A 2) [182]. However, analysis of the stress relaxation function $G(t)$ with the FLG model and comparison with simulations suggests the occurrence of slow relaxation modes at long times. Available evidence from simulations indicates that these modes are collective beyond the level of single polymer molecules [151,197,198]. Their exact molecular origin is still debated but could arise due to linear chain contamination, ring-linear threading, and/or ring-ring threading [199].

Ring-ring and ring-linear chain threading has been confirmed experimentally and by simulations and modeling in the melt [200–206] and in concentrated solutions [197,207–211]. The case where small fractions of rings are added to a linear chain matrix is of particular importance because ring purity is not an issue, yet the rheological implications can be significant, as noted from prior work in the 1980s [47,51]. A recent joint experimental-modeling investigation indicated that the addition of up to 30% PS rings with $Z = 11$ to the respective linear matrix increases its viscosity by up to a factor of 2 and can slow the ring relaxation time by orders of magnitude due to the constraint release effects of the linear chains on the rings [202]. Qualitatively similar experimental observations were recently reported with other polymer chemistries [poly(3,6-dioxa-1,8-octanedithiol) or polyDODT rings] [212] and poly(ethylene oxide) [201]. Threading has been directly observed in single molecule

experiments [197] and corresponding simulations of semidilute solutions of ring-linear blends [198]. These studies show that the presence of threading can be inferred from large fluctuations in ring extension as threads are convectively released during nonequilibrium flow (Sec. III B 6).

3. New ring chemistries to address long-time dynamics

Given challenges in preparing high molecular weight synthetic rings using traditional methods, alternative chemistries have been developed. In a recent study, cyclic poly(phthalaldehyde), cPPA, was prepared in large amounts (>1–10 g scale) without linear contaminants due to the metastable backbone chemistry that rapidly unzips and depolymerizes to monomer if the ring backbone is cleaved (Sec. III C 2) [188]. Ring polymers up to $Z = 59$ were prepared in concentrated samples, and evidence of a slowdown in relaxation dynamics (or an intermediate frequency "plateaulike" relaxation behavior) appeared for rings with a linear equivalent of $Z = 26$ and was clearly evident for $Z = 59$ [Fig. 9(a)] (Sec. III C 4). Stress relaxation experiments for cPPA rings show agreement with the predicted power-law slope in $G(t)$ from the FLG model for $Z < 26$, followed by significant deviation and a smaller magnitude slope than predicted by the FLG model with full dynamic dilution for $Z = 59$ [Fig. 9(a), inset]. However, the magnitude of the apparent plateau modulus for cPPA rings ($Z = 59$) is nearly identical to the plateau modulus G_e of entangled linear cPPA with ($Z = 10$). Due to the cationic polymerization method required for synthesis, cPPA ring samples are relatively polydisperse, and the role of dispersity on the mechanical properties is not yet clear.

Simulations of Kremer–Grest melts were also used to determine $G(t)$ while systematically varying the ring DOP (number of beads) $N_b = 100 - 6400$ at fixed backbone stiffness $k_\theta = 1.5$ [Fig. 9(b)]. Simulations show that the self-similar modes observed in rings with $Z \leq 114$ are preserved, with the observed new behavior (appearance of a foot with lower slope) appearing at longer times and corresponding to a lower value of modulus compared to the linear rubbery plateau modulus. Molecular simulations of high molecular weight rings $N_b = 6400$ ($Z = 229$) with flexible backbones ($k_\theta = 1.5$) show evidence of a slowdown in stress relaxation with a smaller magnitude power-law slope than predicted by the FLG model with full dynamic dilution [Fig. 9(b), inset]. This behavior coincides with a dramatic slowdown in ring COM diffusion that prevented carrying out brute-force diffusion in simulations. Finally, an additional set of MD simulations was performed by varying backbone stiffness $k_\theta = 0 - 4$ at fixed $N_b = 1600$ [Fig. 9(c)]. Simulations showed a monotonic decrease (slower relaxation) in the steepness of the power-law slope of $G(t)$ with increasing stiffness k_θ. Simulated ring melts display a continuous change in terminal power-law that crosses through the regime of values predicted by the FLG model as chain stiffness is varied, which is consistent with a crossover from flexible to semiflexible behavior. This work suggests that slow relaxation modes may become important for high molecular weight rings, but additional work is needed in terms of experimental characterization and molecular simulations.

In a second study, a series of poly(3,6-dioxa-1,8-octanedithiol) or polyDODT polymers was prepared under conditions to produce linear (LDODT), cyclic (RDODT), and linear-cyclic mixtures (LRDODT) [212]. Ultrahigh molecular weight rings were prepared reaching $Z \approx 300$, with claimed linear chain content based on LCCC fractionation of less than 2% for the highest molecular weight rings [212]. Based on a new catalytic activity assay for purity and an 800 MHz NMR characterization and detection for chain ends, the authors reported less than 2% linear contaminants for $Z \approx 300$ RDODT samples, but it is not yet clear how this compares to standard characterization methods using LCCC. PolyDODT is amorphous ($T_g < -50\,^\circ$C) and highly flexible (entanglement molecular weight $M_e \approx 1850$ g/mol for LDODT). LVE experiments on seven different RDODT

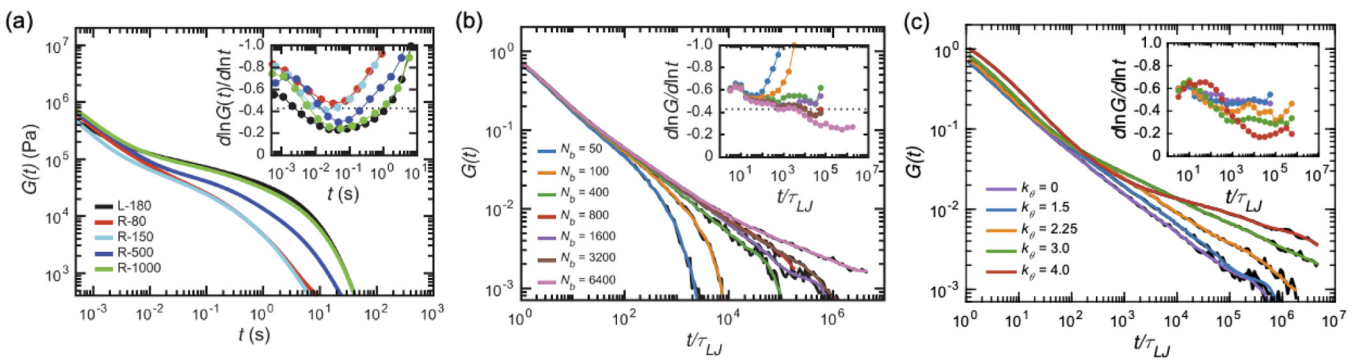

FIG. 9. Stress relaxation and LVE behavior of linear and ring polymer systems using new chemistries. (a) Stress relaxation $G(t)$ master curves from experiments on entangled linear and concentrated cPPA samples as a function of molecular weight. The inset shows derivative slope of $G(t)$ curves, and the dashed line indicates the FLG prediction of $G(t) \propto t^{-3/7}$. Estimates of equivalent $Z = M_w/M_e$ values for the equivalent linear chain for linear samples L-180 (180 kDa) and ring samples R-80 (80 kDa), R-150 (150 kDa), R-500 (500 kDa), and R-1000 (1 MDa) samples are $Z = 10, 4.3, 8.6, 26, 59$, respectively. (b) Stress relaxation $G(t)$ master curves from MD simulations of ring polymer melts as a function of ring degrees of polymerization or number of beads N_b. The inset shows power-law slopes of $G(t)$ curves. MD simulation parameters correspond to the canonical Kremer–Grest flexible backbone model with $k_\theta = 1.5$. Equivalent N/N_e values for MD simulations as a function of N_b and stiffness $k_\theta = 1.5$ are as follows: $N_b = 50, 100, 400, 800, 1600, 3200, 6400$ corresponds to $Z = N/Ne = 1.8, 3.6, 14.3, 28.6, 57.1, 114, 229$, respectively, for the equivalent linear chain. (c) Stress relaxation $G(t)$ curves from MD simulations of ring polymer melts with $N_b = 1600$ for varying backbone stiffness k_θ. The inset shows instantaneous power-law slopes of $G(t)$ curves. All melts are simulated at $\rho = 0.85$, and the Lennard-Jones (LJ) timescale is $\tau_{LJ} = \sqrt{m\sigma^2/\epsilon}$, where m is the bead mass and σ and ϵ are the LJ length and energy scales, respectively. Reproduced with permission from Tu *et al.*, ACS Polymers Au **3**, 307–317 (2023) [188]. Copyright 2023, American Chemical Society.

melts and eight of their solutions show a rubbery plateau in the intermediate frequency region for $Z > 15$. Extensive rheological data obtained with melts and solutions generally confirmed the evolution of an intermediate-frequency rubbery plateau as the molecular weight increases. In addition, upon dilution of the highest molecular weight rings (to a concentration corresponding to $Z < 15$), the rubbery plateau disappeared and the relaxation dynamics quantitatively matched the shapes of the LCCC-fractionated PS systems of similar Z-values. However, these interesting results appear to contradict recent experiments with well-characterized polybutadienes [194]. In this context, the authors referred to these polymer samples as "putative" rings [212]. For the ultrahigh molecular weight ring samples, a second, low-frequency plateau in G' was reported and identified as a slow mode attributed to deep ring-ring interpenetrations. Nevertheless, quantitative analysis of the terminal relaxation time is not yet fully understood (Sec. III C 4) [160,191,200,213].

4. Zero-shear viscosity

Prior work reported that linear chain contaminants significantly affect the ring melt viscosity at concentrations well below their overlap concentration [6], in qualitative agreement with the experimental results [5]. Analysis of simulation results for zero-shear viscosity η_o versus molecular weight M of flexible coarse grained rings yielded a power-law scaling relation of $\eta_o \propto M^{1.4}$ for $Z < 30$ [49]. Moreover, an increase of viscosity by 10% occurred at a volume fraction of linear chains of ≈0.01 in simulations, whereas experimentally a twofold viscosity increase was reported for a fraction of ≈0.0007 [6]. These results suggest that ring purity is a significant albeit subtle issue. Subsequent atomistic simulations compared with limited PEO data suggested a molecular weight power-law scaling of viscosity as $\eta_o \propto M^{1.7}$ for $Z < 12$ [214], however, the increase of viscosity appeared earlier in rings compared to linear chains. Further analysis of LCCC-purified PS data, including those of [5], yielded different values of the zero-shear viscosity η_o, which was described by slow modes at low frequencies or long times [196,200]. These complications create some confusion and point to uncertainties regarding the true zero-shear viscosity value of pure rings, as summarized in [215] and [212]. Zero-shear viscosity was also studied for a few different chemistries, though the data were quite scattered, given the issues discussed above regarding putative linear chain contamination. Nevertheless, the η_o were more consistent than prior experimental data, and their molecular weight dependence seemed to conform to a power-law exponent larger than 1.0 (for $Z < 13$), consistent with simulations and predictions from theory [191].

In another study, a series of LCCC-fractionated PS samples ($0.7 \leq Z \leq 14$) was characterized, revealing a molecular weight power-law scaling of viscosity as $\eta_o \propto M^{1.0}$ over the range $0.7 \leq Z \leq 5$, which is a weaker dependence on M compared to prior experiments and simulations [193]. Later, the same group presented an approach to obtain highly pure ring samples by fractionating the highest molecular weight ring sample (240 kg/mol or $Z \approx 14$) multiple times, measuring the viscoelasticity of the ring-linear blends at different linear contaminant concentrations and extrapolating to zero linear chain concentration [192]. These results showed that the stress relaxation modulus $G(t)$ for the highly purified $Z \approx 14$ sample cannot be fully described by the ring Rouse model, and there were contributions from weak but slow additional relaxation modes (Sec. III C 4). In addition, the resulting viscosity value was found to be much lower than that of the originally LCCC-fractionated sample [193], which raised concerns regarding the level of purity of different samples achieved by different LCCC fractionations in the literature and questioned the degree to which the respective experimental data refer to the properties of pure rings. A recent compilation of viscosity data, in particular, those of [192] and [193] suggested a molecular weight power-law scaling of viscosity as $\eta_o \propto M^{1.0}$ (for $Z \lessapprox 10$) [212,213,215], in contrast with earlier reports [49,191,196,214]. Finally, the recent rheological characterization of putative polyDODT rings showed that samples with $Z > 10$ suggests a molecular weight power-law scaling of viscosity as $\eta_o \propto M^{5.8}$ [212]. However, careful characterization of these samples and more experiments are necessary before drawing more definitive conclusions.

In view of the above results and contradictions, an effort was made recently to reanalyze the available data with LCCC-purified rings of different chemistries, including PSs, polyisoprenes (PIs), and polybutadienes [216]. These results showed that all data exhibited a $G(t)$ with a slope conforming to the FLG model prediction, but they exhibited slow modes as well. Analysis of the data by integrating the $G(t)$, or using simply the FLG model or the FLG combined with slow modes [200] has yielded a rigorous determination of experimental zero-shear viscosities and respective errors and relative contributions of different slow modes (attributed to ring-ring and ring-linear threading). The emerging picture is the following: below the entanglement threshold, the zero-shear viscosity exhibits Rouse scaling with a power-law dependence on molecular weight with an exponent of 1. Above the entanglement threshold, there is a moderately entangled regime with an exponent clearly above 1 (experimental data on PS indicate a value of 1.3) (Fig. 10). The extent of this regime is yet unknown, but the largest Z value examined in experiments is $Z \approx 22$ and in simulations is $Z \approx 60$. In addition to the results discussed above [160,194,212], another regime showing slow dynamics has been postulated (Sec. III C 4). However, additional work is needed to validate this picture.

5. Structure and dynamics: NMR and neutron scattering experiments

A series of PEO rings up to $Z = 44$ was synthesized and characterized in sufficient amounts to perform SANS, NSE, and pulsed field gradient-nuclear magnetic resonance (PFG-NMR) experiments [178,180,190,201,217]. Results for PEO rings with $5 < Z < 44$ revealed the compact structure of ring polymers in the melt such that $R_g \propto N^{0.39}$, which reflects an effective crossover exponent that differs from the

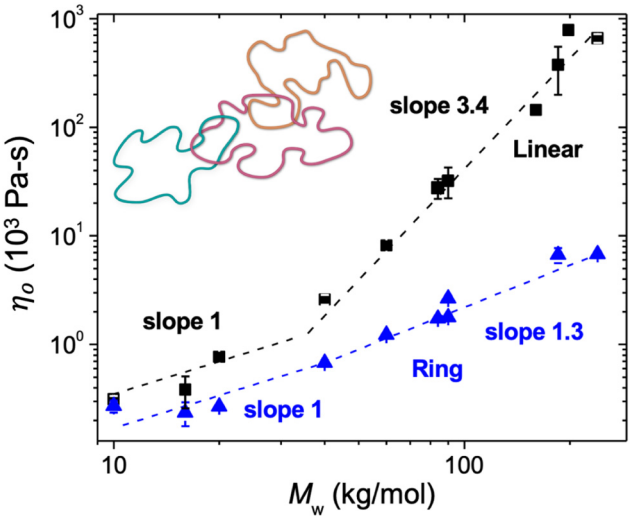

FIG. 10. Zero-shear viscosity of linear PS samples and LCCC-fractionated PS rings as a function of molecular weight (at 160°C). Different symbols refer to different origins of the data (see [216]). The lines with slopes of 1.0 and 1.3 denote the unentangled and moderately entangled regimes for rings, respectively. The cartoon illustrates partially interpenetrated rings. Reproduced with permission from Peponaki *et al.*, Macromolecules 57, 7263–7269 (2024) [216]. Copyright 2024, American Chemical Society.

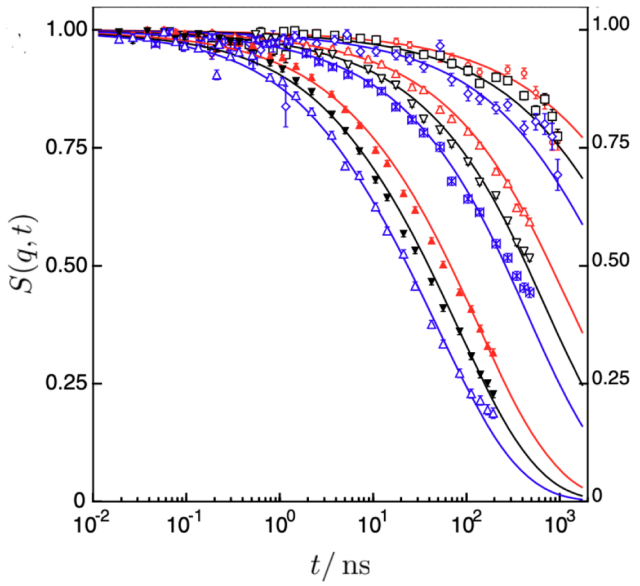

FIG. 11. NSE experiments were used to address the intraring pair correlation function (single chain dynamic structure factor) from PEO ring polymer melts with molecular weights of 87.3 kDa at 140 °C; the q values are 0.042, 0.049, 0.055, 0.069, 0.078, 0.086, 0.11, 0.12, 0.13 Å^{-1}. The solid lines present the best fit using a scaling model based on the FLG assumption for the internal ring motion [182], COM mean-square displacement (MSD) extrapolated from experiments on lower molecular weight rings (10 and 20 kDa) [180,190], and structural parameters determined by SANS [173]. Reproduced with permission from Kruteva *et al.*, Phys. Rev. Lett. **125**, 238004 (2020) [190]. Copyright 2020, American Physical Society.

predicted asymptotic results for crumpled globules of $R_g \propto N^{1/3}$. Scattering studies provided a detailed analysis of the loop structure in rings, indicating Gaussian structures at small length scales only. The loop displacement was consistent with predictions from modeling, and the best agreement was found with the FLG model for $Z = 20$ and 44. Threading of rings by linear chains was also reported, and the PFG-NMR data revealed the appearance of two diffusive modes in ring-linear mixtures [178,180,201,217]. The NSE data with $Z = 44$ did not reveal any unambiguous evidence of the emergence of a rubbery plateau in the range of parameters studied in this work [180,190], though it is thought that the presence of the intermediate-frequency plateau in $G(t)$ may depend on chemistry and backbone flexibility of the rings [188,189]. The structure and local dynamics for PEO rings up to $Z = 10$ were confirmed by atomistic MD simulations [218]. Recently, an analysis of NSE results on relatively large rings was well described by the FLG model [173,190]. Figure 11 shows that the best fit of the dynamic data over short timescales is achieved using the FLG model (Sec. III A 2). Moving forward, additional characterization of the high molecular weight rings for polyDODT and cPPA chemistries demonstrating a number of interesting rheological effects should be studied by SANS and NSE to understand the relation between macroscopic and microscopic properties.

6. Nonlinear rheology

Concerning nonlinear rheology, there is some limited evidence from state-of-the-art experiments and simulations clearly showing that unconcatenated ring melts exhibit drastically different responses compared to their linear counterparts. Bulk rheology experiments using moderately entangled rings with Z values comparable to the equivalent linear chains ($Z = 5$ and 11) show weak shear thinning (power-law scaling of shear viscosity with shear rate $\dot{\gamma}$ such that $\eta \propto \dot{\gamma}^{-0.57}$) (Fig. 12) [195,220]. Nonlinear microrheology experiments on DNA rings similarly show weak shear thinning (power-law scaling of shear viscosity with shear rate $\dot{\gamma}$ such that $\eta \propto \dot{\gamma}^{-0.37}$) [221]. These results are in sharp contrast to their linear entangled counterparts, which show an exponent of −0.7 for microrheology experiments on linear DNA polymers [221] and between −0.8 and −0.9 from bulk rheology experiments on synthetic polymers. Notably, this experimental dependence of viscosity on shear rate was confirmed by MD simulations as well by theoretical modeling, compared in Fig. 12(b) [195]. The latter is based on the development of the shear slit model which involves two distinct length scales associated with shear blobs in the velocity gradient direction ξ_s and (smaller) tension blobs in the flow direction ξ_t, shown in Fig. 12(a). Dissipation that contributes to viscosity, which takes place via modes in the velocity gradient direction that are constrained to within the scale of shear blobs. These modes are uncoupled from the longer wavelength modes that do not contribute. Experiments, modeling, and simulations also confirm the validity of the Cox–Merz rule.

An important aspect of the shear slit model is that it provides scaling predictions for the normal stresses as a function of the shear rate [195,196]. The first and (negative) second normal stress differences N_1 and $-N_2$ are controlled by the tension and shear blobs, respectively, and their associated power-law exponents of their shear rate dependence at rates exceeding the inverse terminal time are around 0.6 and 0.4 [195,196]. Experimental data on normal stresses are more

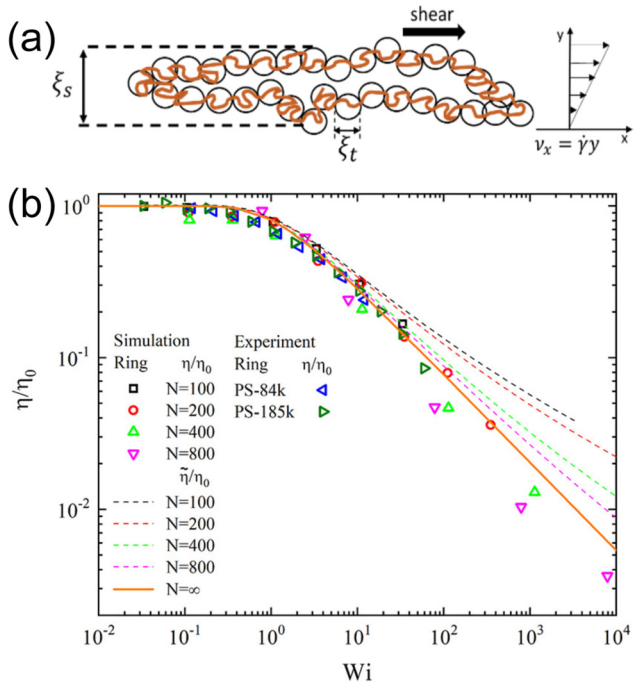

FIG. 12. Ring dynamics and rheology during nonlinear shear. (a) Schematic of a ring polymer in shear flow. Two distinct length scales are considered in the context of the shear slit model including shear blobs in the velocity gradient direction ξ_s and tension blobs in the flow direction ξ_t. (b) Normalized steady-state viscosity vs shear Wi from MD simulations, experiments, and shear slit model predictions of flowing ring melts. Reproduced with permission from Parisi *et al.*, Macromolecules **54**, 2811–2827 (2021) [195]. Copyright 2021, American Chemical Society.

fragmented but suggests that the ratio of second to first normal stresses $-N_2/N_1$ is larger for rings compared to their linear counterparts [196]. The available experimental data conform to this general picture [196] but are limited, and there is clearly a need for more data with different molecular weight ring polymers. The same holds for the simulation results, which are insightful and support the available data [222,223].

Moderately entangled rings ($Z = 11$) have also been subjected to uniaxial extensional fields and found to exhibit unique response, markedly different from that of linear chains [219,224]. In particular, both linear and ring polymers strain-harden, but the hardening of rings is much stronger. Importantly, the extensional viscosity of the rings exhibits a dramatic thickening at very low stretch rates, a regime where the viscosity of the respective linear polymer is higher but exhibits extensional thinning with the well-known slope of -0.5 [224]. This unexpected phenomenon occurred even during very weak elongation flows (the range of stretch rates below the inverse terminal time of the ring, $Wi < 1$), as can be seen in the start-up flow curves for the extensional viscosity in Fig. 13(a). This behavior was explained using MD simulations, which unambiguously showed that under these conditions, separate rings can spontaneously interlock, i.e., they form topological links known as hitch knots that connect them into supramolecular chains [Figs. 13(b)–13(d)] [219]. The experimental data also indicated extensional thinning at high stretch rates, identical to that of entangled linear polymers (their precursors) [224]. These trends were also reproduced by the MD simulations, which were able to resolve steady-state viscosities at even the very low rates where experiments could not.

The nonlinear shear rheology of symmetric ring-linear polymer blends (of the same $Z = 11$) with low ring fraction (15% rings) appeared to be dominated by the contribution of the linear chains. A key result is the strong shear thinning viscosity [211], with a thinning exponent nearly identical to that of linear polymer melts [196]. The same blend with different ring fraction (30% rings) exhibited a peculiar transient response in uniaxial extension which reflected the topological ring-linear interactions [225]. Experiments showed that the blend exhibited strain hardening, which was more

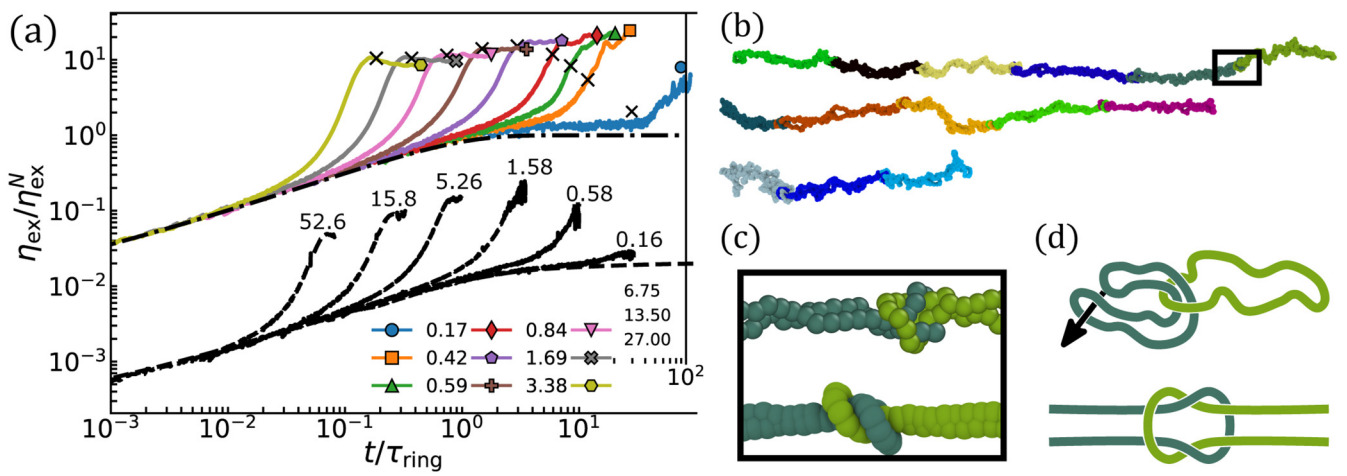

FIG. 13. Ring dynamics and ring-ring linking in ring melts in elongational flow. (a) Startup extensional stress growth curves [219]. Extensional flow predictions from MD simulations (solid color lines) reproduce the anomalous thickening of the viscosity at low *Wi* observed in experiments (dashed black lines). Simulated curves are marked with an X at the strain where experimental filaments failed, capturing the nonmonotonic terminal viscosity measured by experiments. (b) A train of hitched rings in extensional flow. (c) Close-up of an individual hitch knot from (b) before and after primitive path analysis. (d) Illustration of how hitch knots between rings form and are stabilized by an applied tension and can transmit forces even though the rings are not linked from a strictly topological point of view. Reproduced with permission from O'Connor *et al.*, Phys. Rev. Lett. **124**, 027801 (2020) [219]. Copyright 2020, American Physical Society.

substantial than that of its linear component and less than that of the ring. However, unlike its components, the blend exhibited an overshoot in the extensional stress growth coefficient, without reaching steady state. With the help of MD simulations and *in situ* SANS measurements, this overshoot was explained as the consequence of a transient threading-unthreading transition of the rings embedded in the linear network. Up to the overshoot, the rings deformed affinely and contributed to stronger elongation of the linear chains in the blend compared to their pure melt, whereas beyond the overshoot, unthreading dominated the response of the blend [225]. Overall, these findings show how rings can alter the rheology of linear polymers and call for more data from experiments and simulations, to establish scaling relations, as well as understand the role of molecular weight and composition in the case of ring-linear blends.

In semidilute solutions of ring/linear blends, single-molecule experiments [197] and corresponding simulations [198] found that ring polymers undergo large fluctuations in extension in background solutions of majority linear chains [151] and ring-linear blends [197] in extensional flow. Fluctuations in ring extension generally arise due to ring-linear threading events [151], demonstrating the coupling between loopy topology and intermolecular interactions in flow. In semidilute solutions of ring-linear blends, ring relaxation was characterized from high extension, and transient and steady-state stretching dynamics were studied in extensional flow for a series of ring-linear blends with varying ring fraction [197]. Results showed unexpected heterogeneity in ring stretching dynamics of ring-linear blends with multiple molecular subpopulations for ring relaxation, in addition to large conformational fluctuations for rings in a steady extensional flow [197]. A unique set of ring polymer conformations were observed during the transient stretching process, which highlights the prevalence of molecular individualism that arises, in part, due to intermolecular interactions in ring-linear polymer blends [197]. Experiments were complemented by Brownian dynamics (BD) simulations of rings in ring-linear blends with intra- and intermolecular HI and showed that, quite unexpectedly, the large conformational fluctuations of rings arise largely due to HI-driven disturbances to the local extensional flow field instead of being solely dominated by ring-linear topological interactions [198]. Finally, in concentrated solutions, single molecule DNA diffusion experiments at equilibrium have shown that the COM diffusive motion of rings is hindered in solutions of linear chains compared to background solutions of rings due to ring-linear threading interactions [155–157].

7. Glass transition temperature of ring polymers

In addition to the rheological properties of ring polymers, understanding the glass transition temperature is essential for materials applications. Linear polymers are known to exhibit a significant decrease in the glass transition temperature T_g upon decreasing molecular weight. In contrast, the molecular weight dependence on T_g for ring polymers is not fully understood. As discussed below, prior work has reported that the T_g values for rings can show decreases, increases, or no changes as the molecular weight is decreased, but in all cases, smaller magnitude T_g changes are observed compared to linear counterparts. In the case of linear polymers, rheological properties are normally compared at a temperature increment above the nominal glass transition temperature T_g. In some cases, prior literature does not explicitly state T_g values for ring polymers. In such instances, the results are typically given at a reference temperature such as $T_g + 50^oC$ by using the T_g value of the linear chain counterpart, which is used to compare the dynamic properties or viscosities between linear and ring systems. In the case of linear chains, a significant amount of prior literature has reported the molecular weight dependence of the T_g, which is often considered conceptually in terms of conformational entropy or free volume. To first order, both of these frameworks suggest that there should be little to no effect of molecular weight on T_g for rings, either because the conformational entropy of the chains is only weakly dependent on molar mass to low molecular weights or because rings have no free ends to contribute free volume to the melt. Therefore, it is of fundamental interest to examine the molecular weight dependence of T_g for low molecular weight ring polymers.

Early work from Semlyen and co-workers showed that low molecular weight ring polymers exhibit different behavior compared to their linear counterparts using PDMS rings with M_n between 500 and 24 370 g/mol [226]. This work showed that rings and linear chains exhibit a qualitatively different dependence of T_g on M_n. The linear chain T_g depends nearly linearly on $1/M_n$, as expected from free volume arguments [227] and consistent with the expectations of conformational entropy [228,229]. In 1985, Roovers published data suggesting a weaker reduction in the T_g values of PS rings relative to linear analogs as molecular weight decreased [230], but commented "The reason for the residue [residual] decrease of T_g with decreasing molecular weight of the rings is not known," indicating the expectation that rings should not show a significant change in T_g as the molecular weight decreased. However, Semlyen and co-workers [226] found that T_g increased as M_n decreased. Subsequent work from McKenna *et al.* [43] indicated that the Vogel–Fulcher–Tammann temperature T^∞ of the rings, including the low molecular weight rings, was similar to that of the high molecular weight linear PS samples, though there was evidence that T^∞ increased for the lowest molecular weights. At that time, however, it was unknown if the results for PDMS and PS were specific or universal. Additional work [231,232] reported that the upturn in T_g at low molecular weight rings may be followed by a subsequent decrease, with one study suggesting that the peak in T_g may be due to effects of the choice of ring closure moiety in low molecular weight rings.

Recent work on PS rings examined the role of linear chain contamination, suggesting small decrease in T_g of purified rings as molecular weight decreases [233]. Additional work on PS rings reported that the T_g values increase at low M_n, similar to PDMS rings [234]. Interestingly, this work also reported that the specific volume of linear and ring polymer samples increased as a function of M_n, suggesting that conformational entropy plays an important role in the glass formation of rings. On the other hand, multiple prior studies

[43,235–237] on PS that suggest essentially no change in T_g values for rings as molecular weight decreases, yet other studies have reported decreases in T_g at low M_n values [238–240]. Recent work by Song *et al.* [241] used MD simulations to determine the relationship between T_g and M_n for rings, with results suggesting a nearly constant T_g vale for rings down to low molecular weights. Based on these studies, at least from an experimental perspective, the role of linear chain contamination on T_g values for rings remains a topic of investigation. Broadly, there is a need for additional experiments on purified ring samples and further exploration of theories that might provide insights into the impact of the ring architecture on the T_g values of rings and the role of ring-closure moieties on ring stiffness (conformational entropy) or free volumes at low M_n.

C. Emerging challenges with melts and dense solutions of synthetic rings

1. Universality

For linear and branched polymers without loops, dynamic entanglement effects are universal, i.e., one observes the same behavior with similar effective contour length and overall chain architecture independent of details of the molecular structure on monomeric length scales [1,2]. To a lesser extent, the behavior of intrinsically flexible chains depends (at least) on the number of Kuhn segments per entanglement length. Of course, this picture of entanglements changes slightly for bottlebrush or dendronized polymers with relatively large molecular backbone thicknesses. It is not yet clear if quantitative predictions require atomistic simulations or if all universal aspects are captured by coarse-grained models describing chains on the Kuhn length scale [183]. Material-specific tube diameters or obstacle densities can be inferred via primitive path analysis (PPA) [242–247] by simultaneously reducing all polymers to a minimum set of lines with the same topology [248,249] corresponding to pairwise topological interactions [250]. Numerical PPA results are in good agreement with entanglement lengths inferred from rheological experiments for a wide range of polymeric systems [251].

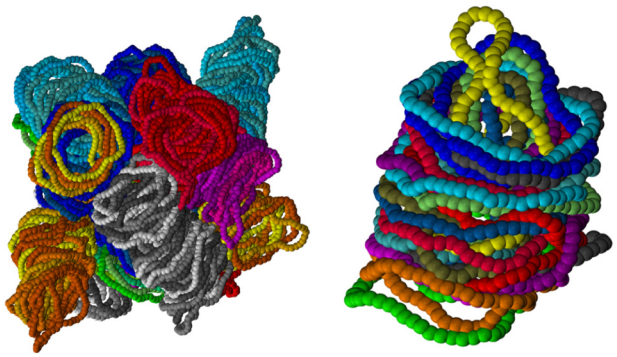

FIG. 14. Snapshots of conformations of nonconcatenated semiflexible rings ($N = 50$, monomer density = 0.4, persistence length $\approx 7.5\sigma$, where σ is the Lennard-Jones length scale) from molecular simulations of concentrated ring solutions. Simulation results show that rings arrange into complex mesophases containing columnar structures of stacked rings where oblate rings can be penetrated by bundles of prolate rings [254,255,258].

It is not yet clear whether the length scale controlling the static properties of rings scales proportionally with the length scale controlling the dynamics of linear chain analogs [6,252]. Atomistic simulations might thus turn out to be even more important for rings [177,200] than linear chain systems. SANS experiments on a set of rings of different molecular weights showed that the size of the elementary loop does not depend on the ring molecular weight and is close to the entanglement length of the corresponding linear chain [173]. In addition, it is not yet clear if the standard dynamical entanglement length [251] is relevant in the more complex mesophases of semiflexible rings [253] that form because the strong energetic penalty for crumpling favors interpenetration, clustering, and stacking of rings (Fig. 14) [254,255]. For such systems, physical properties such as a nonlinear bending rigidity and the ability to kink [36] might be important. Recent simulations have shown that helicity in isolated polymers can affect the topological chirality of polymer knots [256], which suggests that extremely interesting phenomena and topological features could arise for helical polymers. Future studies could address such challenging problems.

As an additional probe into the universality of topological effects, it might also be interesting to explore the structure and dynamics of ring polyelectrolyte solutions such as ring DNA molecules to understand if such phenomena can shed new light on the poorly understood behavior of linear entangled polyelectrolytes [257].

2. Ring purity and high molecular weight rings

Achieving high-purity ring samples and developing accurate and precise methods to characterize sample purity remain a major challenge in ring polymer physics. LCCC is an indispensable tool and arguably the best available method for enhancing the purity of synthetic ring polymer samples, but it is not easy to use and is only available in a few labs. Moreover, although useful, the LCCC method does not generate perfectly pure ring polymer samples and has been shown to yield purified rings with linear contamination levels between 0.1% and 4.5% for PS [192], and possibly up to 6% for different chemistries such as polyDODT [259], which can influence the dynamics and rheology of ring samples. On the other hand, rings with some amount of linear chains may be useful for other studies, for example, when considering the properties of majority linear polymer samples with small fractions of rings [202]. The systematic characterization of rings, including the new chemical families of rings, in the dilute solution and different solvents is important as discussed above. PS rings from the 1980s were synthesized in theta or good solvents, and the more recent samples were prepared in good solvent. Knotting is another concern, and careful analysis of the form factor at different conditions is important. There is limited work with the LCCC fractionated rings on these topics, but available studies show differences depending on the solvent [82]. Nevertheless, additional work needs to be done, especially in view of recent simulations [114].

Some important considerations for preparing ring samples and characterizing ring purity include: (i) deuteration as a function of molecular weight: it is known that deuteration may induce enthalpic effects [260]. However, published data for PEO ring melts up to $Z = 44$ show that the Flory–Huggins parameter values in a blend of deuterated and hydrogenated polymers were negligible. Similar behavior is expected for polybutadiene, but the behavior for extremely high molecular weight rings (e.g., polyDODT rings with $Z \approx 300$) is unknown. (ii) Development of protocols of sample preparation: it is essential to ensure that ring polymers are prepared in equilibrium states, and this is particularly important for polymers with high glass transition temperatures [261]. Blending in the solution and subsequent freeze drying appears to be a reasonably safe method to achieve equilibrium, though it is important that the rate of drying does not inhibit internal relaxation.

A second open challenge relates to the synthesis of high molecular weight ring samples including new ring chemistries. The vast majority of rings synthesized by anionic polymerization have been prepared with relatively small Z values corresponding to the linear chain analogs ($Z \lessapprox 44$) and are only available in small amounts (e.g., PEO, PS, polybutadiene, and PI). Polybutadiene (1,4-addition) would be particularly useful for NSE experiments and rheology; indeed, a recent study with polybutadiene rich in vinyl content and $Z = 22$ suggests this system could provide a path forward [194]. Extremely high molecular weight polymers prepared using new chemistries (e.g., cPPA or polyDODT) would be highly interesting in studying short timescale dynamics, because the COM diffusion will be well separated in time compared to the internal mode relaxation [188]. Additional characterization and experiments with a broader range of molecular weights would be particularly helpful.

Recent experiments on ring polymer melts and concentrated solutions have led to additional open questions regarding ring purity and kinetic degradation (Sec. III B 3) [212]. Experiments on polyDODT showed that the plateau moduli of putative ring samples were indistinguishable from G_e values of the corresponding linear polyDODT (melt or matched-concentration solutions). Although these results are interesting, it is not yet clear whether the LVE data for ring polyDODT are affected by linear chain contaminants. Moreover, the role of kinetic degradation of ring polymers during characterization is not yet fully clear. Prior work based on LCCC characterization has shown that linear chain contaminants in anionically prepared rings can increase by several weight percent during rheological characterization [192].

On the other hand, metastable cPPA rings are considered to be topologically pure, as recent NMR experiments on cPPA rings show extremely rapid and complete kinetic degradation to monomer within <10 seconds upon chemical triggering [188]. The timescales for cPPA ring degradation to monomer are much shorter than the timescales for rheological characterization, suggesting that any putative cleaved rings rapidly convert to monomer during rheological characterization, which precludes the possibility of linear chain contaminants in these samples. Nevertheless, LCCC purification has not yet been attempted on cPPA ring polymer samples.

Overall, these results challenge the field to reconsider the role of linear chain contamination for high molecular weight ring systems, which play an increasingly significant role in the viscoelastic properties as molecular weight increases. The cPPA data of $Z = 59$, with indisputable purity in terms of linear chains, suggest that the PEO samples with $Z = 44$ should be further investigated by rheology and the results compared with NSE data [190]. Additional coarse-grained MD simulations for large $Z > 200$ values are needed, and more computational and experimental work in these directions, in terms of the linear and nonlinear responses, without and with the addition of small amounts of linear chains, is needed.

3. Ring interpenetration, threading, topological glass transition, and knots

In melts and concentrated solutions, ring polymer dynamics are ultimately governed by conformation and structural properties. Schematics of topologically constrained ring polymer conformations from theoretical models shown in Fig. 5 show large open loops, which are indeed observed in simulation snapshots [23,27,49] such as those shown in Fig. 1(c). Studies of the minimal [262,263] and the "magnetic" [23,26] surface enclosed by crumpled rings reveal that the former scales linearly with the ring contour (as expected by the double-folded randomly branched ring model, as shown in Fig. 4), whereas the latter is dominated by open loops with a characteristic size on the order of the radius-of-gyration R_g of the ring polymer (as predicted by the decorated loop and the FLG models, as shown in Fig. 5).

Clearly, there are no open "holes" in dense ring melts. For example, not only is the visible open loop in Fig. 1(c) threaded by at least one additional ring, there may be other invisible open loops that are threaded by other parts of the same ring (Fig. 15) [264]. MD simulations of ring melts revealed substantial ring-ring interpenetrations upon increasing the ring molecular weight or local backbone stiffness [27,188], which suggests that ring polymers are globally compact yet highly porous structures that strongly interpenetrate in concentrated systems [28]. Therefore, ring-ring threading interactions cannot be neglected when considering the dynamics of ring polymers [199]. Additional studies [200,263] showed that ring-ring topological constraints survive for smaller characteristic timescales compared to ring-linear threading interactions at equilibrium. It is not yet clear if these intermolecular effects play a significant role on ring polymer dynamics near equilibrium. Prior work has suggested that threading could lead to slow relaxation modes [5,200] and eventually to a topological glass transition [200,265–267]. A schematic of topological glass formation in a ring polymer liquid is shown in (Fig. 16), where loop 1 slows down due to its interpenetration by loop 2, which in turn slows down due to interpenetration by loop 3 and so forth.

To model concentrated solutions of unknotted and non-concatenated rings on larger scales, it is desirable to coarse-grain over the internal structure of the rings. If explicit topological constraints in an atomistic or mildly coarse-grained polymer model are replaced by effective interactions, the

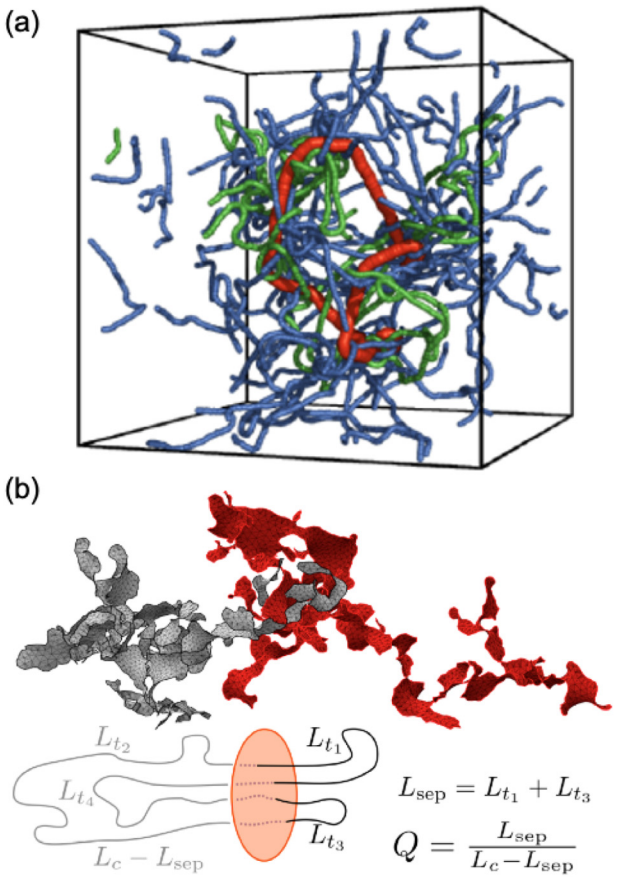

FIG. 15. Rheology of ring polymer melts highlighting the role of threading interactions. (a) Snapshots of polymer conformations from MD simulations (Kremer–Grest model, $k_\theta = 1.5$, $N_b = 400$) in a ring-linear blend (50% linear chains) showing a selected ring polymer (red) threaded by or entangled with additional rings (green) and linear chains (blue). For clarity, not all polymers are shown. Reproduced with permission from Halverson *et al.*, Phys. Rev. Lett. **108**, 038301 (2012) [6]. Copyright 2012, American Physical Society. (b) Two mutually threaded rings from a melt of nonconcatenated ring polymers, shown with their minimal surfaces and threading depth analysis [263,264]. Top: Minimal surfaces of a pair of rings modeled as double-folded polymers on interacting branched primitive trees. Bottom: Schematic of one ring (black and gray) penetrating the minimal surface of another ring (orange) of total contour length L_c. Here, L_{t_i} is the contour length of subchain i penetrating the second ring. Four surface penetrations ($n_p = 4$) split the penetrating ring into the segment pairs (L_{t_1}, L_{t_3}) and (L_{t_2}, L_{t_4}) on opposite sides of the surface: this defines the separation length, L_{sep}, and its complementary, $L_c - L_{sep}$. Reproduced with permission from Smrek and Grosberg, ACS Macro Lett. **5**, 750–754 (2016) [263]. Copyright 2016, American Chemical Society.

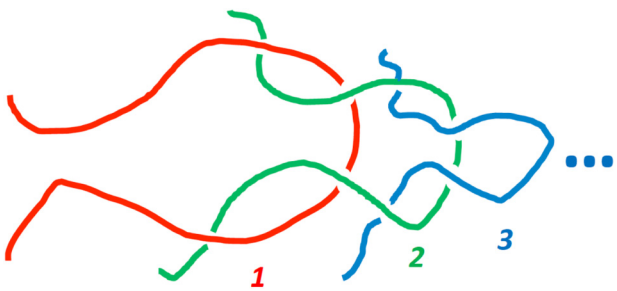

FIG. 16. Schematic of topological glass transition in ring polymer liquids: relaxation of loop 1 (red) is delayed due to its threading by loop 2 (green), which itself is trapped due to threading by loop 3 (blue), and so forth.

latter depend on the knottedness of the rings [268]. Concentrated solutions of unknotted and nonconcatenated rings can be described via multi"blob" models [269]. Although this approach can be used to study the threading interactions between asymmetric ring polymers [270], the standard approach with distance-dependent interactions needs to be augmented by including the relative orientation of semiflexible rings [253] to properly describe clustering, as shown in Fig. 14.

Recent simulations also showed the existence of an entanglement network in large nonconcatenated ring polymers when they are cooled well below the glass transition temperature and undergo crazing [271]. This network formation involves only a fraction of the topological constraints of rings and can support stable craze formation in ring polymer glass under tensile loading. This work offers new routes for characterizing the mechanical properties of ring glasses and also contributes to the understanding of the nature of the entanglements of rings in crazing and beyond. These developments call for experimental studies of glassy ring polymers and ring-linear blends, which will help to elucidate the role of the topology on the physical properties of blends, and may have practical consequences (compared to the crazing properties of entangled linear polymer glasses). In this regard, the possibility of a topologically induced glass transition needs careful assessment by experiments and simulations. In the context of topological effects, the recent simulations showing that cross-linked rings are more stretchable than their linear chain counterparts [59] will certainly motivate new experimental work, as it provides a path to enhance mechanical properties by altering topology. Along the same lines, concatenated rings were recently shown to give rise to enhanced elasticity [272], and slide-ring networks are also highly stretchable.

Finally, whereas much recent work has focused on melts or dense solutions of nonconcatenated unknotted rings, there are many interesting unanswered questions concerning the properties of knotted [100,273–279], supercoiled [207,280–284], and multicyclic [285] rings. Although several prior studies have focused on single molecules and their structure and dynamics as a function of the solvent quality, stiffness, and topological state, the melt limit is highly relevant for genomic applications (Sec. IV).

4. Slow dynamics in ring concentrated solutions and melts

There are several open questions regarding the dynamics of high molecular weight ring polymer melts and concentrated solutions. Based on current understanding, the research on LVE properties of ring melts can be organized into three apparent regimes: unentangled, entangled, and highly entangled. The first unentangled regime ($Z \leq 1$) follows Rouse-ring dynamics with the ring viscosity equal to half of its linear counterpart and with the same molecular weight scaling dependence of zero-shear viscosity ($\eta_\circ \propto M^{1.0}$) [191,193]. A comparison of linear and ring PEO dynamics by NSE experiments in the Rouse regime revealed that the COM diffusion of

rings was unexpectedly faster compared to linear reference polymers with identical molecular weight [177].

The second regime corresponds to an entangled regime with respect to the N_e of the linear chain equivalent (approximately $1 < Z \leq 44$ in experiments [194] and $1 < Z \leq 114$ in simulations [49]). This regime is characterized by a power-law stress relaxation due to self-similar loop relaxation [182], which has been observed in simulations and experiments for common flexible polymer chemistries such as PS [191–194]. However, it remains an open question whether there is an upper limit to this behavior upon increasing the ring molecular weight for a given backbone chemistry. As discussed in Sec. III C 2, experimental characterization of ring polymer systems at high molecular weights is challenging due to the extreme sensitivity of the rheological properties to linear impurities. Thus, mapping out the potential limits of the power-law stress relaxation behavior requires addressing current challenges regarding purity, yield, and stability of synthetic ring polymers even after careful LCCC purification.

The current set of experimental and simulation data also show that the molecular weight dependence of zero-shear viscosity $\eta_\circ$ of entangled rings is weaker than for linear polymer melts over a broad range of molecular weight. Careful analysis of zero-shear viscosity data with three different polymer chemistries and accounting for slow modes indicates a power-law exponent of 1.3, consistent with simulations, as discussed above [216]. However, more work with different chemistries and a broader range of molecular weights is needed to the establish whether power-laws are truly chemically universal, for example, when accounting for properties such as backbone flexibility.

The third regime remains an open question, but it has long been postulated that sufficiently high molecular weight rings might develop new forms of topologically mediated constraints that drive *topological localization* either by forming highly correlated and percolated intermolecular threadings (see Fig. 16) or through the colloidal-like jamming of globular ring conformations. Recent work suggests that rings can show a slowdown in stress relaxation for sufficiently high molecular weight or chain stiffness [188]. MD simulations revealed a slowdown in $G(t)$ relaxation behavior by varying either chain length N_b or chain stiffness k_θ (Sec. III B 3). Such behavior could suggest that an intermediate length scale emerges to break the self-similarity of loop relaxation predicted by models such as the FLG model. Simulations further showed a substantial increase in ring packing number, with more chains coexisting in the volume pervaded by one chain, in addition to suppressed diffusion with increasing chain stiffness, to the point that simulations could no longer resolve bulk diffusion for the highest molecular weight considered ($N_b = 6400$). The origins of the suppressed diffusion in high molecular weight rings were recently investigated using a combination of MD simulations and theory [189], and such dynamic behavior is predicted to depend on backbone stiffness [189]. However, the link between strong ring interpenetration and stress relaxation in $G(t)$ behavior has not yet been definitively established. Nevertheless, these results show that the apparent power-law behavior displayed by $G(t)$ becomes highly sensitive to small changes in the backbone stiffness and N_e at sufficiently high molecular weight [Fig. 9(c)].

There are multiple possible mechanistic interpretations for explaining the dependence of $G(t)$ on stiffness and molecular weight in the highly entangled regime. First, inter-ring threading events become more common at high molecular weight, and the lifetime of such threadings has been found to be much longer than the ring relaxation time and increases with increasing molecular weight [193]. Such threadings might result in large clusters of slowly relaxing material [208] or even a topological glass transition (Sec. III C 3). Second, recent PRISM theory calculations and complementary MD simulations show that the globular conformations of ring polymers become increasingly localized with increasing molecular weight and stiffness, resulting in suppressed and thermally activated regimes of ring diffusion [189]. Such jamming-like localization could result in partial or complete vitrification at the macroscopic scale. Third, it is possible that rings could display loop-size dependent dynamic dilution that varies with chain size and stiffness. The current FLG model assumes that as small loops relax, they act as a dynamically diluting solvent of larger loops. However, the scaling theory permits varying the effectiveness of this dilution, possibly making it length-scale dependent, which could alter or break the self-similarity of the relaxation. Nevertheless, the relevance of any of these possible mechanisms remains an open question. Broadly, developing these new directions would benefit from additional experiments, including further dilution experiments with rings, and additional simulations to understand the molecular origins of the apparent plateaus and power-law behavior in $G(t)$.

Finally, we note that the scenario of a slowdown in ring polymer dynamics due to an activated process is qualitatively different than theoretical predictions of this scenario for linear chain melts [286–288], which predicts that for extremely high molecular weight chains, chain ends become so dilute that the reptation process becomes activated and polymers become trapped in their tubes. For linear chains, the barrier height is predicted to scale as $N^{2/3}$ [287,288]. There are possible hints of this effect in Monte Carlo simulations of lattice models of linear polymer melts using a reptation algorithm [286], but so far neither experiments nor MD simulations of linear polymer melts have observed this theoretically predicted limit, and the available data are consistent with nonactivated reptation.

5. Ring-linear blends

Rings prefer to be threaded by linear chains rather than being constrained by other rings [5,6,201]. This leads to the negative topological Flory interaction parameter χ between rings and linear chains in a blend [205,289] due to the increase of the rings' entropy if topological interactions between rings are replaced by their interactions with linear chains. The negative topological χ could result in the miscibility of weakly immiscible polymers if one of the components of the blend consists of linear chains while the other contains primarily ring polymers [290].

The dynamics of ring-linear blends is extremely heterogeneous and dominated by threading [6,197,198,203,204,206,217,221,291,292]. Interestingly, adding

rings to linear polymers at low ring volume fractions increases blend viscosity and relaxation time, even though the viscosity of pure rings is much lower than that of linear polymers of the same molecular weight. This can be understood based on a theoretical model in which ring dynamics are dominated by constraint release due to the reptation of linear chains threading through rings [202]. This theory predicts an increase of ring-linear blend viscosity with increasing ring composition below significant ring-ring topological interactions.

For ring-linear blends consisting of a relatively small fraction of rings (<50% v/v), the viscosity increases with increasing ring fraction due to ring-linear threading [51,195,203–205,221,289]. Upon increasing the ring fraction in the ring-linear blend, one expects the blend viscosity to reach a maximum and then decrease, as observed in prior simulations [6] and experiments [221]. It is not clear how the relative height of this maximum depends on the molecular weights of blend components and on the difference of the molecular weights between the linear and ring components. Recently, NSE spectroscopy has been used to study ring-linear blends with identical molecular weights, focusing on the internal ring dynamics and its dependence on ring volume fraction. With increasing linear composition, a dynamic crossover from self-similar ring-like relaxation to local reptation-like dynamics was observed. Around a volume fraction of ≈0.5, the blend viscosity exhibits its maximum, and the spectral shapes change from ring- to local reptation- type dynamics. For smaller ring volume fractions, the ring motion is completely enslaved by the linear host. Moving away from equilibrium, the viscosity overshoot in ring-linear blends [293] and multicyclic ring-linear blends [294] was studied in biaxial extensional flow using coarse-grained MD simulations.

Theoretical predictions [202] depend on whether the constraint release process is coherent or ordinary. Coherent constraint release refers to a scenario in which a single linear chain, upon reptating away from its original confining tube, releases $\sqrt{N/N_e}$ common entanglements between it and an adjacent (ring) polymer, whereas in ordinary constraint release, one entanglement is released. Previous experiments and models of linear and star-linear polymer blends [295,296] suggested that constraint release is coherent, but these results were not conclusive because there was constraint release due to the motion of both components of the blend. In ring-linear blends with small ring fractions, constraint release is the only mechanism available for the relaxation of rings. Therefore, such blends are ideal to test the coherence of the constraint release process.

Despite recent work, there is no convincing molecular model describing the dynamics of ring-linear blends with a large fraction of ring polymers and only a small ($\lesssim$5%) fraction of linear chains. A quantitative model describing the limit of large ring content would be crucial for understanding the effect of linear impurities on dynamical properties of ring melts.

Overall, these findings call for additional systematic experiments of ring-linear blends with different molecular weights, new ring chemistries, and additional blend compositions. Blending of low and high molecular weight rings would allow miscibility to be studied in these systems [205,289]. Moreover, the recent predictions of the dependence of topological constraint relaxation time as a function of the ring and linear molecular weights, based on MD simulations, can be tested [206]. Finally, as discussed above, the role of the sample preparation protocol needs to be examined in conjunction with simulations, and together these studies can guide experimental work.

6. Nonlinear rheology

Nonlinear rheological properties of melts of nonconcatenated rings are qualitatively different than melts of linear chains with similar molecular weight. The shear viscosity of ring melts ($Z \leq 15$) decreases with a smaller power-law exponent of shear rate $\dot{\gamma}$ than the shear viscosity of linear polymers melts (Sec. III B 6), as predicted by the recently developed shear slit model [195,196]. The most dramatic nonlinear rheological signature of rings is the strong increase of the extensional viscosity as a function of the extension rate at Weissenberg numbers *Wi* less than unity due to the formation of hitch knots (Fig. 13) [219,224]. Note that hitch knots do *not* change the topological state of the rings in a mathematical sense because they can form and disassemble without backbone crossing or the opening and closing of one of the involved rings. However, once formed, they are locked in by the strong ring extension in flow and can then transmit stresses in a similar manner as two topologically linked rings.

In terms of bulk rheological characterization, there is a need for additional experimental investigations of ring polymer dynamics in shear and extension using different ring polymer chemistries and high molecular weight ring samples, including nonlinear damping, relaxation upon flow cessation, and normal stress measurements. Recent work using state-of-the-art experiments and complementary simulations suggests that this is a highly interesting and critically important research direction [195,196,219]. Of particular significance is the study of the nonlinear rheology of ring-linear blends [197,207,209,209,211,221], together with simulations and structural studies, in the direction of enhancing stretchability or exploring new phenomena associated with interlocking rings. Recent simulation results revealing topological heterogeneities of stretched polymers [297] could serve as a guide for this important new direction, and experiments involving the filament stretching rheometer would greatly aid in understanding the nonlinear rheological behavior in extensional flow.

7. Loopy soft materials beyond rings

The study of rings has shown that loops play a crucial role in the dynamics of polymeric materials. From this view, examination of other loopy structures (e.g., single chain nanoparticles [298], ring bottlebrushes [299], multicyclic polymers [285], dumbbell-shaped polymers [300], tadpole-shaped polymers [301–304], and folded proteins [305]) would be highly useful to inform the study of ring polymer physics. In 1989, Antonetti and co-workers reported the synthesis and characterization of PS micronetworks, which are materials consisting of small particles of cross-linked PS with a fractal distribution of local monomer density [306].

Subsequent work reported the rheological characterization of small spherical PS microgels of size $5< R < 50$ nm prepared by microemulsion polymerization [307]. These compact, fluctutating "rubbery nanospheres" exhibited a zero-shear viscosity that is remarkably smaller than that of linear chains of the same molecular weight. Moreover, the frequency dependence of the mechanical response appears to follow the well-known classic linear chain reptation-type response, including an intermediate time rubbery plateau modulus of essentially identical value as the linear chain analog (similar to high molecular weight cPPA and polyDODT ring experiments [188,212]), along with chain-like power-law scaling of the viscosity with polymer molecular weight. However, it was noted that the putative reptation-like motion of these particles is strictly excluded by the spherical architecture of the molecules. These results suggested the existence of a strong, secondary type of polymer mobility beyond reptation that is more cooperative in its nature than a single-chain mobility.

In 1997, Fuchs and Schweizer modeled this behavior using a nonreptation-based polymer mode coupling theory for dense liquids of compact fluctuating polymeric spheres [308]. Similar phenomena have also emerged in melts of single chain nanoparticles (SCNPs) consisting of dense liquids of collapsed fluctuating fractal globules. Such loopy structures can be threaded by linear chains, giving rise the rheological phenomena analogous to those with ring-linear blends, as shown recently [298]. These findings render the systematic investigation of blends comprising SCNPs and linear chains over a wide material parameter space necessary.

8. *Metastable crumpled linear chains*

Linear chains can be prepared in the unentangled crumpled state in dilute solutions by a rapid quench to poor solvent conditions [309], by melting of polymer crystals [310], or by the decondensation of internally unknotted chromosomes during interphase [35]. In general, these crumpled polymer conformations are likely to be qualitatively different on large scales. However, because the samples are unentangled, they should locally reproduce the generic equilibrium behavior of ring melts on scales up to a slowly relaxation growing length [35]. Such systems can be extremely long lived [34,35], which provides an intriguing scientific motivation for studying crumpling and suggests a possible alternative method to address the challenging synthesis of high molecular weight rings. Preparing equilibrated melt samples for increasing ring molecular weights and studying their dynamics remains a challenge for computational as well as experimental studies [311,312]. Interesting lessons in controlling bulk properties can also be learned from different polymer topologies. As one example, a new class of elastomers was recently reported by end-linking and then deswelling star polymers with low amounts of trapped entanglements, enabling high levels of strain-induced crystallinity of up to 50% [313].

9. *Active systems*

There are several different classes of active ring systems. One class of active rings is achieved by a different effective temperature, corresponding to a higher mobility, in a small section of each ring [314,315], which then diffuses more quickly with the passive part dragged behind. Rings in this nonequilibrium system tend to thread and trap each other in a topological glass scenario with hitch knots playing a crucial role in the final arrested state. It is known that phase segregation occurs in analogous active systems based on linear polymers from both simulations [316] and analytical theory [317], where mobility induces phase segregation in different "hot" and "cold" domains. However, an open question remains regarding whether or not such behavior mechanistically leads to threading in ring-based systems.

IV. BIOLOGICAL AND ACTIVE RING POLYMERS

In biology, living organisms have developed the ability to replicate, transcribe, and separate chromosomal DNA reaching macroscopic contour lengths. Large-scale conformational changes such as the separation of the replicated sister chromatids and the condensation of mitotic chromosomes utilize active loop extrusion [318–320] (Fig. 17) and the enzymatic action of topoisomerases [321,322], which can actively change and regulate the topological state of DNA. Even during interphase, the statistical properties of genomic DNA are better described by stationary rather than equilibrium processes. For example, loop extrusion can lead to observable modifications of the local chromosome structure [318,323–326] which goes beyond the simple analogy to the equilibrium ring melt. The quantitative investigation of these fascinating processes, which are central to life, offers interesting new directions for future research in polymer physics.

Interest in ring polymers was initially motivated decades ago by its importance to understanding naturally occurring circular DNA plasmids and genomes [58,109]. Although our understanding of the physics underlying monodisperse ring polymer solutions has greatly advanced since those seminal studies, several remaining challenges hinder our understanding of more complex biological and active ring polymer

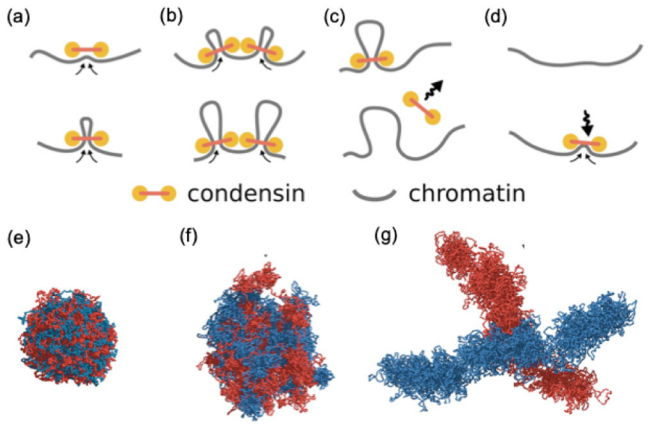

FIG. 17. Biological phenomena involving active loop maintenance chromatin. (a)–(d) Model of loop extrusion from chromatin fibers by condensins. (e)–(g) The conformations of two initially entangled sister chromatids (shown in red and blue) at different time points show that the combination of Brownian dynamics and loop extrusion activity leads to their segregation and disentanglement. Reproduced with permission from Goloborodko *et al.*, eLife **5**, e14864 (2016) [319]. Copyright 2016, eLife Sciences Publications.

systems, such as supercoiled rings [207,284,327], topological composites [210,328], topologically active DNA rings [329], "hot" rings [314,330], kinetoplasts [331,332], and chromatin loops [326]. In the following, we summarize key challenges that need to be addressed to advance our understanding of biological and bioinspired ring polymer systems.

A. Open issues and new directions

1. Theory for complex biological ring systems

Much work has been devoted to developing theoretical models for ring polymer dynamics, as described in Secs. II and III. However, prior theory and experiments have been largely limited to relaxed open circular rings, which represent only a small subset of biological ring polymers. For example, in biology, double-stranded circular DNA (e.g., plasmids) is typically supercoiled [109,110], with substantial torsional stress and writhe, which can act to reduce its radius-of-gyration by promoting intrachain interactions [333], as well as induce branching and extended conformations [284], depending on the DNA length and environmental conditions. Moreover, recent studies have shown that highly concentrated supercoiled DNA polymers adopt more swollen conformations compared to open ring counterparts while at the same time exhibiting faster dynamics, seemingly at odds with the Stokes-Einstein relation describing a collapsed macromolecule [Fig. 18(a)] [284]. DNA and RNA also regularly adopt loopy conformations that bring together two well-separated sections of the long chains [326,334]. The number and spatial distribution of loops, as well as their sizes, have a clear impact on the dynamics of the rings, in particular, in the highly overlapping regime that is typical in biology; yet, the nature of this impact and the underlying physics remains an open question. Another common biological motif is concatenation of rings, as most clearly exemplified by kinetoplasts that comprise a percolated chain-mail structure of concatenated rings that form a larger flat gel-like ring that can fold, bend, and crumple while maintaining its structural integrity [Fig. 18(b)] [331,332]. How can we leverage and extend existing models for ring, branched, and linear polymers to understand these complex structures? What is the role of chirality in determining the local structure and dynamics in unknotted and knotted rings?

2. Bridging microscopic and macroscopic length scales

Although monodisperse ring polymer systems can be fully parameterized and characterized by only a few key length scales, e.g., persistence length, radius-of-gyration, mesh size, and tube diameter, biological or biopolymer-based ring systems often have distinct structural and mechanical properties at different length scales, such that microscopic and macroscopic measurements often yield distinct results [51,209,210]. Yet, methods to characterize rheological properties at intermediate mesoscale ranges that connect these scales remain elusive [209].

The effect of threading of rings by linear chains is particularly sensitive to scale-dependent dynamics due to the dramatic impact that a few threading events can have on bulk dynamics (Sec. III C 5), and the sensitivity to the number of rings and linear chains participating in each discrete threading event. For example, microrheology measurements on

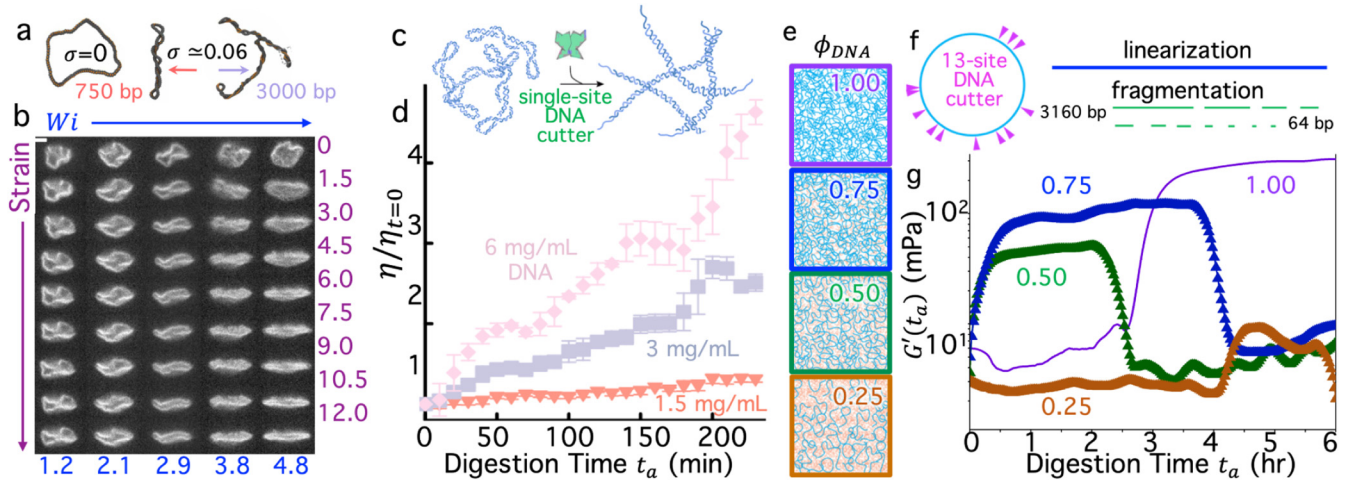

FIG. 18. Naturally occurring topologies and networks of circular DNA and time-varying rheological properties of topologically active DNA solutions and composites. (a) Simulations of dense solutions of supercoiled DNA show that long supercoiled strands can exhibit branching that leads to swelling of the supercoiled conformations above that of open rings. Degree of supercoiling is given by $\sigma = 1/p$, where p is the pitch of twisted backbones. Reproduced with permission from Smrek *et al.*, Sci. Adv. **7**, eabf9260 (2021) [284]. Copyright 2021, American Association for the Advancement of Science. (b) Fluorescent images of kinetoplasts being deformed in planar extensional flow with increasing *Wi* (left to right, blue) and accumulated strain (top to bottom, purple) show varying degrees of stretching and crumpling. Reproduced with permission from Soh and Doyle ACS Macro Lett. **9**, 944–949 (2020) [335]. Copyright 2020, American Chemical Society. (c) and (d) *In situ* conversion of 6 kbp supercoiled circular DNA to linear topology via single-cutter enzyme BamHI causes a steady increase in viscosity η of concentrated DNA solutions as a function of enzymatic digestion time t_a for different DNA concentrations (1.5, 3, 6 mg/ml). Reproduced with permission from Michieletto *et al.*, Nat. Commun. **13**, 4389 (2022) [329]. Copyright 2022, Nature Portfolio. (e) Composites of varying mass fractions of 11 kbp DNA, ϕ_{DNA}, and 500 kDa dextran at total fixed polymer concentration of 11 c^*, where c^* is the overlap concentration, (f) pushed out of equilibrium by the multisite DNA cutter ApoI that first linearizes supercoiled DNA and subsequently cleaves it into 13 polydisperse fragments, (g) resulting in discrete state-switching of bulk rheological properties (G', storage modulus at 1 rad/s) for all composite compositions with the time course and amplitude of state jumps tuned by ϕ_{DNA}. Reproduced with permission from Marfai *et al.*, Adv. Mater. **35**, 2305824 (2023) [208]. Copyright 2023, Wiley.

ring-linear blends of double stranded DNA of identical molecular weight revealed a nonmonotonic dependence of the plateau modulus and shear-thinning exponent as a function of linear chain fraction, both reaching a maximum around a linear fraction of ≈60%–70%—owing to pervasive ring-linear threading events [221]. Single polymer dynamics experiments [83] allowed for direct observation of DNA rings in ring-linear blends, with experiments and complementary simulations showing that transient threading events in flow led to large conformational fluctuations and the broadest range of relaxation timescales for blends with comparable ring and linear DNA fractions [151,197,198]. However, bulk rheology measurements on the same system reported a much weaker dependence of the plateau modulus on blend fraction (i.e., linear chain content) and more pronounced shear thinning of blends [215]. Results from microrheology experiments on DNA-based biopolymer systems were compared, at least qualitatively, to the shear rheology of synthetic ring/linear blends, as previously described [195]. Moreover, such length scale-dependent properties are expected to be even richer in systems of concatenated rings that display hierarchical topological structures that are not self-similar, like kinetoplasts [331], polycatenanes, and olympic rings [336].

3. Emergent properties in biological materials

Mixtures of ring biopolymers with other biological and synthetic polymers—ubiquitous in biology—have been shown to result in emergent properties that are not a simple sum of the properties of the two components [207,210,328,337]. For example, incorporating ring DNA into solutions of polymerizing microtubules has been shown to enhance miscibility of the two components, thereby suppressing microtubule polymerization and reducing the elastic strength of the composite [328]. This phenomenon is unique to ring topologies, whereas linear DNA was shown to induce the opposite effect of enhanced demixing and network stiffening. Moreover, highly overlapping composites of DNA and dextran were shown to exhibit emergent anomalous subdiffusion of ring DNA and enhanced shear-thinning in composites compared to pure solutions of either DNA or dextran [210]. Finally, semidilute blends of supercoiled and open ring DNA were shown to exhibit emergent signatures of entanglement dynamics at concentrations well below the critical entanglement concentration c_e (at around 0.15 c_e) for monodisperse solutions of linear DNA [207]. Although interesting, most of these emergent properties reported in biological ring systems could not be predicted by existing theories and are not yet fully understood.

4. Rheological properties of demixed, heterogeneous, or anisotropic materials

Many biological ring systems are heterogeneous on mesoscopic scales (e.g., the scale of multiple polymers)— arising from demixing, bundling, knotting, or concatenation of different components—and are often anisotropic. For example, kinetoplasts, comprising interconnected networks of concatenated rings, are largely flat circular membranes showing a mechanical response that is highly dependent on the direction of the applied stress [331,332]. Ring-ring concatemers [336] and "daisy-chains" [219] can also adopt directionality associated with the orientation of the linkage, which can make applicability and understanding of bulk rheological properties challenging. Although microrheological methods can be used to probe spatial heterogeneities [209], these methods often require 3D geometries and rely on assumptions that the material can be considered a continuum at the scale of the measurement probe and that material heterogeneities are larger than the probe size. Large sampling is also required for sufficient statistics to characterize heterogeneities measured by data acquired in different spatial regions of the system. Addressing these challenges requires new methods to quantify the dynamics of heterogeneous and anisotropic polymeric materials, as well as new theories to understand the dynamics arising from these complex systems and how they couple with the heterogeneous network structure.

5. Active systems and thermally driven dynamics

Many biological ring polymers undergo active restructuring via the action of enzymes and motors that cut, twist, connect, and loop them. These out-of-equilibrium (or active) dynamics introduce additional relaxation timescales beyond the thermal relaxation timescales of the polymers (of which there are multiple). As enzymes change the size, shape, or structure of the rings, the intrinsic thermal relaxation timescales (determined by the properties of the polymer of interest and its neighbors) also change.

Differentiating between the active and passive contributions to the stress relaxation modulus remains a grand challenge. For example, light scattering measurements of active olympic rings [336], i.e., solutions of relaxed ring DNA that are continuously cut and reconnected via topoisomerase II to form transient concatemers, have shown that this transient concatenation reduces the longest relaxation timescale of the system by eliminating prolonged constraints. However, for timescales shorter than the cutting timescale, the rings are effectively fixed in concatenated states with slower thermal relaxation timescales compared to individual chains. Moreover, because there is expected to be a distribution of concatemer sizes, which has so far proven difficult to quantify, one would expect a distribution of timescales that are not easily separable. Further complicating the issue is the fact that when these systems are in a static concatenated state, the relaxation timescales are quite long, which introduces challenges when using conventional bulk rheological techniques. However, in principle, appropriate implementation of creep and conversion [195] may allow for accurate characterization of these samples.

Similar challenges arise in simulations of active ring systems in which a small fraction of the ring is made to be "hotter" than the rest of the chain, mimicking an athermal "active" contribution to the fluctuation spectrum [314,330]. Of course, it should be noted that there are several different classes of activity that rely on the action of enzymes, artificially higher temperatures (which mimics activity), or the action of motor proteins (e.g., condensin, cohesin, and

polymerases) that can drastically modify polymer conformations and dynamics. Nevertheless, the specific rheological signatures of such activity, and the extent to which they can model experimental biological ring systems, remains an open question.

6. Measuring rheological properties of time-varying systems

In nature, biological rings are out-of-equilibrium, with their structure, dynamics, and interactions changing over time due to enzymatic processes such as cleaving, ligating, and looping. In fact, a characteristic feature of biological systems is that they continuously consume and dissipate energy to remain in a stationary "living" state. A major challenge in characterizing these nonequilibrium systems is that measurements of rheological and dynamical properties require a finite amount of time which can often be longer than the active restructuring timescale. Therefore, interpretation of the stress relaxation modulus is nontrivial. Because these systems violate the fluctuation-dissipation theorem, interpreting passive particle-tracking microrheology results becomes problematic [338]. Current methods to overcome this issue focus on slowing down the active dynamics compared to the measurement timescale, such that the system can be considered in quasisteady state on the timescale of each time-resolved measurement of the modulus [208,329]. However, this approach is limited and may not be feasible in many biological systems subject to active processes driven by molecular-motors or rapid-polymerization and digestion kinetics. Moreover, this quasisteady approach cannot capture the rheological signatures of the active nicking/cleaving/twisting/looping processes. For example, time-resolved particle-tracking microrheology measurements showed that concentrated solutions of ring DNA undergoing slow linearization via single-cutting enzymes exhibited steady viscous thickening over the course of several hours as the fraction of linear chains in the system increased [Figs. 18(c) and 18(d)] [329]. Moreover, bulk rheology measurements on DNA-dextran composites showed that enzyme-driven linearization and fragmentation of ring DNA induced an abrupt switch to a more elastic-like state, in contrast to the steady increase measured in microrheology measurements [Figs. 18(e)–18(g)] [208]. The timing of this abrupt switch did not universally correlate with the linearization timescale across composites, suggesting that the relaxation rate of the DNA undergoing digestion may be slower than the digestion rate. Generally, it is reasonable to expect that any sufficiently strong active driving force (e.g., processes requiring hydrolysis of stored chemical energy such as ATP) will perturb chains to deviate from their equilibrium structure and dynamics. These intriguing results demonstrate the need for experimental and theoretical methods that can couple together and separate the active and thermal contributions to the dynamics of biological ring systems.

V. SUMMARY

Interesting and unexpected phenomena continue to be observed for a wide range of both synthetic and biological ring polymer systems. Although seemingly disparate systems, several overarching themes and grand challenges emerge when considering the full range of synthetic and biological materials. As discussed above, synthetic and biological ring polymers would benefit from additional chemical characterization and control over molecular weight, polydispersity, and purity. It should be noted that nearly all technologically relevant synthetic and biological ring-based materials are neither pure nor prepared in the extremely high molecular weight limit. Moreover, several key questions regarding structure-function relations emerge when considering ring polymer materials with mixed compositions. For example, what can be learned from well-controlled, high molecular materials to better understand industrially relevant materials systems? Are these asymptotic systems relevant references or "anchor points" for understanding more compositionally complex or technologically relevant ring (or other generally loopy) polymer materials? Additional studies will be essential to address these key questions.

Regarding theory and simulations, several key scientific questions remain to be addressed. For example, is it possible to model most relevant ring polymer systems using full atomistic or fine-grained simulations for concentrated systems at very high molecular weight? Alternatively, can we develop new approaches, e.g., data-driven methods, that could potentially provide alternative routes for an improved physical understanding of the relevant phenomena? In addition, the role of chain flexibility or chirality (i.e., weak, tight, racemic variants, packing, and braiding) is not currently well understood for ring polymers, which provides ample opportunities to explore rich and interesting physical phenomena in terms of structure and dynamics. Nevertheless, despite several challenges, the state-of-the-art instrumentation currently available allows for the study of small amounts of samples, weak signals, extended ranges of frequencies and/or rates, single molecule dynamics, and strongly nonlinear responses. Moving forward, a combined approach uniting simulations, theory, and well-controlled experiments, often involving advanced techniques and/or protocols, will be required to address these key questions.

ACKNOWLEDGMENTS

This article is a direct result of collegial talks and discussions that took place at a workshop on Ring Polymer Dynamics held at the Monash University Prato Centre in Prato, Tuscany, in June 2023, as a CECAM Flagship workshop. We gratefully acknowledge financial support of this event by (i) Centre Européen de Calcul Atomique et Moléculaire (CECAM), (ii) DFG SFB TRR 146, Project No. 23363005, (iii) MPI for Polymer Research Mainz; as well as very helpful organizational support from the staff at the Prato Center. The authors gratefully acknowledge Charles Sing for useful discussions.

AUTHOR DECLARATIONS

Conflict of Interest

The authors have no conflicts to disclose.

DATA AVAILABILITY

Data sharing is not applicable to this article as no new data were created or analyzed in this study.

REFERENCES

[1] Doi, M., and S. F. Edwards, *The Theory of Polymer Dynamics* (Oxford University, New York, 1986).

[2] McLeish, T. C. B., "Tube theory of entangled polymer dynamics," Adv. Phys. **51**, 1379–1527 (2002).

[3] McLeish, T., "Polymers without beginning or end," Science **297**, 2005–2006 (2002).

[4] Rubinstein, M., "Dynamics of ring polymers in the presence of fixed obstacles," Phys. Rev. Lett. **57**, 3023–3026 (1986).

[5] Kapnistos, M., M. Lang, D. Vlassopoulos, W. Pyckhout-Hintzen, D. Richter, D. Cho, T. Chang, and M. Rubinstein, "Unexpected power-law stress relaxation of entangled ring polymers," Nat. Mater. **7**, 997–1002 (2008).

[6] Halverson, J. D., G. S. Grest, A. Y. Grosberg, and K. Kremer, "Rheology of ring polymer melts: From linear contaminants to ring-linear blends," Phys. Rev. Lett. **108**, 038301 (2012).

[7] Robertson, R. M., S. Laib, and D. E. Smith, "Diffusion of isolated DNA molecules: Dependence on length and topology," Proc. Natl. Acad. Sci. U.S.A. **103**, 7310–7314 (2006).

[8] Wijesekera, A., D. L. Vigil, and T. Ge, "Molecular simulations revealing effects of non-concatenated ring topology on phase behavior of symmetric diblock copolymers," Macromolecules **57**, 5092–5104 (2024).

[9] Zardalidis, G., J. Mars, J. Allgaier, M. Mezger, D. Richter, and G. Floudas, "Influence of chain topology on polymer crystallization: Poly(ethylene oxide) (PEO) rings versus linear chains," Soft Matter **12**, 8124–8134 (2016).

[10] Tubiana, L., G. Alexander, A. Barbensi, D. Buck, J. Cartwright, M. Chwastyk, M. Cieplak, I. Coluzza, S. Copar, D. J. Craik, M. D. Stefano, R. Everaers, P. Faisca, F. Ferrari, A. Giacometti, D. Goundaroulis, E. Haglund, Y.-M. Hou, N. Ilieva, S. E. Jackson, A. Japaridze, N. Kaplan, A. Klotz, H. Li, C. N. Likos, E. Locatelli, T. Lopez-Leon, T. Machon, C. Micheletti, D. Michieletto, A. Niemi, W. Niemyska, S. Niewieczerzal, F. Nitti, E. Orlandini, S. Pasquali, A. P. Perlinska, R. Podgornik, R. Potestio, N. M. Pugno, M. Ravnik, R. Ricca, C. M. Rohwer, A. Rosa, J. Smrek, A. Souslov, A. Stasiak, D. Steer, J. Sulkowska, P. Sulkowski, D. W. L. Sumners, C. Svaneborg, P. Szymczak, T. Tarenzi, R. Travasso, P. Virnau, D. Vlassopoulos, P. Ziherl, and S. Zumer, "Topology in soft and biological matter," Phys. Rep. **1075**, 1–137 (2024).

[11] Poelma, J. E., K. Ono, D. Miyajima, T. Aida, K. Satoh, and C. J. Hawker, "Cyclic block copolymers for controlling feature sizes in block copolymers lithography," ACS Nano **6**, 10845–10854 (2012).

[12] Feinberg, E. C., H. L. Hernandez, C. L. Plantz, E. B. Meija, N. R. Sottos, S. R. White, and J. S. Moore, "Cyclic poly(phthalaldehyde): Thermoforming a bulk transient material," ACS Macro Lett. **7**, 47–52 (2018).

[13] Alberts, B., A. Johnson, J. Lewis, M. Raff, K. Roberts, and P. Walter, *Molecular Biology of the Cell*, 6th ed. (Garland, New York, NY, 2014).

[14] Rao, S. S. P., "M. H. Huntley, N. C. Durand, E. K. Stamenova, I. D. Bochkov, J. T. Robinson, A. L. Sanborn, I. Machol, A. D. Omer, E. S. Lander, and E. L. Aiden, A 3D map of the human genome at kilobase resolution reveals principles of chromatin looping," Cell **159**, 1665–1680 (2014).

[15] Mallinson, J., and I. Collins, "Macrocycles in new drug discovery," Future Med. Chem. **4**, 1409–1438 (2012).

[16] Rubinstein, M., and R. H. Colby, *Polymer Physics* (Oxford University, Oxford, UK, 2003).

[17] Kapnistos, M., D. Vlassopoulos, J. Roovers, and L. G. Leal, "Linear rheology of architecturally complex macromolecules: Comb polymers with linear backbones," Mcromolecules **38**, 7852–7862 (2005).

[18] Edwards, S. F., "Statistical mechanics with topological constraints: I," Proc. Phys. Soc. **91**, 513–519 (1967).

[19] Prager, S., and H. L. Frisch, "Statistical mechanics of a simple entanglement," J. Chem. Phys. **46**, 1475–1483 (1967).

[20] Svaneborg, C., H. A. Karimi-Varzaneh, N. Hojdis, F. Fleck, and R. Everaers, "Multiscale approach to equilibrating model polymer melts," Phys. Rev. E **94**, 032502 (2016).

[21] Vettorel, T., A. Y. Grosberg, and K. Kremer, "Statistics of polymer rings in the melt: A numerical simulation study," Phys. Biol. **6**, 025013 (2009).

[22] Vettorel, T., A. Y. Grosberg, and K. Kremer, "Territorial polymers," Phys. Today **62**, 72 (2009).

[23] Schram, R. D., A. Rosa, and R. Everaers, "Local loop opening in untangled ring polymer melts: A detailed 'Feynman test' of models for the large scale structure," Soft Matter **15**, 2418–2429 (2019).

[24] Flory, P., *Statistical Mechanics of Chain Molecules* (Interscience, New York, 1969).

[25] Müller, M., J. P. Wittmer, and M. E. Cates, "Topological effects in ring polymers: A computer simulation study," Phys. Rev. E **53**, 5063–5074 (1996).

[26] Müller, M., J. P. Wittmer, and M. E. Cates, "Topological effects in ring polymers. II. Influence of persistence length," Phys. Rev. E **61**, 4078–4089 (2000).

[27] Halverson, J. D., W. B. Lee, G. S. Grest, A. Y. Grosberg, and K. Kremer, "Molecular dynamics simulation study of nonconcatenated ring polymers in a melt: I. Statics," J. Chem. Phys. **134**, 204904 (2011).

[28] Rosa, A., and R. Everaers, "Ring polymers in the melt state: The physics of crumpling," Phys. Rev. Lett. **112**, 118302 (2014).

[29] Singh, M. K., M. Hu, Y. Cang, H.-P. Hsu, H. Therien-Aubin, K. Koynov, G. Fytas, K. Landfester, and K. Kremer, "Glass transition of disentangled and entangled polymer melts: Single-chain-nanoparticles approach," Macromolecules **53**, 7312–7321 (2020).

[30] Cremer, T., and C. Cremer, "Chromosome territories, nuclear architecture and gene regulation in mammalian cells," Nat. Rev. Genet. **2**, 292–301 (2001).

[31] Halverson, J. D., J. Smrek, K. Kremer, and A. Y. Grosberg, "From a melt of rings to chromosome territories: The role of topological constraints in genome folding," Rep. Prog. Phys. **77**, 022601 (2014).

[32] Singh, M. K., N. L. van Berkum, L. Williams, M. Imakaev, T. Ragoczy, A. Telling, I. Amit, B. R. Lajoie, P. J. Sabo, M. O. Dorschner, R. Sandstrom, B. Bernstein, M. A. Bender, M. Groudine, A. Gnirke, J. Stamatoyannopoulos, L. A. Mirny, E. S. Lander, and J. Dekker, "Comprehensive mapping of long-range interactions reveals folding principles of the human genome," Science **326**, 289–293 (2009).

[33] Grosberg, A., Y. Rabin, S. Havlin, and A. Neer, "Crumpled globule model of the three-dimensional structure of DNA," Europhys. Lett. **23**, 373–378 (1993).

[34] Sikorav, J.-L., and G. Jannink, "Kinetics of chromosome condensation in the presence of topoisomerases: A phantom chain model," Biophys. J. **66**, 827–837 (1994).

[35] Rosa, A., and R. Everaers, "Structure and dynamics of interphase chromosomes," PLoS Comput. Biol. **4**, e1000153 (2008).

[36] Rosa, A., N. B. Becker, and R. Everaers, "Looping probabilities in model interphase chromosomes," Biophys. J. **98**, 2410–2419 (2010).
[37] Chan, B., and M. Rubinstein, "Activity-driven chromatin organization during interphase: Compaction, segregation, and entanglement suppression," Proc. Natl. Acad. Sci. U.S.A. **121**, e2401494121 (2024).
[38] Fiers, W., and R. L. Sinsheimer, "The structure of the DNA of bacteriophage phi-X174. III. Ultracentrifugal evidence for a ring structure," J. Mol. Biol. **5**, 424–434 (1962).
[39] Hotta, Y., and A. Bassel, "Molecular size and circularity of DNA in cells of mammals and higher plants," Proc. Natl. Acad. Sci. U.S.A. **53**, 356–362 (1965).
[40] Semlyen, J. A., B. R. Wood, and P. Hodge, "Cyclic polymers: Past, present and future," Polym. Adv. Technol. **5**, 473–478 (1994).
[41] Dodgon, K., and J. A. Semlyen, "Studies of cyclic and linear poly(dimethyl siloxanes): 1. Limiting viscosity number–molecular weight relationships," Polymer **18**, 1265–1268 (1977).
[42] Ederle, Y., K. S. Naraghi, and P. J. Lutz, "Synthesis of cyclic macromolecules," in *Materials Science and Technology* (Wiley, Weinheim, Germany, 1999).
[43] McKenna, G. B., G. Hadziioannou, P. J. Lutz, G. Hild, C. Strazielle, C. Straupe, P. Rempp, and A. J. Kovacs, "Dilute solution characterization of cyclic polystyrene molecules and their zero-shear viscosity in the melt," Macromolecules **20**, 498–512 (1987).
[44] Roovers, J., and P. M. Toporowski, "Synthesis of high molecular weight ring polystyrenes," Macromolecules **16**, 843–849 (1983).
[45] Roovers, J., "Organic cyclic polymers," in *Cyclic Polymers*, 2nd ed. (Kluwer Academic, New York, NY, 2000).
[46] Roovers, J., and P. M. Toporowski, "Synthesis and characterization of ring polybutadienes," J. Polym. Sci., Part B: Polym. Phys. **26**, 1251–1259 (1988).
[47] Roovers, J., "Viscoelastic properties of polybutadiene rings," Macromolecules **21**, 1517–1521 (1988).
[48] McKenna, G. B., B. J. Hostetter, N. Hadjichristidis, L. J. Fetters, and D. J. Plazek, "A study of the linear viscoelastic properties of cyclic polystyrenes using creep and recovery measurements," Macromolecules **22**, 1834–1852 (1989).
[49] Halverson, J. D., W. B. Lee, G. S. Grest, A. Y. Grosberg, and K. Kremer, "Molecular dynamics simulation study of nonconcatenated ring polymers in a melt: II. Dynamics," J. Chem. Phys. **134**, 204905 (2011).
[50] Orrah, D. J., J. A. Semlyen, and S. B. Ross-Murphy, "Studies of cyclic and linear poly(dimethylsiloxnes): 27. Bulk viscosities and densities above the critical molar mass for entanglement," Polymer **29**, 1452–1454 (1988).
[51] McKenna, G. B., and D. J. Plazek, "The viscosity of blends of linear and cyclic molecules of similar molecular mass," Polym. Commun. **27**, 304–306 (1986).
[52] Orrah, D. J., J. A. Semlyen, and S. B. Ross-Murphy, "Studies of cyclic and linear poly(dimethylsiloxnes): 28. Viscosities and densities of ring and chain poly(dimethylsiloxane) blends," Polymer **29**, 1455–1458 (1988).
[53] Lee, H. C., H. Lee, W. Lee, T. Chang, and J. Roovers, "Fractionation of cyclic polystyrene from linear precursor by HPLC at the chromatographic critical condition," Macromolecules **33**, 8119–8121 (2000).
[54] Chang, T., "Polymer characterization by interaction chromatography," J. Polym. Sci., Part B: Polym. Phys. **43**, 1591–1607 (2005).
[55] Chang, T., "Chromatographic separation of polymers," in *Recent Progress in Separation of Macromolecules and Particulates*, ACS Symposium Series, edited by Y. Wang, W. Gao, S. Orski, and X. M. Liu (ACS, Washington, DC, 2018), pp. 1–17.
[56] Ziebarth, J. D., A. A. Gardiner, Y. Wang, Y. Jeong, J. Ahn, T. Jin, and T. Chang, "Comparison of critical adsorption points of ring polymers with linear polymers," Macromolecules **49**, 8780–8788 (2016).
[57] Khokhlov, A. R., and S. K. Nechaev, "Polymer chain in an array of obstacles," Phys. Lett. **112**, 156–160 (1985).
[58] Obukhov, S. P., M. Rubinstein, and T. Duke, "Dynamics of a ring polymer in a gel," Phys. Rev. Lett. **73**, 1263–1266 (1994).
[59] Wang, J., T. C. O'Connor, G. S. Grest, and T. Ge, "Superstretchable elastomer from cross-linked ring polymers," Phys. Rev. Lett. **128**, 237801 (2022).
[60] Kruteva, M., J. Allgaier, and D. Richter, "Topology matters: Conformation and microscopic dynamics of ring polymers," Macromolecules **56**, 7203–7229 (2023).
[61] *Cyclic Polymers*, edited by J. A. Semlyen (Elsevier, New York, NY, 2002).
[62] *Topological Polymer Chemistry: Progress of Cyclic Polymers in Syntheses, Properties and Functions*, edited by Y. Tezuka (World Scientific, Singapore, 2013).
[63] Haque, F. M., and S. M. Grayson, "The synthesis, properties and potential applications of cyclic polymers," Nat. Chem. **12**, 433–444 (2020).
[64] de Gennes, P. G., *Scaling Concepts in Polymer Physics* (Cornell University, Ithaca, 1979).
[65] Douglas, J., and K. F. Freed, "Renormalization and the two-parameter theory," Macromolecules **17**, 2344–2354 (1984).
[66] Freire, J. J., R. Prats, J. Pla, and J. Garcia de la Torre, "Hydrodynamic properties of flexible branched chains. Monte Carlo nonpreaveraged calculations for stars and preaveraged results for combs," Macromolecules **17**, 1815–1821 (1984).
[67] Lipson, J. E. G., D. S. Gaunt, M. K. Wilkinson, and S. G. Whittington, "Lattice models of branched polymers: Combs and brushes," Macromolecules **20**, 186–190 (1987).
[68] Ohno, K., and K. Binder, "Scaling theory of star polymers and general polymer networks in bulk and semi-infinite good solvents," J. Phys. **49**, 1329–1351 (1988).
[69] Batoulis, J., and K. Kremer, "Thermodynamic properties of star polymers: Good solvents," Macromolecules **22**, 4277–4285 (1989).
[70] Douglas, J. F., J. Roovers, and K. F. Freed, "Characterization of branching architecture through 'universal' ratios of polymer solution properties," Macromolecules **23**, 4168–4180 (1990).
[71] Mourey, T. H., S. R. Turner, M. Rubinstein, J. M. J. Frechet, C. J. Hawker, and K. L. Wooley, "Unique behavior of dendritic macromolecules: Intrinsic viscosity of polyether dendrimers," Macromolecules **25**, 2401–2406 (1992).
[72] Okumoto, M., Y. Tasaka, Y. Nakamura, and T. Norisuye, "Excluded-volume effects in star polymer solutions: Six-arm star polystyrene in cyclohexane near the θ temperature," Macromolecules **32**, 7430–7436 (1999).
[73] Striolo, A., J. M. Prausnitz, and A. Bertucco, "Osmotic second virial coefficient, intrinsic viscosity and molecular simulation for star and linear polystyrenes," Macromolecules **33**, 9583–9586 (2000).
[74] Tande, B. M., N. J. Wagner, M. E. Mackay, C. J. Hawker, and M. Jeong, "Viscosimetric, hydrodynamic, and conformational properties of dendrimers and dendrons," Macromolecules **34**, 8580–8585 (2001).
[75] Ballauff, M., and C. N. Likos, "Dendrimers in solution: Insight from theory and simulation," Angew. Chem. Int. Ed. **43**, 2998–3020 (2004).
[76] Maiti, P. K., and W. A. Goddard, "Solvent quality changes the structure of G8 PAMAM dendrimer, a disagreement with some experimental interpretations," J. Phys. Chem. B **110**, 25628–25632 (2006).
[77] Bosko, J. T., and J. R. Prakash, "Universal behavior of dendrimer solutions," Macromolecules **44**, 660–670 (2011).
[78] Santra, A., K. Kumari, R. Padinhateeri, B. Dünweg, and J. R. Prakash, "Universality of the collapse transition of sticky polymers," Soft Matter **15**, 7876–7887 (2019).

[79] Öttinger, H. C., *Stochastic Processes in Polymeric Fluids* (Springer, Berlin, 1996).
[80] Kröger, M., A. Alba-Perez, M. Laso, and H. C. Öttinger, "Variance reduced Brownian simulation of a bead-spring chain under steady shear flow considering hydrodynamic interaction effects," J. Chem. Phys. **113**, 4767–4773 (2000).
[81] Hadziioannou, G., P. M. Cotts, G. ten Brinke, C. C. Han, P. Lutz, C. Strazielle, P. Rempp, and A. J. Kovacs, "Thermodynamic and hydrodynamic properties of dilute solutions of cyclic and linear polystyrenes," Macromolecules **20**, 493–497 (1987).
[82] Gooßen, S., A. R. Brás, W. Pyckhout-Hintzen, A. Wischnewski, D. Richter, M. Rubinstein, J. Roovers, P. J. Lutz, Y. Jeong, T. Chang, and D. Vlassopoulos, "Influence of the solvent quality on ring polymer dimensions," Macromolecules **48**, 1598–1605 (2015).
[83] Schroeder, C. M., "Single polymer dynamics for molecular rheology," J. Rheol. **62**, 371–403 (2018).
[84] Zimm, B. H., and W. H. Stockmayer, "The dimensions of chain molecules containing branches and rings," J. Chem. Phys. **17**, 1301–1314 (1949).
[85] Semlyen, J. A., "Ring-chain equilibria and the conformations of polymer chains," in *Mechanisms of Polyreactions-Polymer Characterization* (Springer, Berlin, 1976), pp. 41–75.
[86] Higgins, J., K. Dodgson, and J. Semlyen, "Studies of cyclic and linear poly(dimethyl siloxanes): 3. Neutron scattering measurements of the dimensions of ring and chain polymers," Polymer **20**, 553–558 (1979).
[87] Higgins, J., K. Ma, L. Nicholson, J. Hayter, K. Dodgson, and J. Semlyen, "Studies of cyclic and linear poly(dimethyl siloxanes): 12. Observation of diffusion behaviour by quasielastic neutron scattering," Polymer **24**, 793–799 (1983).
[88] Roovers, J., "Dilute-solution properties of ring polystyrenes," J. Polym. Sci. Pol. Phys. Ed. **23**, 1117–1126 (1985).
[89] Ragnetti, M., D. Geiser, H. Höcker, and R. C. Oberthür, "Small angle neutron scattering (SANS) of cyclic and linear polystyrene in toluene," Makromol. Chem. **186**, 1701–1709 (1985).
[90] Lutz, P., G. B. McKenna, P. Rempp, and C. Strazielle, "Solution properties of ring-shaped polystyrenes," Makromol. Chem., Rapid Commun. **7**, 599–605 (1986).
[91] Hodgson, D. F., and E. J. Amis, "Dilute solution behavior of cyclic and linear polyelectrolytes," J. Chem. Phys. **95**, 7653–7663 (1991).
[92] Takano, A., Y. Kushida, Y. Ohta, K. Masuoka, and Y. Matsushita, "The second virial coefficients of highly-purified ring polystyrenes in cyclohexane," Polymer **50**, 1300–1303 (2009).
[93] Kramers, H. A., "The behavior of macromolecules in inhomogeneous flow," J. Chem. Phys. **14**, 415–424 (1946).
[94] Yamakawa, H., *Modern Theory of Polymer Solutions* (Harper and Row, New York, 1971).
[95] Prentis, J. J., "Spatial correlations in a self-repelling ring polymer," J. Chem. Phys. **76**, 1574–1583 (1982).
[96] Uehara, E., and T. Deguchi, "Statistical and hydrodynamic properties of topological polymers for various graphs showing enhanced short-range correlation," J. Chem. Phys. **145**, 164905 (2016).
[97] Zhu, L., X. Wang, J. Li, and Y. Wang, "Radius of gyration, mean span, and geometric shrinking factors of bridged polycyclic ring polymers," Macromol. Theory Simul. **25**, 482–496 (2016).
[98] Zifferer, G., and W. Preusser, "Monte Carlo simulation studies of the size and shape of ring polymers," Macromol. Theory Simul. **10**, 397–407 (2001).
[99] Suzuki, J., A. Takano, and Y. Matsushita, "The theta-temperature depression caused by topological effect in ring polymers studied by monte carlo simulation," J. Chem. Phys. **135**, 204903 (2011).
[100] Narros, A., A. J. Moreno, and C. N. Likos, "Effects of knots on ring polymers in solvents of varying quality," Macromolecules **46**, 3654–3668 (2013).
[101] Li, B., Z. Sun, L. An, and Z.-G. Wang, "The scaling behavior of the second virial coefficient of linear and ring polymer," Sci. China Chem. **59**, 619–623 (2016).
[102] Gartner, T. E., F. M. Haque, A. M. Gomi, S. M. Grayson, M. J. A. Hore, and A. Jayaraman, "Scaling exponent and effective interactions in linear and cyclic polymer solutions: Theory, simulations, and experiments," Macromolecules **52**, 4579–4589 (2019).
[103] Miyaki, Y., Y. Einaga, H. Fujita, and M. Fukuda, "Flory's viscosity factor for the system polystyrene + cyclohexane at 34.5 °C," Macromolecules **13**, 588–592 (1980).
[104] Miyaki, Y., and H. Fujita, "Excluded-volume effects in dilute polymer solutions. 11. Tests of the two-parameter theory for radius of gyration and intrinsic viscosity," Macromolecules **14**, 742–746 (1981).
[105] Hayward, R. C., and W. W. Graessley, "Excluded volume effects in polymer solutions. 1. Dilute solution properties of linear chains in good and theta solvents," Macromolecules **32**, 3502–3509 (1999).
[106] Vidakovic, P., and F. Rondelez, "Temperature dependence of the hydrodynamic radius of flexible coils in solutions. 3. Experimental evidence for the crossover between Gaussian and excluded-volume single chain statistics," Macromolecules **18**, 700–708 (1985).
[107] Schäfer, L., *Excluded Volume Effects in Polymer Solutions* (Springer, Berlin, 1999).
[108] ten Brinke, G., and G. Hadziioannou, "Topological constraints and their influence on the properties of synthetic macromolecular systems. 1. Cyclic macromolecules," Macromolecules **20**, 480–485 (1987).
[109] Marko, J. F., and E. D. Siggia, "Bending and twisting elasticity of DNA," Macromolecules **27**, 981–988 (1994).
[110] Bauer, W. R., F. H. C. Crick, and J. H. White, "Supercoiled DNA," Sci. Am. **243**, 118–133 (1980).
[111] Hild, G., C. Strazielle, and R. Rempp, "Cyclic macromolecules. Synthesis and characterization of ring-shaped polystyrenes," Eur. Polym. J. **19**, 721–727 (1983).
[112] Ohta, Y., Y. Nakamura, Y. Matsushita, and A. Takano, "Synthesis, separation and characterization of knotted ring polymers," Polymer **53**, 466–470 (2012).
[113] Takano, A., Y. Ohta, K. Masuoka, K. Matsubara, T. Nakano, A. Hieno, M. Itakura, K. Takahashi, S. Kinugasa, D. Kawaguchi, Y. Takahashi, and Y. Matsushita, "Radii of gyration of ring-shaped polystyrenes with high purity in dilute solutions," Macromolecules **45**, 369–373 (2012).
[114] Santra, A., and J. Ravi Prakash, "Universality of dilute solutions of ring polymers in the thermal crossover region between theta and athermal solvents," J. Rheol. **66**, 775–792 (2022).
[115] Garcia Bernal, J. M., M. M. Tirado, J. J. Freire, and J. Garcia de la Torre, "Monte carlo calculation of hydrodynamic properties of linear and cyclic polymers in good solvents," Macromolecules **24**, 593–598 (1991).
[116] Duval, M., P. Lutz, and C. Strazielle, "Hydrodynamic dimensions of ring-shaped macromolecules in a good solvent," Die Makromol. Chem., Rapid Commun. **6**, 71–76 (1985).
[117] Bloomfield, V., and B. H. Zimm, "Viscosity, sedimentation, et cetera, of ring- and straight-chain polymers in dilute solution," J. Chem. Phys. **44**, 315–323 (1966).
[118] Fukatsu, M., and M. Kurata, "Hydrodynamic properties of flexible-ring macromolecules," J. Chem. Phys. **44**, 4539–4545 (1966).
[119] Rubio, A. M., J. J. Freire, M. Bishop, and J. H. R. Clarke, "Theta state, transition curves, and conformational properties of cyclic chains," Macromolecules **28**, 2240–2246 (1995).

[120] Jeong, Y., Y. Jin, T. Chang, F. Uhlik, and J. Roovers, "Intrinsic viscosity of cyclic polystyrene," Macromolecules **50**, 7770–7776 (2017).
[121] Schaub, B., D. B. Creamer, and H. Johannesson, "Intrinsic viscosities for linear and ring polymers using renormalization-group techniques," J. Phys. A: Math. Gen. **21**, 1431–1455 (1988).
[122] Vargas-Lara, F., B. A. Pazmino Betancourt, and J. F. Douglas, "A comparison between the solution properties of knotted ring and star polymers," J. Chem. Phys. **149**, 161101 (2018).
[123] Pan, S., D. Ahirwal, D. A. Nguyen, P. Sunthar, T. Sridhar, and J. R. Prakash, "Viscosity radius of polymers in dilute solutions: Universal behaviour from DNA rheology and Brownian dynamics simulations," Macromolecules **47**, 7548–7560 (2014).
[124] Adam, M., and M. Delsanti, "Light scattering by dilute solution of polystyrene in a good solvent," J. Phys. **37**, 1045–1049 (1976).
[125] Adam, M., and M. Delsanti, "Dynamical properties of polymer solutions in good solvent by rayleigh scattering experiments," Macromolecules **10**, 1229–1237 (1977).
[126] Venkataswamy, K., A. M. Jamieson, and R. G. Petschek, "Static and dynamic properties of polystyrene in good solvents: Ethylbenzene and tetrahydrofuran," Macromolecules **19**, 124–133 (1986).
[127] Reith, D., B. Müller, F. Müller-Plathe, and S. Wiegand, "How does the chain extension of poly (acrylic acid) scale in aqueous solution? A combined study with light scattering and computer simulation," J. Chem. Phys. **116**, 9100–9106 (2002).
[128] Douglas, J. F., and K. F. Freed, "Renormalization and the two-parameter theory. 2. Comparison with experiment and other two-parameter theories," Macromolecules **18**, 201–211 (1985).
[129] Düenweg, B., D. Reith, M. Steinhauser, and K. Kremer, "Corrections to scaling in the hydrodynamic properties of dilute polymer solutions," J. Chem. Phys. **117**, 914–924 (2002).
[130] Sunthar, P., and J. R. Prakash, "Dynamic scaling in dilute polymer solutions: The importance of dynamic correlations," Europhys. Lett. **75**, 77–83 (2006).
[131] Clisby, N., and B. Dünweg, "High-precision estimate of the hydrodynamic radius for self-avoiding walks," Phys. Rev. E **94**, 052102 (2016).
[132] Fixman, M., "Inclusion of hydrodynamic interaction in polymer dynamical simulations," Macromolecules **14**, 1710–1717 (1981).
[133] Liu, B., and B. Dünweg, "Translational diffusion of polymer chains with excluded volume and hydrodynamic interactions by Brownian dynamics simulation," J. Chem. Phys. **118**, 8061–8072 (2003).
[134] Jendrejack, R. M., M. D. Graham, and J. J. de Pablo, "Hydrodynamic interactions in long chain polymers: Application of the Chebyshev polynomial approximation in stochastic simulations," J. Chem. Phys. **113**, 2894–2900 (2000).
[135] Jendrejack, R. M., J. J. De Pablo, and M. D. Graham, "Stochastic simulations of DNA in flow: Dynamics and the effects of hydrodynamic interactions," J. Chem. Phys. **116**, 7752–7759 (2002).
[136] Hsieh, C.-C., L. Li, and R. G. Larson, "Modeling hydrodynamic interaction in Brownian dynamics: Simulations of extensional flows of dilute solutions of DNA and polystyrene," J. Non-Newtonian Fluid Mech. **113**, 147–191 (2003).
[137] Schroeder, C. M., E. S. G. Shaqfeh, and S. Chu, "Effect of hydrodynamic interactions on DNA dynamics in extensional flow: Simulation and single molecule experiment," Macromolecules **37**, 9242–9256 (2004).
[138] Prakash, J. R., "Universal dynamics of dilute and semidilute solutions of flexible linear polymers," Curr. Opin. Colloid Interface Sci. **43**, 63–79 (2019).
[139] Kumar, K. S., and J. R. Prakash, "Equilibrium swelling and universal ratios in dilute polymer solutions: Exact Brownian dynamics simulations for a delta function excluded volume potential," Macromolecules **36**, 7842–7856 (2003).
[140] Hsiao, K.-W., C. M. Schroeder, and C. E. Sing, "Ring polymer dynamics are governed by a coupling between architecture and hydrodynamic interactions," Macromolecules **49**, 1961–1971 (2016).
[141] Tu, M. Q., M. Lee, R. M. Robertson-Anderson, and C. M. Schroeder, "Direct observation of ring polymer dynamics in the flow-gradient plane of shear flow," Macromolecules **53**, 9406–9419 (2020).
[142] Liebetreu, M., and C. N. Likos, "Hydrodynamic inflation of ring polymers under shear," Commun. Mater. **1**, 1–11 (2020).
[143] Smith, D. E., and S. Chu, "Response of flexible polymers to a sudden elongational flow," Science **281**, 1335–1340 (1998).
[144] Smith, D. E., H. E. Babcock, and S. Chu, "Single-polymer dynamics in steady shear flow," Science **283**, 1724–1727 (1999).
[145] Laib, S., R. M. Robertson-Anderson, and D. Smith, "Preparation and characterization of a set of linear DNA molecules for polymer physics and rheology studies," Macromolecules **39**, 4115–4119 (2006).
[146] Paiva, W. A., S. D. Alakwe, J. Marfai, M. V. Jennison-Henderson, R. A. Achong, T. Duche, A. A. Weeks, R. M. Robertson-Anderson, and N. J. Oldenhuis, "From bioreactor to bulk rheology: Achieving scalable production of highly concentrated circular DNA," Adv. Mater. **36**, 2405490 (2024).
[147] Li, Y., K.-W. Hsiao, C. A. Brockman, D. Y. Yates, R. M. Robertson-Anderson, J. A. Kornfield, M. J. San Francisco, C. M. Schroeder, and G. B. McKenna, "When ends meet: Circular DNA stretches differently in elongational flows," Macromolecules **48**, 5997–6001 (2015).
[148] Liebetreu, M., M. Ripoll, and C. N. Likos, "Trefoil knot hydrodynamic delocalization on sheared ring polymers," ACS Macro Lett. **7**, 447–452 (2018).
[149] Farimani, R. A., Z. Ahmadian, C. N. Likos, and R. M. Ejtehadi, "Effects of linking on the shear response of connected ring polymers: Catenanes and bonded rings flow differently," Phys. Rev. Lett. **132**, 148101 (2024).
[150] Schneck, C., J. Smrek, C. N. Likos, and A. Zöttl, "Supercoiled ring polymers under shear flow," Nanoscale **16**, 8880–8899 (2024).
[151] Zhou, Y., K.-W. Hsiao, K. E. Regan, D. Kong, G. B. McKenna, R. M. Robertson-Anderson, and C. M. Schroeder, "Effect of molecular architecture on ring polymer dynamics in semidilute linear polymer solutions," Nat. Commun. **10**, 1753 (2019).
[152] Boydston, A. J., Y. Xia, J. A. Kornfield, I. A. Gorodetskaya, and R. H. Grubbs, "Cyclic ruthenium-alkylidene catalysts for ring-expansion metathesis polymerization," J. Am. Chem. Soc. **130**, 12775–12782 (2008).
[153] Chang, Y. A., and R. M. Waymouth, "Recent progress on the synthesis of cyclic polymers via ring-expansion strategies," J. Polym. Sci., Part A: Polym. Chem. **55**, 2892–2902 (2017).
[154] Zhou, L., L. T. Reilly, C. Shi, E. C. Quinn, and E. Y.-X. Chen, "Proton-triggered topological transformation in superbase-mediated selective polymerization enables access to ultrahigh-molar-mass cyclic polymers," Nat. Chem. **16**, 1357–1365 (2024).
[155] Robertson, R. M., and D. E. Smith, "Self-diffusion of entangled linear and circular DNA molecules: Dependence on length and concentration," Macromolecules **40**, 3373–3377 (2007).
[156] Robertson, R. M., and D. E. Smith, "Strong effects of molecular topology on diffusion of entangled DNA molecules," Proc. Natl. Acad. Sci. U.S.A. **104**, 4824–4827 (2007).
[157] Chapman, C. D., S. Shanbhag, D. E. Smith, and R. M. Robertson-Anderson, "Complex effects of molecular topology on diffusion in entangled biopolymer blends," Soft Matter **8**, 9177–9182 (2012).

[158] Zhou, Y., and C. M. Schroeder, "Transient and average unsteady dynamics of single polymers in large-amplitude oscillatory extension," Macromolecules **49**, 8018–8030 (2016).
[159] Zhou, Y., and C. M. Schroeder, "Single polymer dynamics in large amplitude oscillatory extension," Phys. Rev. Fluids **1**, 053301 (2016).
[160] Tu, M. Q., H. V. Nguyen, E. Foley, M. I. Jacobs, and C. M. Schroeder, "3D manipulation and dynamics of soft materials in 3D flows," J. Rheol. **67**, 877–890 (2023).
[161] Edwards, S. F., "The statistical mechanics of a polymerized material," Proc. Phys. Soc. **92**, 9–16 (1967).
[162] de Gennes, P.-G., "Reptation of a polymer chain in the presence of fixed obstacles," J. Chem. Phys. **55**, 572–579 (1971).
[163] Schleger, P., B. Farago, C. Lartigue, A. Kollmar, and D. Richter, "Clear evidence of reptation in polyethylene from neutron spin-echo spectroscopy," Phys. Rev. Lett. **81**, 124–127 (1998).
[164] Monkenbusch, M., M. Kruteva, and D. Richter, "Dynamic structure factors of polymer melts as observed by neutron spin echo: Direct comparison and reevaluation," J. Chem. Phys. **159**, 034902 (2023).
[165] Cates, M. E., and J. M. Deutsch, "Conjectures on the statistics of ring polymers," J. Phys. **47**, 2121–2128 (1986).
[166] Daoud, M., and J. F. Joanny, "Conformation of branched polymers," J. Physique **42**, 1359–1371 (1981).
[167] Everaers, R., A. Y. Grosberg, M. Rubinstein, and A. Rosa, "Flory theory of randomly branched polymers," Soft Matter **13**, 1223–1234 (2017).
[168] Rosa, A., and R. Everaers, "Beyond flory theory: Distribution functions for interacting lattice trees," Phys. Rev. E **95**, 012117 (2017).
[169] Rosa, A., and R. Everaers, "Conformational statistics of randomly branching double-folded ring polymers," Eur. Phys. J. E **42**, 7 (2019).
[170] Gutin, A. M., A. Y. Grosberg, and E. I. Shakhnovich, "Polymers with annealed and quenched branchings belong to different universality classes," Macromolecules **26**, 1293–1295 (1993).
[171] Grosberg, A. Y., "Annealed lattice animal model and flory theory for the melt of non-concatenated rings: Towards the physics of crumpling," Soft Matter **10**, 560–565 (2014).
[172] Rosa, A., and R. Everaers, "Computer simulations of melts of randomly branching polymers," J. Chem. Phys. **145**, 164906 (2016).
[173] Kruteva, M., J. Allgaier, M. Monkenbusch, L. Porcar, and D. Richter, "Self-similar polymer ring conformations based on elementary loops: A direct observation by sans," ACS Macro. Lett. **9**, 507–511 (2020).
[174] Smrek, J., and A. Y. Grosberg, "Understanding the dynamics of rings in the melt in terms of the annealed tree model," J. Phys.: Condens. Matter **27**, 064117 (2015).
[175] Ghobadpour, E., M. Kolb, M. R. Ejtehadi, and R. Everaers, "Monte carlo simulation of a lattice model for the dynamics of randomly branching double-folded ring polymers," Phys. Rev. E **104**, 014501 (2021).
[176] Ghobadpour, E., M. Kolb, I. Junier, and R. Everaers, "The emergent dynamics of double-folded randomly branching ring polymers," arXiv.2503.01446 (2025).
[177] Brás, A. R., R. Pasquino, T. Koukoulas, G. Tsolou, O. Holderer, A. Radulescu, J. Allgaier, V. G. Mavrantzas, W. Pyckhout-Hintzen, D. Vlassopoulos, D. Richter, "Structure and dynamics of polymer rings by neutron scattering: Breakdown of the rouse model," Soft Matter **7**, 11169–11176 (2011).
[178] Gooßen, S., A. Brás, M. Krutyeva, M. Sharp, P. Falus, A. Feoktystov, U. Gasser, W. Pyckhout-Hintzen, A. Wischnewski, and D. Richter, "Molecular scale dynamics of large ring polymers," Phys. Rev. Lett. **113**, 168302 (2014).
[179] Brás, A. R., S. Gooßen, M. Krutyeva, A. Radulescu, B. Farago, J. Allgaier, W. Pyckhout-Hintzen, A. Wischnewski, and D. Richter, "Compact structure and non-gaussian dynamics of ring polymer melts," Soft matter **10**, 3649–3655 (2014).
[180] Kruteva, M., J. Allgaier, M. Monkenbusch, I. Hoffmann, and D. Richter, "Structure and dynamics of large ring polymers," J. Rheol. **65**, 713–727 (2021).
[181] Obukhov, S., A. Johner, J. Baschnagel, H. Meyer, and J. P. Wittmer, "Melt of polymer rings: The decorated loop model," Europhys. Lett. **105**, 48005 (2014).
[182] Ge, T., S. Panyukov, and M. Rubinstein, "Self-similar conformations and dynamics in entangled melts and solutions of nonconcatenated ring polymers," Macromolecules **49**, 708–722 (2016).
[183] Everaers, R., H. A. Karimi-Varzaneh, F. Fleck, N. Hojdis, and C. Svaneborg, "Kremer–Grest models for commodity polymer melts: Linking theory, experiment, and simulation at the Kuhn scale," Macromolecules **53**, 1901–1916 (2020).
[184] Tomiyoshi, Y., T. Murashima, and T. Kawakatsu, "Single-chain slip-spring simulation for entangled nonconcatenated ring polymer melts," Macromolecules **58**, 1804–1816 (2025).
[185] Mei, B., Z. E. Dell, and K. S. Schweizer, "Microscopic theory of long-time center-of-mass self-diffusion and anomalous transport in ring polymer liquids," Macromolecules **53**, 10431–10445 (2020).
[186] Dell, Z. E., and K. S. Schweizer, "Intermolecular structural correlations in model globular and unconcatenated ring polymer liquids," Soft Matter **14**, 9132–9142 (2018).
[187] Mei, B., Z. E. Dell, and K. S. Schweizer, "Theory of transient localization, activated dynamics, and a macromolecular glass transition in ring polymer liquids," ACS Macro Lett. **10**, 1229–1235 (2021).
[188] Tu, M. Q., O. Davydovich, B. Mei, P. K. Singh, G. S. Grest, K. S. Schweizer, T. C. O'Connor, and C. M. Schroeder, "Unexpected slow relaxation dynamics in pure ring polymers arise from intermolecular interactions," ACS Polymers Au **3**, 307–317 (2023).
[189] Mei, B., G. S. Grest, S. Liu, T. C. O'Connor, and K. S. Schweizer, "Unified understanding of the impact of semiflexibility, concentration, and molecular weight scaling on macromolecular-scale ring diffusion," Proc. Natl. Acad. Sci. U.S.A. **121**, e2403964121 (2024).
[190] Kruteva, M., M. Monkenbusch, J. Allgaier, O. Holderer, S. Pasini, I. Hoffmann, and D. Richter, "Self-similar dynamics of large polymer rings: A neutron spin echo study," Phys. Rev. Lett. **125**, 238004 (2020).
[191] Pasquino, R., T. C. Vasilakopoulos, Y. C. Jeong, H. Lee, S. Rogers, G. Sakellariou, J. Allgaier, A. Takano, A. R. Bras, T. Chang, S. Goossen, W. Pyckhout-Hintzen, A. Wischnewski, N. Hadjichristidis, D. Richter, M. Rubinstein, and D. Vlassopoulos, "Viscosity of ring polymer melts," ACS Macro Lett. **2**, 874–878 (2013).
[192] Doi, Y., A. Matsumoto, T. Inoue, T. Iwamoto, A. Takano, Y. Matsushita, Y. Takahashi, and H. Watanabe, "Re-examination of terminal relaxation behavior of high-molecular-weight ring polystyrene melts," Rheol. Acta **56**, 567–581 (2017).
[193] Doi, Y., K. Matsubara, Y. Ohta, T. Nakano, D. Kawaguchi, Y. Takahashi, A. Takano, and Y. Matsuhita, "Melt rheology of ring polystyrenes with ultrahigh purity," Macromolecules **48**, 3140–3147 (2015).
[194] Kamble, S., D. Parisi, Y. Jeong, T. Chang, and D. Vlassopoulos, "Stress relaxation of critically fractionated entangled polybutadiene ring melts," Rheol. Acta **63**, 483–491 (2024).
[195] Parisi, D., S. Costanzo, Y. Jeong, J. Ahn, T. Chang, D. Vlassopoulos, J. D. Halverson, K. Kremer, T. Ge, M. Rubinstein, G. S. Grest, W. Srinin, A. Y. Grosberg, "Nonlinear shear rheology of entangled polymer rings," Macromolecules **54**, 2811–2827 (2021).
[196] Parisi, D., M. Kaliva, S. Costanzo, Q. Huang, P. J. Lutz, J. Ahn, T. Chang, M. Rubinstein, and D. Vlassopoulos, "Nonlinear rheometry

of entangled polymeric rings and ring-linear blends," J. Rheol. **65**, 695–711 (2021).

[197] Zhou, Y., C. D. Young, K. E. Regan, M. Lee, S. Banik, D. Kong, G. B. McKenna, R. M. Robertson-Anderson, C. E. Sing, and C. M. Schroeder, "Dynamics and rheology of ring-linear blend semidilute solutions in extensional flow: Single molecule experiments," J. Rheol. **65**, 729–744 (2021).

[198] Young, C. D., Y. Zhou, C. M. Schroeder, and C. E. Sing, "Dynamics and rheology of ring-linear blend semidilute solutions in extensional flow: Modeling and molecular simulations," J. Rheol. **65**, 757–777 (2021).

[199] Ubertini, M. A., J. Smrek, and A. Rosa, "Entanglement length scale separates threading from branching of unknotted and non-concatenated ring polymers in melts," Macromolecules **55**, 10723–10736 (2022).

[200] Tsalikis, D. G., V. G. Mavrantzas, and D. Vlassopoulos, "Analysis of slow modes in ring polymers: Threading of rings controls long-time relaxation," ACS Macro Lett. **5**, 755–760 (2016).

[201] Gooßen, S., M. Kruteva, M. Sharp, A. Feoktystov, J. Allgaier, W. Pyckhout-Hintzen, A. Wischnewski, and D. Richter, "Sensing polymer chain dynamics through ring topology: A neutron spin echo study," Phys. Rev. Lett. **115**, 148302 (2015).

[202] Parisi, D., J. Ahn, T. Chang, D. Vlassopoulos, and M. Rubinstein, "Stress relaxation in symmetric ring-linear polymer blends at low ring fractions," Macromolecules **53**, 1685–1693 (2020).

[203] Katsarou, A. F., A. J. Tsamopoulos, D. G. Tsalikis, and V. G. Mavrantzas, "Dynamic heterogeneity in ring-linear polymer blends," Polymers **12**, 752 (2020).

[204] Tsalikis, D. G., and V. G. Mavrantzas, "Size and diffusivity of polymer rings in linear polymer matrices: The key role of threading events," Macromolecules **53**, 803–820 (2020).

[205] Grest, G. S., T. Ge, S. J. Plimpton, M. Rubinstein, and T. C. O'Connor, "Entropic mixing of ring/linear polymer blends," ACS Polymers Au **3**, 209–216 (2023).

[206] Vigil, D. L., T. Ge, M. Rubinstein, T. C. O'Connor, and G. S. Grest, "Measuring topological constraint relaxation in ring-linear polymer blends," Phys. Rev. Lett. **133**, 118101 (2024).

[207] Peddireddy, R., M. Lee, Y. Zhou, S. Adalbert, S. Anderson, C. M. Schroeder, and R. M. Robertson-Anderson, "Unexpected entanglement dynamics in semidilute blends of supercoiled and ring DNA," Soft Matter **16**, 152–161 (2020).

[208] Marfai, J., R. McGorty, and R. M. Robertson-Anderson, "Cooperative rheological state-switching of enzymatically-driven composites of circular DNA and dextran," Adv. Mater. **35**, 2305824 (2023).

[209] Peddireddy, R., R. Clairmont, P. Neill, R. McGorty, and R. M. Robertson-Anderson, "Optical-tweezers-integrating-differential-dynamic-microscopy maps the spatiotemporal propagation of nonlinear strains in polymer blends and composites," Nat. Commun. **13**, 5180 (2022).

[210] Khanal, P., R. Peddireddy, J. Marfai, R. McGorty, and R. M. Robertson-Anderson, "DNA topology dictates emergent bulk elasticity and hindered macromolecular diffusion in DNA-dextran composites," J. Rheol. **66**, 699–715 (2022).

[211] Peddireddy, K. R., R. Clairmont, and R. M. Robertson-Anderson, "Polymer threadings and rigidity dictate the viscoelasticity of entangled ring-linear blends and their composites with rigid rod microtubules," J. Rheol. **67**, 125–138 (2023).

[212] Chen, D. K., K. Molnar, H. Kim, C. A. Helfer, G. Kaszas, J. E. Puskas, J. A. Kornfield, and G. B. McKenna, "Linear viscoelastic properties of putative cyclic polymers synthesized by reversible radical recombination polymerization (R3P)," Macromolecules **56**, 1013–1032 (2023).

[213] McKenna, G. B., D. Chen, S. C. H. Mangalara, D. Kong, and S. Banik, "Some open challenges in polymer physics," Polymer Engineering and Science **62**, 1325–1355 (2022).

[214] Tsalikis, D. G., P. V. Alatas, L. D. Peristeras, and V. G. Mavrantzas, "Scaling laws for the conformation and viscosity of ring polymers in the crossover region around me from detailed molecular dynamics simulations," ACS Macro Lett. **7**, 916–920 (2018).

[215] Kong, D., S. Banik, M. J. San Francisco, M. Lee, R. M. Robertson-Anderson, C. M. Schroeder, and G. B. McKenna, "Rheology of entangled solutions of ring-linear DNA blends," Macromolecules **55**, 1205–1217 (2022).

[216] Peponaki, K., D. G. Tsalikis, N. Patelis, T. Chang, and D. Vlassopoulos, "Revisiting the viscosity of moderately entangled ring polymer melts," Macromolecules **57**, 7263–7269 (2024).

[217] Kruteva, M., J. Allgaier, and D. Richter, "Direct observation of two distinct diffusive modes for polymer rings in linear polymer matrices by pulsed field gradient (PFG) NMR," Macromolecules **50**, 9482–9493 (2017).

[218] Tsalikis, D. G., T. Koukoulas, V. G. Mavrantzas, R. Pasquino, D. Vlassopoulos, W. Pyckhout-Hintzen, A. Wischnewski, M. Monkenbusch, and D. Richter, "Microscopic structure, conformation, and dynamics of ring and linear poly(ethylene oxide) melts from detailed atomistic molecular dynamics simulations: Dependence on chain length and direct comparison with experimental data," Macromolecules **50**, 2565–2584 (2017).

[219] O'Connor, T. C., T. Ge, M. Rubinstein, and G. S. Grest, "Topological linking drives anomalous thickening of ring polymers in weak extensional flows," Phys. Rev. Lett. **124**, 027801 (2020).

[220] Yan, Z.-C., S. Costanzo, Y. Jeong, T. Chang, and D. Vlassopoulos, "Linear and nonlinear shear rheology of a marginally entangled ring polymer," Macromolecules **49**, 1444–1453 (2016).

[221] Peddireddy, R., M. Lee, C. M. Schroeder, and R. M. Robertson-Anderson, "Viscoelastic properties of ring-linear DNA blends exhibit nonmonotonic dependence on blend composition," Phys. Rev. Res. **2**, 023213 (2020).

[222] Yoon, J., J. Kim, and C. Baig, "Nonequilibrium molecular dynamics study of ring polymer melts under shear and elongation flows: A comparison with their linear analogs," J. Rheol. **60**, 673–685 (2016).

[223] A. J. Tsamopoulos, A. F. Katsarou, D. G. Tsalikis, and V. G. Mavrantzas, "Shear rheology of unentangled and marginally entangled ring polymer melts from large-scale nonequilibrium molecular dynamics simulations," Polymers **11**, 1194 (2019).

[224] Huang, Q., J. Ahn, D. Parisi, T. Chang, O. Hassager, S. Panyukov, M. Rubinstein, and D. Vlassopoulos, "Unexpected stretching of entangled ring macromolecules," Phys. Rev. Lett. **122**, 208001 (2019).

[225] Borger, A., W. Wang, T. C. O'Connor, T. Ge, G. S. Grest, G. V. Jensen, J. Ahn, T. Chang, O. Hassager, K. Mortensen, D. Vlassopoulos, and Q. Huang, "Threading–unthreading transition of linear-ring polymer blends in extensional flow," ACS Macro Lett. **9**, 1452–1457 (2020).

[226] Clarson, S. J., K. Dodgson, and J. A. Semlyen, "Studies of cyclic and linear poly(dimethylsiloxanes): 19. Glass transition temperatures and crystallization behaviour," Polymer **26**, 930–934 (1985).

[227] Fox, T., and P. Flory, "Second-order transition temperatures and related properties of polystyrene. I. Influence of molecular weight," J. Appl. Phys. **21**, 581–591 (1950).

[228] Gibbs, J., and E. DiMarzio, "Nature of the glass transition and the glassy state," J. Chem. Phys. **28**, 373–383 (1958).

[229] McKenna, G., "Glass formation and glassy behavior," in *Omprehensive Polymer Science: Vol. 2. Polymer Properties*, edited by C. Booth and C. Price (Oxford, UK, 1989), pp. 311–363.
[230] Roovers, J., "The melt properties of ring polystyrenes," Macromolecules **18**, 1359–1361 (1985).
[231] Clarson, S. J., J. A. Semlyen, and K. Dodgson, "Cyclic polysiloxanes: 4. Glass transition temperatures of poly(phenylmethylsiloxanes," Polymer **32**, 2823–2827 (1991).
[232] Hogen-Esch, T., J. Sundararajan, and W. Toreki, "Synthesis and characterization of topologically interesting vinyl polymers," Makromol. Chem. **47**, 23–42 (1991).
[233] Gao, L., J. Oh, Y. Tua, T. Chang, and C. Li, "Glass transition temperature of cyclic polystyrene and the linear counterpart contamination effect," Polymer **170**, 198–203 (2019).
[234] Liu, X., D. Chen, Z. He, M. Zhang, and H. Hu, "Molecular weight dependence of the glass transition of cyclic polystyrene," Polym. Comm. **32**, 123–125 (1991).
[235] Simon, S. L., P. Bernazzani, and G. B. McKenna, "Effects of freeze-drying on the glass temperature of cyclic polystyrenes," Polymer **44**, 8025–8032 (2003).
[236] Santangelo, P., C. M. Roland, D. Chang, T. Cho, and J. Roovers, "Dynamics near the glass temperature of low molecular weight cyclic polystyrene," Macromolecules **34**, 9002–9005 (2001).
[237] Zhang, L., R. Elupula, S. Grayson, and J. Torkelson, "Suppression of the fragility-confinement effect via low molecular weight cyclic or ring polymer topology," Macromolecules **50**, 1147–1154 (2017).
[238] Gan, Y., D. Dong, and T. Hogen-Esch, "Effects of lithium bromide on the glass transition temperatures of linear and macrocyclic poly(2-vinylpyridine) and polystyrene," Macromolecules **28**, 383–385 (1995).
[239] Rique-Lurbet, L., M. Schappacher, and A. Deffieux, "New strategy for the synthesis of cyclic polystyrenes: Principle and application," Macromolecules **27**, 6318–6324 (1994).
[240] Alberty, K. A., T. Hogen-Esch, and S. Carlotti, "Synthesis and characterization of macrocyclic vinyl-aromatic polymers. molecular weight-dependent glass transition temperatures and emission of macrocyclic polystyrene," Macromol. Chem. Phys. **206**, 1035–1042 (2005).
[241] Song, X.-Y., Z.-Y. Yang, Q.-L. Yuan, S.-W. Li, Z.-Q. Tang, Y.-T. Dong, S.-C. Jiang, and W.-S. Xu, "Understanding mass dependence of glass formation in ring polymers," Chinese J. Polym. Sci. **41**, 1447–1461 (2023).
[242] Everaers, R., S. K. Sukumaran, G. S. Grest, C. Svaneborg, A. Sivasubramanian, and K. Kremer, "Rheology and microscopic topology of entangled polymeric liquids," Science **303**, 823–826 (2004).
[243] Sukumaran, S. K., G. S. Grest, K. Kremer, and R. Everaers, "Identifying the primitive path mesh in entangled polymer liquids," J. Polym. Sci, Part B: Polym. Phys. **43**, 917–933 (2005).
[244] Kröger, M., "Shortest multiple disconnected path for the analysis of entanglements in two- and three-dimensional polymeric systems," Comp. Phys. Commun. **168**, 209–232 (2005).
[245] Shanbhag, S., and R. G. Larson, "Chain retraction potential in a fixed entanglement network," Phys. Rev. Lett. **94**, 076001 (2005).
[246] Zhou, Q., and R. G. Larson, "Primitive path identification and statistics in molecular dynamics simulations of entangled polymer melts," Macromolecules **38**, 5761–5765 (2005).
[247] Tzoumanekas, C., and D. N. Theodorou, "Topological analysis of linear polymer melts: A statistical approach," Macromolecules **39**, 4592–4604 (2006).
[248] Edwards, S. F., "The theory of rubber elasticity," Britich Polymer Journal **9**, 140–143 (1977).
[249] Rubinstein, M., and E. Helfand, "Statistics of the entanglement of polymers: Concentration effects," J. Chem. Phys. **82**, 2477–2483 (1985).
[250] Everaers, R., "Topological versus rheological entanglement length in primitive-path analysis protocols, tube models, and slip-link models," Phys. Rev. E **86**, 022801 (2012).
[251] Uchida, N., G. S. Grest, and R. Everaers, "Viscoelasticity and primitive path analysis of entangled polymer liquids: From f-actin to polyethylene," J. Chem. Phys. **128**, 044902 (2008).
[252] Müller, M., J. P. Wittmer, and J.-L. Barrat, "On two intrinsic length scales in polymer physics: Topological constraints vs. entanglement length," Europhys. Lett. **52**, 406 (2000).
[253] Bernabei, M., P. Bacova, A. J. Moreno, A. Narros, and C. N. Likos, "Fluids of semiflexible ring polymers: Effective potentials and clustering," Soft Matter **9**, 1287–1300 (2013).
[254] Slimani, M. Z., P. Bacova, M. Bernabei, A. Narros, C. N. Likos, and A. J. Moreno, "Cluster glasses of semiflexible ring polymers," ACS Macro Lett. **3**, 611–616 (2014).
[255] Poier, P., P. Bačová, A. J. Moreno, C. N. Likos, and R. Blaak, "Anisotropic effective interactions and stack formation in mixtures of semiflexible ring polymers," Soft Matter **12**, 4805–4820 (2016).
[256] Zhao, Y., J. Rothorl, P. Bensenius, P. Virnau, and K. Daoulas, "Can polymer helicity affect topological chirality of polymer knots?" ACS Macro. Lett. **12**, 234–240 (2023).
[257] Colby, R. H., "Structure and linear viscoelasticity of flexible polymer solutions: Comparison of polyelectrolyte and neutral polymer solutions," Rheol. Acta **49**, 425–442 (2010).
[258] Stano, R., J. Smrek, and C. N. Likos, "Cluster formation in solutions of polyelectrolyte rings," ACS Nano **17**, 21369–21382 (2023).
[259] Molnar, K., H. Kim, D. Chen, C. A. Helfer, G. Kaszas, G. B. McKenna, J. A. Kornfield, C. Yuan, and J. E. Puskas, "PolyDODT: A macrocyclic elastomer with unusual properties," Polym. Chem. **13**, 668–676 (2022).
[260] Bates, F. S., L. J. Fetters, and G. D. Wignall, "Thermodynamics of isotopic polymer mixtures: Poly(vinylethylene) and poly(ethylethylene)," Macromolecules **21**, 1086–1094 (1988).
[261] Hsu, H.-P., M. K. Singh, Y. Cang, H. Therien-Aubin, M. Mezger, R. Berger, I. Lieberwirth, G. Fytas, and K. Kremer, "Free standing dry and stable nanoporous polymer films made through mechanical deformation," Adv. Sci. **10**, 2207472 (2023).
[262] Lang, M., "Ring conformations in bidisperse blends of ring polymers," Macromolecules **46**, 1158–1166 (2013).
[263] Smrek, J., and A. Y. Grosberg, "Minimal surfaces on unconcatenated polymer rings in melt," ACS Macro Lett. **5**, 750–754 (2016).
[264] Smrek, J., K. Kremer, and A. Rosa, "Threading of unconcatenated ring polymers at high concentrations: Double-folded versus time-equilibrated structures," ACS Macro Lett. **8**, 155–160 (2019).
[265] Obukhov, S. P., "Topologically induced glass transition in freely rotating rods," (1997), Kavli Institute for Theoretical Physics, Workshop on Jamming and Rheology: Constrained Dynamics on Microscopic and Macroscopic Scales.
[266] Michieletto, D., and M. S. Turner, "A topologically driven glass in ring polymers," Proc. Natl. Acad. Sci. U.S.A. **113**, 5195–5200 (2016).
[267] Michieletto, D., N. Nahali, and A. Rosa, "Glassiness and heterogeneous dynamics in dense solutions of ring polymers," Phys. Rev. Lett. **119**, 197801 (2017).
[268] Narros, A., A. J. Moreno, and C. N. Likos, "Influence of topology on effective potentials: Coarse-graining ring polymers," Soft Matter **6**, 2435–2441 (2010).
[269] Narros, A., C. N. Likos, A. J. Moreno, and B. Capone, "Multi-blob coarse graining for ring polymer solutions," Soft Matter **10**, 9601–9614 (2014).

[270] Staňo, R., C. N. Likos, and J. Smrek, "To thread or not to thread? Effective potentials and threading interactions between asymmetric ring polymers," Soft Matter **19**, 17–30 (2022).
[271] Wang, J., and T. Ge, "Crazing reveals an entanglement network in glassy ring polymers," Macromolecules **54**, 7500–7511 (2021).
[272] Hu, P., J. Madsen, Q. Huang, and A. Ladegaard Skov, "Elastomers without covalent cross-linking: Concatenated rings giving rise to elasticity," ACS Macro Lett. **9**, 1458–1463 (2020).
[273] Frank-Kamenetskii, M. D., A. V. Lukashin, and A. V. Vologodskii, "Statistical mechanics and topology of polymer chains," Nature **258**, 398–402 (1975).
[274] Michels, J., and F. Wiegel, "Probability of knots in a polymer ring," Phys. Lett. A **90**, 381–384 (1982).
[275] Marcone, B., E. Orlandini, A. L. Stella, and F. Zonta, "What is the length of a knot in a polymer?" J. Phys. A: Math. Gen. **38**, L15–L21 (2005).
[276] Grosberg, A. Y., "A few notes about polymer knots," Polym. Sci. Ser. A **51**, 70–79 (2009).
[277] Tubiana, L., E. Orlandini, and C. Micheletti, "Probing the entanglement and locating knots in ring polymers: A comparative study of different arc closure schemes," Prog. Theor. Phys. Supplement **191**, 192–204 (2011).
[278] Dai, L., "Developing the tube theory for polymer knots," Phys. Rev. Res. **2**, 022014 (2020).
[279] Zhang, J., H. Meyer, P. Virnau, and K. C. Daoulas, "Can soft models describe polymer knots?" Macromolecules **53**, 10475–10486 (2020).
[280] Benham, C. J., "Elastic model of supercoiling," Proc. Natl. Acad. Sci. U.S.A. **74**, 2397–2401 (1977).
[281] Vologodskii, A. V., and N. R. Cozzarelli, "Conformational and thermodynamic properties of supercoiled DNA," Annu. Rev. Biophys. Biomol. Struct. **23**, 609–643 (1994).
[282] Chirico, G., and J. Langowski, "Kinetics of DNA supercoiling studied by Brownian dynamics simulation," Biopolym.: Original Res. Biomolecules **34**, 415–433 (1994).
[283] Marko, J. F., and E. D. Siggia, "Statistical mechanics of supercoiled DNA," Phys. Rev. E **52**, 2912–2938 (1995).
[284] Smrek, J., J. Garamella, R. M. Robertson-Anderson, and D. Michieletto, "Topological tuning of DNA mobility in entangled solutions of supercoiled plasmids," Sci. Adv. **7**, eabf9260 (2021).
[285] Yan, Z.-C., M. D. Hossain, M. J. Monteiro, and D. Vlassopoulos, "Viscoelastic properties of unentangled multicyclic polystyrenes," Polymers **10**, 973 (2018).
[286] Deutsch, J. M., "The dynamics of entangled polymers," J. Phys. **48**, 141–150 (1987).
[287] Rubinstein, M., and S. P. Obukhov, "Memory effects in entangled polymer melts," Phys. Rev. Lett. **71**, 1856–1859 (1993).
[288] Semenov, A. N., and M. Rubinstein, "Dynamics of strongly entangled polymer systems: Activated reptation," Eur. Phys. J. B **1**, 87–94 (1998).
[289] Kruteva, M., M. Monkenbusch, J. Allgaier, W. Pyckhout-Hintzen, L. Porcar, and D. Richter, "Structure of polymer rings in linear matrices: Sans investigation," Macromolecules **56**, 4835–4844 (2023).
[290] Khokhlov, A., and S. Nechaev, "Topologically driven compatibility enhancement in the mixtures of rings and linear chains," J. Phys. II **6**, 1547–1555 (1996).
[291] Nam, S., J. Leisen, V. Breedveld, and H. W. Beckham, "Melt dynamics of blended poly(oxyethylene) chains and rings," Macromolecules **42**, 3121–3128 (2009).
[292] Papadopoulos, G. D., D. G. Tsalikis, and V. G. Mavrantzas, "Microscopic dynamics and topology of polymer rings immersed in a host matrix of longer linear polymers: Results from a detailed molecular dynamics simulation study and comparison with experimental data," Polymers **8**, 283 (2016).
[293] Murashima, T., K. Hagita, and T. Kawakatsu, "Viscosity overshoot in biaxial elongational flow: Coarse-grained molecular dynamics simulation of ring–linear polymer mixtures," Macromolecules **54**, 7210–7225 (2021).
[294] Murashima, T., K. Hagita, and T. Kawakatsu, "Topological transition in multicyclic chains with structural symmetry inducing stress-overshoot phenomena in multicyclic/linear blends under biaxial elongational flow," Macromolecules **55**, 9358–9372 (2022).
[295] Green, P. F., and E. J. Kramer, "Matrix effects on the diffusion of long polymer chains," Macromolecules **19**, 1108–1114 (1986).
[296] Brochard-Wyart, F., A. Ajdari, L. Leibler, M. Rubinstein, and J. L. Viovy, "Dynamics of stars and linear chains dissolved in a polymer melt," Macromolecules **27**, 803–808 (1994).
[297] Hsu, H.-P., and K. Kremer, "Clustering of entanglement points in highly strained polymer melts," Macromolecules **52**, 6756–6772 (2019).
[298] Pyromali, C., N. Patelis, M. Cutrano, M. Gosika, E. Glynos, A. J. Moreno, G. Sakellariou, J. Smrek, and D. Vlassopoulos, "Non-monotonic composition dependence of viscosity when adding single-chain nanoparticles to entangled polymers," Macromolecules **57**, 4826–4832 (2024).
[299] Elardo, M. J., A. M. Levenson, A. P. Kitos Vasconcelos, M. N. Pomfreta, and M. R. Golder, "A general synthesis of cyclic bottlebrush polymers with enhanced mechanical properties via graft-through ring expansion metathesis polymerization," Chem. Sci. **15**, 17193–17199 (2024).
[300] Doi, Y., A. Takano, Y. Takahashi, and Y. Matsuhita, "Viscoelastic properties of dumbbell-shaped polystyrenes in bulk and solution," Macromolecules **54**, 1366–1374 (2021).
[301] Doi, Y., Y. Ohta, A. Takano, Y. Takahashi, and Y. Matsushita, "Precise synthesis and characterization of tadpole-shaped polystyrenes with high purity," Macromolecules **46**, 1075–1081 (2013).
[302] Doi, Y., A. Takano, Y. Takahashi, and Y. Matsushita, "Melt rheology of tadpole-shaped polystyrenes," Macromolecules **48**, 8667–8674 (2015).
[303] Rosa, A., J. Smrek, M. S. Turner, and D. Michieletto, "Threading-induced dynamical transition in tadpole-shaped polymers," ACS Macro Lett. **9**, 743–748 (2020).
[304] Doi, Y., A. Takano, Y. Takahashi, and Y. Matsushita, "Melt rheology of tadpole-shaped polystyrenes with different ring sizes," Soft Matter **16**, 8720–8724 (2020).
[305] Dharmaraj, V. L., P. D. Godfrin, Y. Liu, and S. D. Hudson, "Rheology of clustering protein solutions," Biomicrofluidics **10**, 043509 (2016).
[306] Antonietti, M., K. J. Folsch, H. Sillescu, and T. Pakula, "Micronetworks by end-linking of polystyrene. 2. Dynamic mechanical behavior and diffusion experiments in the bulk," Macromolecules **22**, 2812–2817 (1989).
[307] Antonietti, M., T. Pakula, and W. Bremser, "Rheology of small spherical polystyrene microgels: A direct proof for a new transport mechanism in bulk polymers besides reptation," Macromolecules **28**, 4227–4233 (1995).
[308] Fuchs, M., and K. S. Schweizer, "Mode-coupling theory of the slow dynamics of polymeric liquids: Fractal macromolecular architectures," J. Chem. Phys. **106**, 347–375 (1997).
[309] Grosberg, A. Y., S. K. Nechaev, and E. I. Shakhnovich, "The role of topological constraints in the kinetics of collapse of macromolecules," J. Phys. France **49**, 2095–2100 (1988).
[310] Rastogi, S. D. R. Lippits, G. W. M. Peters, R. Graf, Y. Yao, andH. W. Spiess, , "Heterogeneity in polymer melts from melting of polymer crystals," Nat. Mater. **4**, 635–641 (2005).

[311] Vettorel, T., and K. Kremer, "Development of entanglements in a fully disentangled polymer melt," Macromol. Theory Simul. **19**, 44–56 (2010).

[312] Singh, M. K., M. Hu, Y. Cang, H.-P. Hsu, H. Therien-Aubin, K. Koynov, G. Fytas, K. Landfester, and K. Kremer, "Glass transition of disentangled and entangled polymer melts: Single-chain-nanoparticles approach," Macromolecules **53**, 7312–7321 (2020).

[313] Hartquist, C., S. Lin, J. H. Zhang, S. Wang, M. Rubinstein, and X. Zhao, "An elastomer with ultrahigh strain-induced crystallization," Sci. Adv. **9**, eadj0411 (2023).

[314] Smrek, J., I. Chubak, C. N. Likos, and K. Kremer, "Active topological glass," Nat. Commun. **11**, 26 (2020).

[315] Chubak, I., C. N. Likos, K. Kremer, and J. Smrek, "Emergence of active topological glass through directed chain dynamics and non-equilibrium phase segregation," Phys. Rev. Res. **2**, 043249 (2020).

[316] Grosberg, A. Y., and J.-F. Joanny, "Nonequilibrium statistical mechanics of mixtures of particles in contact with different thermostats," Phys. Rev. E **92**, 032118 (2015).

[317] Smrek, J., and K. Kremer, "Small activity differences drive phase separation in active-passive polymer mixtures," Phys. Rev. Lett. **118**, 098002 (2017).

[318] Alipour, E., and J. F. Marko, "Self-organization of domain structures by DNA-loop-extruding enzymes," Nucleic Acids Res. **40**, 11202–11212 (2012).

[319] Goloborodko, A., M. V. Imakaev, J. F. Marko, and L. Mirny, "Compaction and segregation of sister chromatids via active loop extrusion," eLife **5**, e14864 (2016).

[320] Ganji, M., I. A. Shaltiel, S. Bisht, E. Kim, A. Kalichava, C. H. Haering, and C. Dekker, "Real-time imaging of DNA loop extrusion by condensin," Science **360**, 102–105 (2018).

[321] Cozzarelli, N. R., "DNA gyrase and the supercoiling of DNA," Science **207**, 953–960 (1980).

[322] Champoux, J. J., "DNA topoisomerases: Structure, function, and mechanism," Annu. Rev. Biochem. **70**, 369–413 (2001).

[323] Sanborn, A. L., S. S. P. Rao, S.-C. Huang, N. C. Durand, M. H. Huntley, A. I. Jewett, I. D. Bochkov, D. Chinnappan, A. Cutkosky, J. Li, K. P. Geeting, A. Gnirke, A. Melnikov, D. McKenna, E. K. Stamenova, E. S. Lander, and E. L. Aiden, "Chromatin extrusion explains key features of loop and domain formation in wild-type and engineered genomes," Proc. Natl. Acad. Sci. U.S.A. **112**, E6456–E6465 (2015).

[324] Fudenberg, G., M. Imakaev, C. Lu, A. Goloborodko, N. Abdennur, and L. A. Mirny, "Formation of chromosomal domains by loop extrusion," Cell Rep. **15**, 2038–2049 (2016).

[325] Polovnikov, K., S. Belan, M. Imakaev, H. B. Brandão, and L. A. Mirny, "Fractal polymer with loops recapitulates key features of chromosome organization," bioRxiv 2022–02 (2022).

[326] Chan, B., and M. Rubinstein, "Theory of chromatin organization maintained by active loop extrusion," Proc. Natl. Acad. Sci. U.S.A. **120**, e2222078120 (2023).

[327] Krajina, B. A., and A. J. Spakowitz, "Large-scale conformational transitions in supercoiled DNA revealed by coarse-grained simulation," Biophys. J. **111**, 1339–1349 (2016).

[328] Peddireddy, R., D. Michieletto, G. Aguirre, J. Garamella, P. Khanal, and R. M. Robertson-Anderson, "DNA conformation dictates strength and flocculation in DNA–microtubule composites," ACS Macro. Lett. **10**, 1540–1548 (2021).

[329] Michieletto, D., P. Neill, S. Weir, D. Evans, N. Crist, V. A. Martinez, and R. M. Robertson-Anderson, "Topological digestion drives time-varying rheology of entangled DNA fluids," Nat. Commun. **13**, 4389 (2022).

[330] Papale, A., J. Smrek, and A. Rosa, "Nanorheology of active–passive polymer mixtures differentiates between linear and ring polymer topology," Soft Matter **17**, 7111–7117 (2021).

[331] Klotz, A. R., B. W. Soh, and P. S. Doyle, "Equilibrium structure and deformation response of 2D kinetoplast sheets," Proc. Natl. Acad. Sci. U.S.A. **117**, 121–127 (2020).

[332] Polson, J. M., E. J. Garcia, and A. R. Klotz, "Flatness and intrinsic curvature of linked-ring membranes," Soft Matter **17**, 10505–10515 (2021).

[333] Latulippe, D. R., and A. L. Zydney, "Radius of gyration of plasmid DNA isoforms from static light scattering," Biotechnol. Bioeng. **107**, 134–142 (2010).

[334] Petermann, E., L. Lan, and L. Zou, "Sources, resolution and physiological relevance of R-loops and RNA–DNA hybrids," Nat. Rev. Mol. Cell Biol. **23**, 521–540 (2022).

[335] Soh, B. W., and P. S. Doyle, "Deformation response of catenated DNA networks in a planar elongational field," ACS Macro Lett. **9**, 944–949 (2020).

[336] Krajina, B. A., A. Zhu, S. C. Heilshorn, and A. J. Spakowitz, "Active DNA olympic hydrogels driven by topoisomerase activity," Phys. Rev. Lett. **121**, 148001 (2018).

[337] O'Connor, T. C., T. Ge, and G. S. Grest, "Composite entanglement topology and extensional rheology of symmetric ring-linear polymer blends," J. Rheol. **66**, 49–65 (2022).

[338] Mason, T. G., K. Ganesan, J. H. van Zanten, D. Wirtz, and S. C. Kuo, "Particle tracking microrheology of complex fluids," Phys. Rev. Lett. **79**, 3282–3285 (1997).